DETERMINATION OF THE CRYSTAL GROWTH, BIRTH OF CRYSTAL NUCLEI, DYNAMICS AND STABILITY OF THE CRYSTALLIZER

By

CHARLES UMEJEI ONWUEGBUNEM OKONKWO

A DISSERTATION PRESENTED TO THE GRADUATE COUNCIL
OF THE UNIVERSITY OF FLORIDA IN
PARTIAL FULFILLMENT OF THE REQUIREMENTS
FOR THE DEGREE OF DOCTOR OF PHILOSOPHY

UNIVERSITY OF FLORIDA

1982

This project
is
dedicated
to
my parents
for their continual love,
encouragement, and support
throughout the years

ACKNOWLEDGMENTS

Glory be to God for seeing me through the many years of my educational experience.

I wish to thank the chairman of my doctoral supervisory committee, Dr. Hong Lee, for his guidance in this research, and Dr. Robert Coldwell for his assistance with the computer subroutine (simple).

Thank you to Dr. Robert Gould and Dr. Ranganatha Narayanan for their encouragemenet.

Special thanks go to Dr. Charles Burnap and Dr. Ulrich Kurzweg for the many fruitful discussions I have had with them during the course of my studies at this university.

Thank you to Linda McClintic and Elaine Everett for their encouragement. Also sincere thanks go to Vita Zamorano for her diligence and cooperation in typing the manuscript.

In conclusion, a special word of thanks is extended to my family for their moral support, prayers, love and patience. Thank you Mom, Dad, Thomas, Elizabeth, Paul, Rosaline, Francis and Fidelis for your understanding, encouragement and assistance throughout my educational experience.

TABLE OF CONTENTS

KEY TO SYMBOLS

a	Withdrawal rate of intermediate size product
a_i	Dimensional constants in balance equations (3-53) and (3-54)
$\tilde{a}_i$	Constants in the fit for $n(\zeta,t)$
a_n	Coefficients in characteristic equation
A1	Constant in W(z), example data
A2	Constant in $\eta_o(z)$, example data
A3	Constant in R(z), example data
A_n	Constants in series for N(z)
A_T	Total crystal area
b	Size dependent birth function
b	Size dependent part of birth function in equation (3-45)
b	Net birth function in equation (A-20), Appendix A
b^*	Dimensionless derivative of concentration dependent part of birth function
B1	Constant in W(z), example data
B	Birth function of crystals in equation (3-33)
B^o	Birth rate at zero size
$\overline{B}$	Cummulative birth function measured in steady state crystallizer and defined in equation (3-17a)
c	Concentration
c	Constant in ASL model, equation (2-10)
c_s	Saturation concentration

$\bar{c}$	Steady state concentration
$\bar{c}$	Reference concentration
c_1, c_2	Constants in the fit for number size distribution, steady state case
C1,C2,C3	Constants in $\Gamma_3(z)$, example data
C_1	Absolute error in n, Appendix B
C_i	Concentration of the i-th stream
C_m	Metastable concentration
C_o	Inlet concentration in equation (3-37)
CS1,CS2,CS3	Constants in $\Gamma_1(z)$, example data
C*	Dimensionless inlet concentration
D	Death rate of entities, Appendix A
EM	Constant in W(z), example data
EM_2	Constant in R(z), example data
EMH	Constant in $n_o(z)$, example data
ENINT	Integral of size distribution for seed crystals
f_n	Appropriate set of orthonormal functions
F_{Ai}	Fitted values for steady state size distribution
Fi	Experimental data for steady state number size distribution
F(z)	Integral of h(z)
g	Concentration dependent part of growth rate in equation (3-44)
g(x)	Vector function in equation (2-22)
g*	Dimension derivative of the concentration dependent part of growth rate
h_i	Classification function
h(z)	Quantity occurring in equation (3-65a)
i	Ratio of nucleation to growth rate (nucleation-growth sensitivity parameter)

I_m	Quantities occurring in equation (3-90)
j	Exponent to which suspension density is raised
J(z)	Quantity occurring in equation (3-69a)
k_v	Volumetric shape factor
K_2, K_3	Constants in B(c), equation (1-3)
K_c	Constant in equation (3-95)
K_n	Constant in B^o, equation (1-1)
K_N	Constant in equation (2-16)
L_c	Critical size of crystal
L_D	Dominant size
L_f^*	Maximum size of crystal fines
L_f	Dimensionless maximum size of crystal fines
L_K	Discrete size
L_m	Quantities occurring in equation (3-90)
L_{max}	Maximum largest size measured
L_n^m	Associate Laguerre polynomials
$\begin{matrix} m \\ n \end{matrix}$	Modified orthonomal set of functions, example data
L_o	Lower limit of integration, equation (2-4)
L_p	Maximum size for intermediate size crystals
L_w, L_1	Lowest size measured
M	Matrix
m_o	Amplitude of dimensionless time dependent concentration
m_k	k-th moment of number size distribution
M_T	Suspension density
n	Number size distribution
n_i	Inlet number size distribution for seed crystals in inlet feed

n_{in}	Dimensionless number size distribution for seeds
n_m	Size distribution for the m-th stage
n^o	Number of zero size crystals per unit volume
$\bar{N}$	Groups of quantities defined in equation (3-17c)
N(z)	Size dependent part of dimensionless number size distribution
P	Nucleation-growth sensitivity parameter occurring in equation (3-95)
P_n	Quantities occurring in equation (3-90)
Q	Volumetric flow rate
Q*	Quantity defined in equation (3-75)
r	Fraction change in concentration due to dissolving and recycling fines
R	Recycle ratio of dissolved fines
R(z)	Dimensionless size dependent part of birth rate
S	Sum of square error
t	Time
t_g	Time of particle growth after birth
t_m	Discrete time
t_w, t_l	Lowest time measured
T	Reference time
u	Dimensionless concentration dependent part of birth function
v	Dimensionless concentration dependent part of growth function
v_l	Growth rate, Appendix A
v_e	External velocity, Appendix A
v_i	Internal velocity, Appendix A
V	Volume of crystallizer's contents

V	Crystallizer's volume, Appendix A
V_L	Volume of clear liquor volume
V_S	Slurry volume
W	Dimensionless size dependent part of growth rate
x	Spatial coordinate, Appendix A
$\bar{X}$	Quantity defined in equation (3-17b)
y	Spatial coordinate, Appendix A
y	Dimensionless concentration
y_o	Time independent dimensionless concentration in perturbation analysis
z	Spatial coordinate, Appendix A
Z	Dimensionless size
Z^*	Withdrawal rate of oversize products

Greek Symbols

α	Fractional error in n, Appendix B
α_i	Constant in expression in steady state birth function, equation (3-8)
α_i	Constants relating residence times of crystals to their corresponding flow rate in different size ranges
α_{mn}	Quantities in equation (3-79)
β	Product recycle rate
β_{mn}	Quantities in equation (3-79)
χ	Square root of chi-square error
χ_n	Quantities in equation (3-79)
δ_m	Quantities in equation (3-79)
α_m	Quantities in equation (3-90)

η	Dimensionless number-size distribution
ε	Perturbation error
ε	Error in cummulative birth rate, Appendix B
ε_c	Ratio of clear liquor volume to slurry volume
γ	Constant in equation (2-10)
γ_1, γ_2	Constants in fit for $n(\zeta)$, steady state case
γ_n	Quantities in equation (3-79)
Γ_1	Group of terms defined in (3-47)
Γ_2	Group of terms defined in (3-49)
Γ_3	Group of terms defined in (3-50)
λ	Eigen value in stability analysis
Λ_{mn}	Quantities in equation (3-90)
μ_m	Microns
ν_5	Dimensionless residence time
Ω	Quantity in equation (3-74)
ϕ	Size dependent part of growth rate
ψ	Some entities, Appendix A
ψ_{mn}	Quantities in equation (3-90)
ρ	Density of crystal
σ	Concentration dependent part of birth rate
τ	Residence time
τ_4	Average residence time of crystals in crystallizers
τ_i	Residence time of seed crystals
τ_i	Residence times of crystals in different size ranges in equation (3-34)
θ	Solid fines recycle rate
θ	Dimension time

Abstract of Dissertation Presented to the Graduate Council of the University of Florida in Partial Fulfillment of the Requirements for the Degree of Doctor of Philosophy

DETERMINATION OF THE CRYSTAL GROWTH, BIRTH OF CRYSTAL NUCLEI, DYNAMICS AND STABILITY OF THE CRYSTALLIZER

By

Charles Umejei Onwuegbunem Okonkwo

August 1982

Chairman: Hong H. Lee
Major Department: Chemical Engineering

The task of quantifying growth and nucleation rates in a crystallizer grows increasingly difficult as one demands more accuracy in the calculation of these qualities, growth and nucleation rates. The associated stability problem of the crystallizer becomes very complex as more efficient and useful criteria are sought. The search for very good criteria necessitates that the research work with more complete balance equations.

Novel methods for quantifying growth and nucleation rates in steady and unsteady state crystallizers are developed. There were no assumptions made in the development of these methods which utilize some minimization procedure. The only approximation was in the minimization procedure. When applied to some literature data, the methods gave good results. In addition, the critical size, L_c, at which the growth rate is zero could be determined by these methods.

Very comprehensive and meaningful stability criteria are developed for the complex crystallizer via perturbation techniques. The complex crystallizer was a well-mixed suspension crystallizer equipped with dissolving and recycling of undissolved crystals and product classification. The criteria were derived from the complete crystallizer's balance equations. The only approximation was that the concentration dependent parts of the birth and growth functions were linear in concentration. In addition, the fourth order characteristic equation, from which the criteria are derived, is used in monitoring the effects of various crystallizer's parameters on the system's stability. These effects were simulated via the Root-Locus method. When applied to some example data, the characteristic equation gave results that are in agreement with experimental observations. The computer simulation and the criteria agree in all cases. New ways of stably operating a crystallizer under conditions in which the crystallizer may be inherently unstable were obtained.

CHAPTER I
INTRODUCTION

The preparation and handling of solids are influenced not only by gross chemical composition, but also by particle size distribution, morphology and surface chemistry. These parameters are in turn often fixed by processes that occur as the solid forms and is separated from its mother liquor. Crystallization products include food materials, pharmaceuticals, fertilizers and commodity chemicals. A few uses of crystallization include the following: (1) in process development, (2) in separation techniques, (3) in polymerization processes, and (4) in controlling product quality and shape. Thus if one wants to know about behavior of solids--reaction rates, caking, blending, toxicology, storage, dusting, bioavailability, etcetera--an adequate knowledge of the crystallization process will prove worthy. Sometimes a problem that is not initially viewed as a crystallization problem becomes one in the end.

Unlike most chemical processes, particle conservation balance is required in addition to mass, momentum, and energy balances to determine process yields and energy requirements. The population balance is an added complication which makes solution of the balance equations extremely difficult, if not impossible.

Primary and secondary nucleation are the two forms of crystallization. Primary crystallization is further subdivided into homogeneous and heterogeneous nucleation. Classical homogeneous nucleation is that which occurs only because of supersaturation as the driving force. In other words, it is conceived as the coming together of sufficient solute molecules to form a critical mass capable of surviving as a solid phase. An example of this is found in simple cooling and temperature reduction of a solution or in the evaporation of a portion of the solvent of a solution. Heterogeneous primary nucleation is similar to homogeneous nucleation except for the presence of a foreign solid which acts as an active site for nucleation. This foreign substance is of a different chemical composition. Again heterogeneous nucleation has supersaturation as its driving force. In general primary nucleation occurs at high supersaturation levels and nucleation and growth kinetics have a high order dependence on supersaturation. On the other hand, secondary nucleation is one which can occur at very low supersaturation provided there is some form energy and a seed crystal of the same chemical composition as material being crystallized. Secondary nuclei can form in saturated and undersaturated solution. For the nuclei formed to survive the solution must be slightly supersaturated. Secondary nucleation is not a strong function of nucleation and growth kinetics. The driving force is the presence of the seed crystal and energy. This

energy might be one of several forms such as crystal impeller collisions, ultrasonic waves or fluid shear on the crystal surface.

Crystallizers which operate at high and low supersaturation levels irrespective of the throughput or process conditions are classified as class I and class II systems respectively. Class II systems are usually high yield and fast growing while the contrary is true for class I systems. Primary and secondary nucleation are phenomena with high probability of occurrence in class I and class II systems respectively.

Though primary crystallization has been for a long time a topic of interdisciplinary interest among various scientists and engineers and has been extensively researched, a better understanding of the phenomenon of secondary nucleation awaits still much work to be at par with its counterpart. It was no more than thirty years ago when chemical engineers began work in secondary nucleation when they realized that it was the dominant form of nucleation in industrial crystallizers which usually operate at low supersaturation. Since then, several authors (Miller and Saeman, 1951; Murray and Larson, 1965; Timm and Larson, 1968; Clontz and McCabe, 1971; Randolph and Cise, 1972; Strickland-Constable, 1972; Ottens and de Jong, 1973; Sung et al., 1973; Bauer et al., 1974; Garside and Jancic, 1976; Lee, 1978; Garside and Jancic, 1979; Randolph and Puri, 1981) have addressed one aspect or the other of

secondary nucleation. Some of the aspects of secondary nucleation that have been of interest to chemical engineers are the following: (a) factors such as the crystallizer environment affecting the crystallizer (these may include effects of impurities, crystallizer hydrodynamics, impeller speed, surface regeneration time, hardness of contacting surface--the effects of these factors are usually treated via empirical correlations); (b) mechanisms involved in the crystallization process such as that responsible for nucleation and growth or the effect of impurities; (c) dynamics, stability and control of crystallizer; and (d) quantification of nucleation (birth of secondary nuclei) and crystal growth. Of the aforementioned areas the last is most critical in understanding the phenomenon of secondary nucleation. Knowledge about accurate quantification of nucleation and growth is important in understanding other areas as well.

The mixed-suspension-mixed-product-removal (MSMPR) pioneered by Randolph and Larson (1971) is a simple continuous crystallizer with inlet and outlet flow and in many ways is analogous to the continuous stirred tank reactor (CSTR). The main difference is the simultaneous occurrence of nucleation and growth in the MSMPR crystallizer. The name MSMPR crystallizer as used in the literature is a steady state crystallizer of the above description but obeying certain constraints that are rarely satisfied in practice.

Though the MSMPR crystallizer is valid for the large size region of constant growth rate (that is the McCabe ΔL law), researchers have used the MSMPR theory for the small size region. Because of the complexity introduced by the simultaneous occurrence of the two fundamental quantities --birth and growth rates--authors working with the steady state crystallizer have simply ignored the birth function in the population balance equation even when there is nuclei generation by contact nucleation. Contact nucleation is a form of secondary nucleation where energy is provided by contacting the seed crystal. Khambaty and Larson (1978) failed to account for nuclei generation in their steady state crystallizer experiment involving contact nucleation in addition to assuming that nuclei are born at zero size. Garside and Jancic (1979), like their predecessors, found it necessary to invoke the "zero size nuclei" assumption in their attempt to determine birth and growth rates in a steady state crystallizer. Authors have had more problems in determining the two fundamental quantities in an unsteady state crystallizer. To alleviate the problem Randolph and Cise (1972), while working with an unsteady state crystallizer, assumed zero birth rate in the population balance in order to calculate growth rate and to calculate birth rate they assumed zero growth. Similarly, Garside and Jancic (1976) obtained birth and growth rates in an unsteady state crystallizer via a differential technique, a method which not only gives gross errors, but also is very

impractical considering the type of experimental data that one works with. While the above list is by no means exhaustive, it is representative of the general trend adopted by most researchers. The above mentioned problems are addressed in the first part of my work.

Dynamics and Stability

MSMPR crystallizers inherently produce a wide crystal size distribution with a large coefficient of variation (C.V.) and a dominant size $L_D = 3G\tau$, where G and τ are constant growth rate and residence time respectively. This wide distribution is industrially undesirable. Design specifications for commercial products might require a narrow or large distribution or somewhere between the two. Sometimes one might desire some nucleation when there is little or none, while at other times there may be undesirable excessive nucleation. These and other problems dictate the need for controlling CSD. One way to change the CSD is to incorporate some selective removal whereby crystals of a certain size range are preferentially removed. Preferential removal, dissolution and recycle of fines generally lead to an increase in characteristic dimension (such as dominant or average crystal size) and spread of the distribution, while preferential removal of coarse products leads to a narrower distribution with a concomitant reduction in dominant size. Incorporation of clear liquor advance has the effect of increasing crystal residence time

which in turn has little or no effect in increasing dominant size. While it should be remembered that the purpose of designing selective crystal removal into a crystallizer is to force the CSD to a larger dominant size or narrow the distribution, actual incorporation of selective removal often leads to sustained oscillations. This action results in no improvement in product quality. It would be desirable to be able to operate the crystallizer without the incursion of instability even in regions where the system is inherently unstable by choosing appropriate control strategy. Ability to do this requires very meaningful stability criteria.

Several researchers have investigated various aspects of stability and control of one form of crystallizer or the other. Some of these are complex in nature. Unlike the MSMPR crystallizer which is analogous to the CSTR reactor as used in reaction engineering, complex crystallizers have no such counterpart. Complex crystallizers do not easily lend themselves to mathematical description and solution. The type of crystallization considered varied from slow growth rate kinetics (class I systems), where residual supersaturation is appreciable, to fast growth systems (class II systems) with negligible residual supersaturation.

Miller and Saeman (1947) while working with an industrial ammonium nitrate producing crystallizer observed cyclic fluctuations in particle size distribution. Similar observations were made by Finn and Wilson (1954) during a fermentation

process and by Thomas and Mallison (1961) in the field of continuous polymerization process. Yu and Douglas (1975) showed in their paper that a class I MSMPR crystallizer could be operated to give oscillations in the size distribution. These oscillations were the results of interactions within the system and these interactions were in turn the direct result of disturbances.

Randolph (1962) quantified stability of class II MSMPR in the following manner: $\frac{dL_n B^o}{dL_n G} < 21$. The logarithms of nuclei birth rate and grow rate are $\ell_n B$ and $\ell_n G$ respectively. By assuming the empirical power-law nucleation growth kinetics as expressed in equation (1-1),

$$B^o = K_n G^i \tag{1-1}$$

he obtained the following constraint:

$$\frac{dL_n B^o}{dL_n G} = i < 21 \ . \tag{1-2}$$

In equation (1-1) B^o is the nuclei birth rate defined via the assumption of zero size nuclei; G is the size independent growth rate and "i" is the kinetic order of birth to growth. Oscillations generated by kinetic values as high as 21 are referred to as high-order cycling.

Sherwin, Shinnar, and Katz (1967) derived stability criteria for an isothermal class I MSMPR crystallizer using Volmer's nucleation model in equation (1-2) and assuming nuclei birth rate is size independent.

$$B(c) = K_2 \exp(-K_3/(\ell_n c/c_s)^2) \qquad (1\text{-}3)$$

In equation (1-3), B(c) represents the concentration dependence of birth function, K_2 and K_3 are constants, and c and c_s are the concentration and saturation concentration, respectively. They claimed that instability was due to the nonlinear nature of the dependence of nucleation on supersaturation and that size dependency of the growth rate has a stabilizing effect. Attempts to treat size dependence of growth rate up to second order resulted in nonlinear moment equations which were not closed. Similar attempts not to linearize B(c) resulted in a closed set of nonlinear moment equations which were solved numerically. The authors concluded for the case of size independent growth rate and B(c) as defined by equation (1-3) that the tendency towards cycling increased with increasing particle size. Considering the assumptions in their model these conclusions are questionable.

Hulburt and Stefango (1969) modeled a double draw-off crystallizer by assuming size independent growth and birth rates and Volmer's nucleation model. They numerically solved the coupled nonlinear population and mass balance equations. The assumption of zero nuclei size was made in deriving these equations. They concluded that one of the draw-off streams, the clear liquid overflow, seemed to enhance stability. They also concluded that both increased seed addition and increased seed size in feed stream enhanced stability for high growth rate conditions.

Randolph, Beer and Keener (1973) showed the birth-growth stability constraint of a complex R-Z crystallizer to be a function of "i," fines exponential decay factor, λ, product classification size, L_p, and normalized product classification rate, z. Their model assumes that the birth and growth rates were size independent and that nuclei were of zero size. Beckman (1976) experimentally demonstrated sustained limit-cycle behavior in an R-Z type crystallizer equipped with clear liquor advance and product classification. He concluded that cycling behavior was chiefly induced by product classification.

Crystallizer Control

Timm and Gupta (1970) investigated the stability control of class II MSMPR crystallizer using fines seeding and fines destruction plus recycle as manipulated variables. They concluded that controlling the zero moment tended to stabilize the system while controlling the second moment tended to destabilize a normally stable system. Lei, Shinnar, and Katz (1971a) investigated the stability of a class I crystallizer with a point fines trap via spectral method. The control variable was fines crystal area. They were able to stabilize the system by manipulating the throughput rate while by manipulating fines destruction and recycle rate the system's stability was not enhanced. The idea of a point fines trap (zero mass of fines in trap) has

no practical value since industrial crystallizers operate with appreciable amounts of crystal mass in fines trap.

In order to avoid the excruciating mathematical complexity that would result, the aforementioned researchers found it necessary to make one assumption or the other even in situations when the conditions of their assumptions are never realized in practice. In consideration of the above problems, the second part of this work is devoted to obtaining more general stability criteria from which meaningful control strategy can be obtained. The crystallizer in this study will be discussed in detail in a later chapter. While it is more general, it is in many ways physically similar to the R-Z crystallizer modeled by Randolph, Beer, and Keener (1973), and will henceforth be referred to as "the Complex Crystallizer."

CHAPTER II
LITERATURE REVIEW

The concept of the population balance is mainly responsible for the progress and development witnessed in crystallization thus far. The study of crystallization has shifted from what was originally considered an art to what is becoming, more and more, an engineering science. The development of crystallization science started with nucleation-growth kinetics and steady state system analysis and progressed to dynamic system analysis. The various aspects of crystallization have not been equally embraced by the many works published on this subject. More attention is now being directed to the very important but least addressed areas of crystallization.

Nucleation and Growth

Saeman (1956) investigated the simplest continuous crystallizer--the mixed-suspension-mixed-product-removal (MSMPR) crystallizer. For this he essentially derived equations for the steady state crystal size distribution (CSD) in a mixed suspension. By first generating nuclei he no longer had to consider the birth function as part of the particle balance. Then he obtained the balance equation (2-1) with respect to time of growth after particle birth.

$$\frac{dn}{dt_g} + \frac{n}{\tau} = 0 \qquad (2\text{-}1)$$

The number of particles per unit volume per unit size and the residence time of these particles are n and τ, respectively. The variable t_g represents time (time of particle growth after birth). The solution to equation (2-1) is given by

$$n(t_g) = n(t_g=0)\ \exp(-t_g/\tau)\,. \qquad (2\text{-}2)$$

By assuming that growth was not a function of particle size, this allowed him to relate time of growth, t_g, to growth rate, G, and crystal size, L, in the following manner:

$$L = Gt_g\,. \qquad (2\text{-}3)$$

Substituting (2-3) in (2-2) and assuming that initial distribution of particles are nuclei of size L_o, he obtained.

$$n(L) = n(L_o)\ \exp\left(-\frac{L}{G\tau}\right)\,. \qquad (2\text{-}4)$$

In particular he chose $L_o = 0$ and obtained the standard MSMPR crystallizer equation,

$$n(L) = n(0)\exp\left(\frac{-L}{G\tau}\right) = n^o\ \exp\left(\frac{-L}{G\tau}\right)\,. \qquad (2\text{-}5)$$

Saeman then compared his theoretical distribution with that obtained from an Oslo-Krystal type crystallizer producing ammonium nitrate crystals under conditions of hindered settling and found good agreement. Similar work was done by Robinson and Roberts (1957) who obtained the theoretical

crystal size distribution resulting from a cascade of MSMPR crystallizers with nucleation in the first stage only, but same residence time in all stages. The size distribution for the m-th stage could be represented by

$$n_m(L) = \frac{n_1(0)\ (\frac{L}{G\tau})^{m-1}}{(m-1)!} \exp(-\frac{L}{G\tau}) \ ; \quad m = 1,2,... \tag{2-6}$$

Randolph and Larson (1962) later extended the work of Robinson and Roberts (1957) to include nucleation in all stages (and equal residence time for each unit). By so doing, they were able to extend application to more industrial crystallizers. The size distribution of the m-th stage for this type of crystallizer is

$$n_m(L) = (\frac{-L}{G\tau}) \sum_{k=1}^{m} \frac{n(0)\ (L/G\tau)^{k-1}}{(k-1)!} \ . \tag{2-7}$$

Abegg and Balakrishnan (1971) obtained the distribution in equations (2-6) and (2-7) in their attempt to model the mixing in different crystallizers. They found good agreement between the theoretical distributions, equations (2-6) and (2-7), and data taken from Draft Tube Battle (DTB) and Forced Circulation (FC) crystallizers respectively.
Hulbert and Katz (1964) derived with great generality the distribution of some entities over any associated property. This entity and associated property can be, for instance, particulate entity and particle size respectively. The

associated property can also be age or any other quantity that varies with time. Their model was then applied to particle nucleation and agglomeration, referred to as net birth (birth and death) and growth in crystallization terminology. Randolph (1964) in a "Note to the Editor" derived essentially the same population balance and noted that it would be of major importance in advancing the theoretical understanding of continuous crystallization.

Murray and Larson (1965) designed and constructed a continuous mixed suspension salting out crystallizer to test both the MSMPR model as well as the unsteady state model given by equation (2-8),

$$\frac{\partial n}{\partial t} = \frac{-r\partial n}{\partial \zeta} - \frac{n}{\tau}. \qquad (2\text{-}8)$$

They obtained nucleation and growth rates for the MSMPR model and some of the first transient data in the literature. They experienced great difficulty in the description of the very small crystals which dominate the size distribution behavior in terms of numbers. As a result determinations of nucleation and growth rates for this small size range were in error. Timm and Larson (1968) obtained nucleation and growth kinetics for three materials using steady state and transient data. They found that unsteady state experiments have some advantages over steady state experiments in determining the kinetic order of nucleation rate to growth rate. McCabe and Stevens (1951) found the growth rate of copper sulfate in a

suspension maintained by means of an agitator to be dependent on crystal size if the relative velocities of the crystals to solution velocity differ and if these relative velocities are in the effective low range. They found that larger crystals grew faster than small ones because larger crystals have higher relative velocity.

Youngquist and Randolph (1972) while working with a class II system involving ammonium sulfate obtained with great difficulty the nucleation rate after making several assumptions. They remarked that a rigorous quantitative definition of and use of secondary nucleation kinetics must await quantitative separation of size dependent growth and birth rates $G(\zeta)$, $b(\zeta)$ in the small size range. They said, "the increased detail and accuracy of secondary nucleation measurements made in this study have indicated the near impossibility of quantitatively characterizing secondary nucleation using the MSMPR technique as well as casting doubt on the general applicability of gross secondary nucleation kinetis so obtained" (p. 429). It will become obvious from this study, outlined in a later chapter, that one can go much further with the quantitative determination of birth and growth functions than they had thought. Randolph and Cise (1972), while working with an unsteady state class II system involving potassium sulfate, thought that it was patently impossible to uniquely specify both size dependent functions $G(\zeta)$ and $b(\zeta)$ using only the single size dependent measurement $n(\zeta)$, without further simplifying assumptions

or other independent measurements. Faced with this dilemma they assumed zero birth rate in the population balance in order to calculate the growth rate and to calculate birth rate they assumed zero growth rate, thus suppressing population changes due to convective number flux. Similarly, Garside and Jancic (1976) while working with potash alum in an unsteady state crystallizer used a differential technique to obtain birth and growth rates. This method is not only in gross error, but also impractical as regards typical experimental data.

Garside and Jancic (1979) found it necessary to invoke the "zero size" assumption in their attempt to determine birth and growth rates in a steady state crystallizer. They rearranged the steady state population balance as shown in equation (2-9):

$$b(\zeta) = n(\zeta)G(\zeta)\frac{d\ell_n n(\zeta)}{d\zeta} + \frac{1}{G(\zeta)\tau} + \frac{d\ell_n G(\zeta)}{d\zeta} . \quad (2\text{-}9)$$

They said that $b(\zeta)$ can be calculated if only $G(\zeta)$ is known. Then they used surface integration rate and mass transfer correlations to estimate the terms in equation (2-9) that involve $G(\zeta)$. Their semi-log plot of particle number versus size showed some curvature. They agreed that for small sizes, particularly below 15μm, overall growth was strongly size dependent. Khambaty and Larson (1978) in their experiment with magnesium sulfate heptahydrate crystals obtained a curved line on a semi-log plot of particle number versus size

and attributed the curvature to size dependency of the small crystals. They ignored the birth function in the population balance despite the fact that there was crystal generation by contact. They also invoked the zero size assumption. Rousseau and Parks (1981) similarly studied size dependency of the growth rate of magnesium sulphate heptahydrate crystal and obtained some curvature in the semi-log plot of particle number versus size. They similarly concluded that growth rate was strongly dependent on crystal size for the 44 to 1000μm size measured in the class II MSMPR crystallizer. The size dependent growth rate was obtained via the two parameter reduced version of the Abegg-Stevens-Larson (ASL) model given in equations (2-10) and (2-11):

$$G = g^{o}(1+\gamma L)^{c} \; ; \qquad c<1 \tag{2-10}$$

$$\gamma = 1/(G^{o}\tau) \tag{2-11}$$

The parameter, G^{o}, is the growth rate of nuclei and the parameters γ and c are simply constants.

The purpose of studying nucleation and growth in crystallizers is to be able to control crystal size distribution in these crystallizers, which are often plagued by oscillatory crystal size distribution dynamics. The associated dynamic behavior of crystallizers presents serious industrial problems.

Dynamics and Stability

Many investigators have dealt with the dynamic behavior of crystallizers. Some have addressed problems associated with class I crystallizers while others have directed attention to class II systems. In addition, some of the works have approached crystallizer instability from the nucleation-growth-kinetics viewpoint while others have taken the viewpoint that the mode of operation is the primary cause of crystallizer instability.

Cycling of crystal size distribution has been reported in class I crystallizers. Bennett (1962) observed cycling with an industrial crystallizer with a 15-hour period and a large amplitude swing of particle weight on a 12 SSM screen. Song and Douglas (1975) designed a laboratory scale sodium shloride crystallizer in which they produced oscillatory outputs using constant inputs. The experimental values of the oscillatory output agreed slightly with their theoretical predictions based on steady state measurements of growth rate and nucleation rate kinetic parameters of an isothermal MSMPR class I system. Only one cycle was observed in the experiment. Their theoretical work for this system is described in an earlier paper.

Sherwin, Shinnar and Katz (1967) carried out a theoretical investigation of the effect of feed seeding and fines dissolving and recycling on the stability of a class I system. These authors have expressed their stability criterion in terms of ratio b/g which they defined as

$$b/g = \frac{\bar{G}\left.\frac{dB}{dc}\right|_{\bar{c}}}{\bar{B}\left.\frac{dG}{dc}\right|_{\bar{c}}} \approx i \quad . \tag{2-12}$$

In equation (2-12) "bar" represents steady state values; G is a linear function of supersaturation,

$$G = k_1(c-c_s) \quad . \tag{2-13}$$

In equation (2-13) k_1 is a constant. The quantity B was approximated with Volmer's nucleation model defined earlier in equation (1-2), and in which the quantity $(\bar{c}/c_s - 1)$ is assumed very small. By expanding B up to first order in c/c_s and utilizing the above assumption, equation (2-12) can be written as

$$b/g \approx \frac{2K_3}{\left(\frac{\bar{c}}{c_s} - 1\right)^2} = i \quad . \tag{2-14}$$

For a clear feed, it was found that the system becomes unstable when $b/g > 21$. Seeded feed was found to improve stability strongly while volume fraction (void fraction) of solution had an insignificant effect. Another observation made was that the system stability increases significantly if nuclei had a finite size and that the region of stable operation enlarges with increasing nuclei size. The kinetic order of nucleation rate to growth rate played a significant role in determining the system stability.

Sherwin et al. (1969) were the first to uncover the extreme importance of product classification in causing crystallizer instability, in spite of the fact that their model was too idealized to be of practical value for engineering simulation. It was assumed in the model that as soon as a particle reached product size it was instantly removed thus producing mono-sized product crystals. It was found that extreme classification enhanced the sensitivity of the crystallizer to disturbances and increased the tendency toward cyclic fluctuations. Hulbert and Stenfango (1969) investigated a double draw-off crystallizer by assuming size independent growth and birth rates, zero size nuclei and Volmer's nucleation model. These assumptions resulted in a coupled nonlinear population and mass balance equations which were numerically solved. They found that one of the draw-off streams, the clear liquor overflow, tended to increase particle size and crystal solid content due to the longer particle retention time. As Bennett and Van Buren (1969) had already pointed out, increasing particle retention time does not always result in larger product crystals. In addition, the clear liquor overflow seemed to enhance the system stability. Another conclusion reached by Hulburt and Stefango was that increased feed seeding and increased seed size in feed stream enlarged the stability region for high growth conditions.

Nyvlt and Mullin (1970) observed damped oscillatory behavior while experimenting with a 200-liter draft-tube

crystallizer fitted with an elutriating leg and containing sodium thiosulfate as the specimen under investigation. The data obtained were too scanty to conclusively demonstrate sustained limit cycle behavior.

Lei et al. (1971a) carried out a theoretical study of the stability and dynamic behavior of a continuous crystallizer equipped with a fines trap. The fines had a fixed size. Nucleation was assumed to occur at a fixed size and growth rate was assumed independent of size. Their study showed that cycling in crystallizers can be reduced or eliminated by adjusting the operation of a fines trap, especially when the size of the fines is increased slightly. They also noted that fines dissolution and recycle do not always stabilize a crystallizer system, and can, in fact, destabilize the system depending on the conditions of operation.

Using perturbation methods Yu and Douglas (1975) carried out a theoretical investigation of the stability of a class I MSMPR crystallizer, and from which they concluded that, in some cases, oscillatory behavior can produce yields that exceed the predicted steady state value. The study entertained many assumptions in the derivation of the balance equations and process parameters used do not correspond to typical industrial conditions.

Attention has been directed to class II crystallizers by some investigators. Oscillatory behavior has been observed in some class II systems. Miller and Saeman (1947) observed oscillatory behavior of the crystal size distribution while

working with and industrial ammonium nitrate producing crystallizer (an Oslo type crystallizer). Kerr-McGee (in Beckman, 1976) observed cyclic fluctuations in an industrial potassium chloride crystallizer as shown in Figure 1. The severity of the fluctuations caused continous rippling of the weight distribution of product crystals. Cycling behaviors have been observed in a continuous polymerization process by Finn and Wilson (1954) and in a fermentation process by Thomas and Mallison (1961).

Randolph and Larson (1965) investigated the problem of stability in a class II MSMPR. The dynamic population balance equation (2-15) in conjunction with boundary condition equation (2-16) and initial condition (2-17) were transformed into moment equations, which were then solved on an analog computer.

$$\frac{\partial n}{\partial t} + \frac{G\partial n}{\partial \zeta} + \frac{n}{\tau} = 0 \qquad (2\text{-}15)$$

$$n(\zeta=0) = K_N G^i \qquad (2\text{-}16)$$

$$\bar{n}(\zeta) = \bar{n}(0)\ \exp(-\zeta/\tau) \qquad (2\text{-}17)$$

The coefficient, K_N, of G^i is a constant and "τ" is the crystallizer residence time. All other symbols in equation (2-15) are as defined in previous sections. The bar represents steady state values. Step changes in production rate and in nuclei dissolving rate were introduced into the system, and the resulting disturbances in the zeroth,

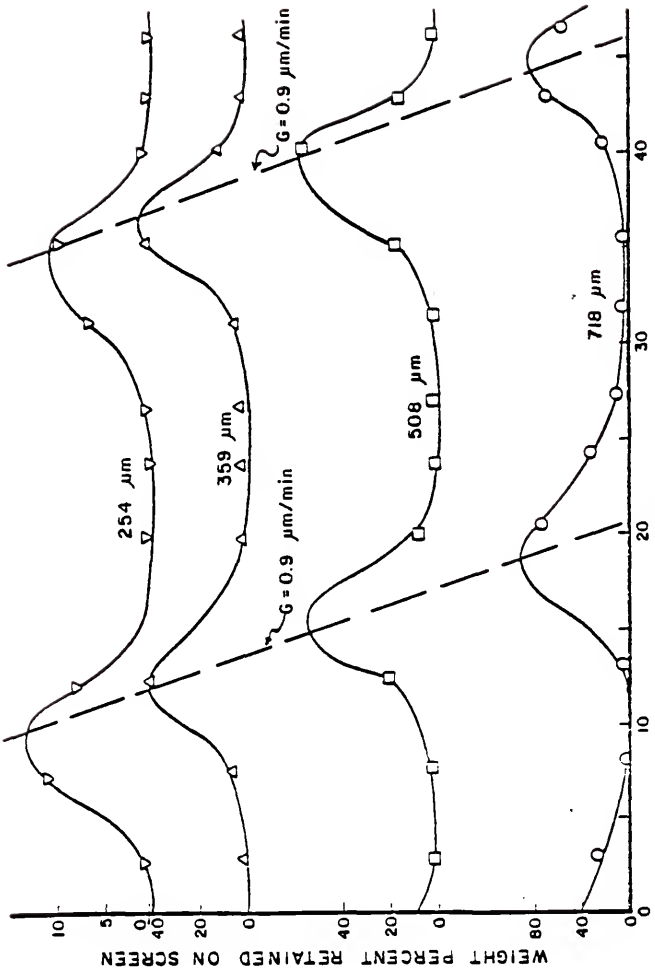

Figure 1. Unstable CSD Behavior in an Industrial KCl Crystallizer--source: Kerr-McGee in Beckman (1976), p. 18.

first, and second moments were plotted as functions of time. The plots showed cyclic fluctuations.

Randolph and Larson (1971) modeled a class II MSMPR crystallizer with equation (2-15) which was first transformed into a closed set of moment equations in time. The characteristic equation of this closed set of ordinary differential equations was obtained via Laplace transformation technique. Routh-Horwitz method was used to establish stability criterion which guaranteed stability of a crystallizer obeying equation (2-15), whenever the slope of the log-log plot of nucleation rate versus growth rate was less than 21. Randolph and Larson (1969) included product classification and fines dissolution and recycle in their crystallization. They concluded that the net effect of fines dissolution and recycle is to force growth rate to a higher level, producing the same production on larger average size crystals having less total area. They noted that if the higher supersaturation produced from the fines dissolution and recycle resulted in a greater than proportionate increase in nucleation rate (as would be the case if nucleaction rate were a stronger function of supersaturation than growth rate), then size improvement would be somewhat less than expected. They also noted that this internal feedback (that is, an increase in supersaturation causing an increase in nucleation rate) might affect the system in such a way that disturbances to the system might not damp out, thereby causing sustained oscillation of the crystal

size distribution. They further remarked that imperfect classification of larger product crystals is almost always accompanied by a reduction in average size, unless nucleation is independently controlled. Using the concept of a classification function, Randolph et al. (1973) modeled an R-Z crystallizer and showed the stability of such a crystallizer to be a function of "i," fines dissolution and recycle, product classification size, L_p, and normalized product classification rate, z. Beckman (1976) experimentally demonstrated sustained limit cycle behavior in an R-Z type crystallizer equipped with clear liquor advance and product classification. He then solved the population balance equation (with a perturbed steady state solution as initial condition) via Laplace transform technique to obtain the dynamic behavior of the crystallizer. He then compared his semianalytic solution with a regular-falsi method of numerical solution.

Saeman (1956) in his study of the simplest continuous MSMPR crystallizer noted that regardless of the classification device used, a crystallizer cannot put out large crystals unless conditions which are conducive to growth of large crystals are maintained in the suspension. They also remarked that positive and direct means for size control lie largely in the provision of effective means of segregation and elimination of excess fines. He recommended that fines should be eliminated at an average age that is less than or equal to one-tenth that of the product crystals, and that whatever the classification device used for removing fines,

it must not inadvertently overload with large intermediate size crystals. Saeman further showed that classification could yield a narrow distribution as well as one with relatively larger dominant size.

Cohen and Keener (1975) used a multiple time scale perturbation technique on a third order system of nonlinear ordinary differential equations to predict the bifurcation of time periodic solution of a class II MSMPR crystallizer. Their model is essentially represented by equations (2-18), (2-19) and (2-20).

$$\frac{\partial n}{\partial t} + \frac{1}{\int_0^\infty \zeta^2 n(\zeta,t)d\zeta} \frac{\partial n}{\partial \zeta} + n = 0 , \quad \zeta>0, \ t>0 \qquad (2\text{-}18)$$

$$n(0,t) = \frac{1}{\left[\int_0^\infty \zeta^2 n(\zeta,t)d\zeta\right]^i} , \quad t > 0 \qquad (2\text{-}19)$$

$$n(\zeta,0) = f(\zeta) = e^{-\zeta} \qquad (2\text{-}20)$$

The function, $f(\zeta)$, is the initial steady state distribution of the CSD. By defining the K-th moment as in equation (2-21), they transformed their equations into a set of nonlinear ordinary differential equations of the moments.

$$m_k(t) = \frac{1}{k!} \int_0^\infty \zeta^k n(\zeta,t)d\zeta \qquad (2\text{-}21)$$

In order to study their moment equations they investigated a general system of nonlinear ordinary differential equations represented by equation (2-22):

$$\frac{dX}{dt} = PX + \xi^2 AX + g(X) \quad . \qquad (2\text{-}22)$$

Here X is a three-component vector, P and A are constant matrices, and g(X) is a smooth nonlinear vector function containing no linear terms near the equilibrium point. In other words, derivatives with respect to each component of X varnish at the equilibrium point. In addition, the function g itself varnishes at the equilibrium point. If we represent $X^T = (x,y,z)$, then this condition is represented by equation (2-23).

$$g_i(0,0,0) = g_{ix}(0,0,0) = g_{iy}(0,0,0) = g_{iz}(0,0,0) = 0$$
$$i = 1,2,3 \qquad (2\text{-}23)$$

The parameter, ξ, is very small ($0<\xi<<1$). The subscripts x,y,z represent first order partials with respect to x, y, and z respectively. By casting the nonlinear ordinary differential equations of the moment into the form of equation (2-22), they were able to show oscillation in the crystal size distribution,n, and the growth rate, G, defined by equation (2-24).

$$G(t) = 1/\left(\int_0^\infty \zeta^2 n(\zeta,t)d\zeta\right) \quad . \qquad (2\text{-}24)$$

Their analysis predicted both amplitude and period of oscillation. The authors noted that including the mass balance would present a formidable task. In addition, they eliminated the birth function from the population balance, equation

(2-18), and by representing it as a size independent function and assuming a power law type of nucleation-growth kinetics, they included it as a boundary condition. Because of the many assumptions made their whole analysis is questionable.

Nyvlt and Mullin (1970) carried out a numerical study of a class II MSMPR crystallizer equipped with an elutriator via a Monte Carlo simulation technique. They used their study to explain experimental data obtained from a pilot plant. They concluded that crystallizers with or without product classification can exhibit periodic changes in production rate, product crystal size, supersaturation, magma density and other related parameters, and in some cases, the steady state may not be reached. The cyclic period, which is comparatively long in most cases, depends on the supersaturation rate and on the fraction of product crystals removed during classification. They noted that the stability of the system increases with increasing growth rate, increasing magma density, decreasing nucleation order, i, decreasing minimum product size, and decreasing quantity of crystals withdrawn per unit time. They also remarked that seeding would have the same effect as decreasing the effective nucleation rate and should lead to a stabilization of the system.

Good stability criteria is a prerequisite for an effective control scheme for dynamic crystallizers.

Control

Publications in control of crystallizer dynamics are very few. A good predictive model in terms of good stability criteria is a prerequisite for effective control. Simple proportional control of some crystallizer variable has been used by most of the investigators.

Bollinger and Lamb (1962) and Luyben and Lamb (1963) have outlined the basic design of feed forward control. Han (1967) investigated a feed forward control of class I MSMPR crystallizers by using feed concentration as the disturbance, supersaturation as the controlled variable and flow rate as the manipulated variable. By controlling the supersaturation, he intended to control production rate. Han's control scheme worked better when the system was operated in the stable instead of the unstable region of birth-growth kinetics.

Lei, Shinnar and Katz (1971b) investigated a feedback control of a class I MSMPR crystallizer equipped with a fines trap. Because of its relatively easy accessibility by light transmission measurement, the total surface area of fines in the fines trap was used as the controlled variable, with flow rate through the crystallizer as the manipulated variable. This scheme showed good control even when the crystallizer was operated in the unstable region. However, attempts to use fines recirculation rate (that is, the amount of fines destroyed) as the manipulated variable did not readily stabilize an unstable operation.

The above results were derived from a linearized stability analysis of a crystallizer equipped with point fines trap and in which a simple proportional control was incorporated.

Timm and Gupta (1970) investigated a feedforward/feedback control of a class II MSMPR by using flow rate out of the crystallizer as the disturbance, seeding and fines destruction and recirculation rate as manipulated variables and cumulative number of crystals as the controlled variable. The control scheme monitoring the cummulative number of crystals was demonstrated to be superior to the one monitoring the total area of crystals within the crystallizer. The control scheme with total area of suspended crystal magma as the controlled variable was worse than no control. The simple proportional control was capable of stabilizing the system within an inherently unstable region. The feedforward/feedback scheme showed remarkable improvement over conventional feedback control.

Beckman (1976), using proportional control of nuclei density with fines destruction and recirculation rate as the manipulated variable, studied the control of a class I MSMPR crystallizer equipped with fines destruction, clear liquor advance and product classification. He theoretically predicted the proportional control constant necessary for stability. The system was amenable to control. From a computer simulation utilizing experimentally determined nucleation and process parameters, he obtained a value for the proportional control constant which agreed with that predicted theoretically by his model. Beckman assumed nuclei were of

zero size and growth rate was size independent. By neglecting the birth function in the population balance, he included it as a size independent function in the boundary condition.

CHAPTER III
THEORY AND METHODOLOGY

As pointed out in earlier chapters, previous investigators encountered tremendous difficulty in their endeavor to simultaneously quantify the two fundamental quantities, growth and nucleation rates for all sizes. Apparently it was realized by these researchers that the most important tool towards understanding crystallization phenomenon in steady state crystallizers is the ability to quantify growth and nucleation rates. The MSMPR technique pioneered by Randolph and Larson (1962, 1971) was not capable of explaining experimental steady state data for the small size range where most of the nucleation occurs. It was designed for the large size region where growth rate is independent of size and for the size region where particle birth is negligible. Youngquist and Randolph (1972) in their work with a class II system remarked that a rigorous quantitative definition of and use of secondary nucleation kinetics must await quantitative separation of size dependent growth and birth rates $G(\zeta)$, $b(\zeta)$ in the small size range. They said that their work indicated the near impossibility of quantitatively characterizing secondary nucleation using the MSMPR technique as well as casting doubt on the general applicability of gross secondary nucleation so obtained. It is now

obvious that empirical correlations involving crystallizer process parameters and environment must await the rigorous quantification of growth and nucleation rates.

It is the unraveling of the simultaneous quantification of growth and nucleation rates to which the next section is devoted.

Growth and Birth Rates in Steady State Crystallizer

Consider the following crystal population balance equation (3-1), the derivation of which is included in detail in the appendix:

$$\frac{1}{V}\frac{\partial}{\partial t}(Vn) + \frac{\partial(Gn)}{\partial \zeta} = b + \frac{1}{V}(n_i Q_i - n_o Q_o) \qquad (3\text{-}1)$$

where

t = time

n = number of crystals per unit volume per unit size in crystallizer, #/Mℓ-μm)

ζ = crystal characteristic size, μm

G = crystal growth rate, μm/min

b = net birth rate of crystal nuclei, #/(mℓ-μm-min)

n_i = number of crystal seeds in inlet (feed) stream per unit volume per unit size, #/mℓ-μm)

n_o = number of crystals in outlet stream per unit volume per unit size, #/(mℓ-μm)

Q_i = inlet volumetric flow rate, (mℓ/min)

Q_o = outlet volumetric flow rate, (mℓ/min).

For a constant volume, well mixed, steady state crystallizer with no seeds in inlet feed, the above equation reduces to equation (3-2):

$$\frac{\partial}{\partial \zeta}(Gn) = b(\zeta) - \frac{1}{\tau} n(\zeta) \qquad (3\text{-}2)$$

where $\tau = \frac{V}{Q_o}$ is the average crystal residence time. Most researchers usually assume the McCabe ΔL Law to hold and take growth rate, G, to be indendent of size and in addition assume zero birth rate even in situations where secondary nuclei are being generated by contacting the seed crystal. When these assumptions are made, equation (3-3) is obtained:

$$\frac{G\partial n}{\partial \zeta} + \frac{n}{\tau} = 0 \ . \qquad (3\text{-}3)$$

The solution to equation (3-3) is given by equation (3-4):

$$n(\zeta) = n(L_o)\exp(-(\zeta - L_o)/(G\tau)) \ . \qquad (3\text{-}4)$$

Further they assume nuclei are born at size zero (that is $L_o=0$) so that equation (3-4) becomes

$$n(\zeta) = n^o \exp(\zeta/(G\tau)) \qquad (3\text{-}5)$$

where n^o is an abbreviation for n(0).

A curved population balance on a semilog plot of n versus size is of the form shown in Figure 2. Since equation (3-3) is not capable of explaining experimental data of the form represented in Figure 2, it suggests that one

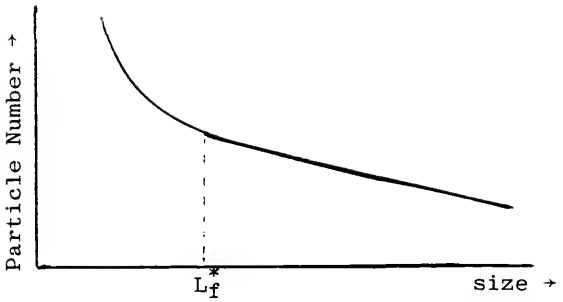

Figure 2. Plot of Population Density Versus Size.

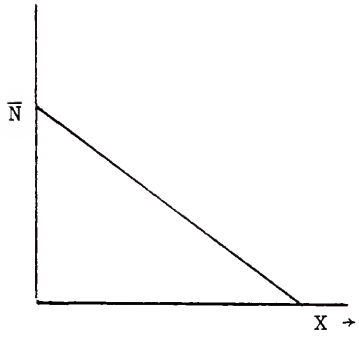

Figure 3. Plot of $\bar{N}$ Versus $\bar{X}$.

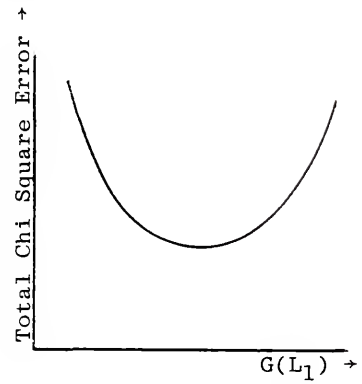

Figure 4. Plot of Total Chi Square Error Versus G(L_1) Values.

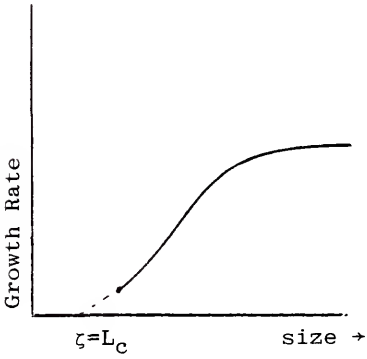

Figure 5. Growth Rate Versus Size.

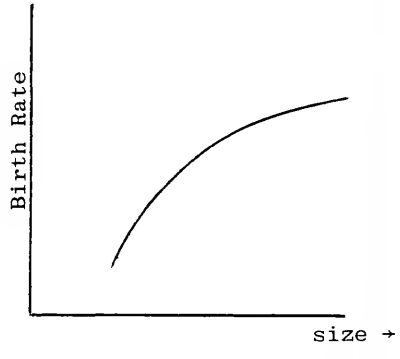

Figure 6. Birth Rate Versus Size.

should work with the more complete equation (3-2) for the steady state crystallizer.

Before proceeding, it is necessary to define a critical size, L_c, as that at which the growth rate is zero (that is $G(L_c)=0$). This definition is motivated by the fact that the growth rate, G, is a monotone increasing function of size in the interval, I = $(0,\infty)$. The shape of it is well documented. Integrating equation (3-2) with respect to size and applying the condition in equation (3-6) yields equation (3-7).

$$G(L_c) = 0 \tag{3-6}$$

$$G(\zeta)n(\zeta) = \int_{L_c}^{\zeta} b(\Lambda)d\Lambda - \frac{1}{\tau}\int_{L_c}^{\zeta} n(\Lambda)d\Lambda \tag{3-7}$$

The shapes or functional forms of the functions $b(\zeta)$ and $n(\zeta)$ are very well established from experimental as well as theoretical considerations. The shapes of these functions are exponential. For this reason, these functions are represented by equations (3-8) and (3-9).

$$b(\zeta) = \alpha_1 e^{-\alpha_2(\zeta-L_c)} \tag{3-8}$$

$$n(\zeta) = c_1\exp(-\gamma_1\zeta) + c_2\exp(-\gamma_2\zeta) \tag{3-9}$$

The parameters α_1, α_2, c_1, c_2, γ_1, and γ_2 are constants. Usually the parameters c_1, c_2, γ_1, and γ_2 can be determined from a nonlinear least squares fit of number size

distribution data. Substitution of equations (3-8) and (3-9) into equation (3-7) gives

$$G(\zeta)n(\zeta) = \int_{L_c}^{\zeta} \alpha_1 \exp(-\alpha_2(\Lambda - L_c))d\Lambda - \frac{1}{\tau}\int_{L_c}^{\zeta} [c_1\exp(-\gamma_1\Lambda) + c_2\exp(-\gamma_2\Lambda)]d\Lambda \quad . \quad (3\text{-}10)$$

We make the following definitions:

$$F_i = G(\zeta_i)n(\zeta_i) \quad , \qquad i = 1,2,\ldots,n \qquad (3\text{-}11)$$

$$F_{A_i} = \int_{L_c}^{\zeta_i} \alpha_1 \exp(-\alpha_2(\Lambda - L_c))d\Lambda - \frac{1}{\tau}\int_{L_c}^{\zeta_i} [c_1\exp(-\gamma_1\Lambda) + c_2\exp(-\gamma_2\Lambda)]d\Lambda \quad , \quad i = 1,2,\ldots,n \quad . \quad (3\text{-}12)$$

Experimental data are always reported for the size interval, $I_1 = [L_w, L_{max}]$, where L_w and L_{max} denote the respective lowest and maximum experimentally measured sizes. The size denoted as L_f^* in Figure 2 is that beyond which growth rate is constant as indicated by the straight line portion of the plot in the interval $I_2 = [L_f^*, L_{max}]$. It is for this same size interval that the MSMPR technique usually applies.

Once $n(\zeta)$ is obtained by fitting experimental data as represented by equation (3-9), it is used to interpolate for more values so that $n(\zeta_i)$ is available in much finer partition; in other words, the interval, $[L_w, L_{max}]$, is subdivided into much finer partitions than the original

experimental data. The only unknown values α_1, α_2, and L_c can be obtained by minimizing the sum, S, defined by equation (3-13) over α_1, α_2, and L_c.

$$S = \sum_{i=1}^{N} \left[(F_i - F_{Ai})/F_i\right]^2 \qquad (3\text{-}13)$$

Another version constitutes confining the minimization to the interval, $I_2 = [L_f^*, L_{max}]$, for which F_i is known for each "i." The minimization procedure is carried out via an appropriate nonlinear least square method. The determination of α_1, α_2, and L_c immediately yields the function, $b(\zeta)$ and $G(\zeta)$ can be calculated from equation (3-10). The integrations in equation (3-10) are to be carried out analytically. This concludes the analysis for the quantification of the two fundamental quantities, $G(\zeta)$ and $b(\zeta)$. It should be noted that no assumption was made in the population balance equation. The only approximation made is in the minimization procedures. This approximation is in general negligible since minimization procedures usually have built-in tolerances, some smaller than 10^{-6}, that must be satisfied before convergence is attained. I proceed to the determination of $G(\zeta)$ and $b(\zeta)$ for the unsteady state crystallizer.

Growth and Birth Rates in Unsteady State Crystallizer

The difficulty in quantifying the two fundamental quantities in an unsteady state crystallizer is compounded by the transient nature, which is an added dimension to the steady state case. Randolph and Cise (1972) attested to this difficulty in their experiment with an unsteady state Class II crystallizer involving potassium sulphate. They remarked that it was patently impossible to uniquely specify both size dependent functions $G(\zeta)$ and $b(\zeta)$ using only the single size dependent measurement $n(\zeta)$, without further simplifying assumptions or other independent measurements. Lee (1978) was the first to conceptualize a method of attack that set the direction for determining the two fundamental quantities in his study of the Single Seeded Batch Crystallizer (SSBCR). The following study will proceed along the same lines of thought.

Equation (3-1) shall form the basis of our analysis for a constant volume, well mixed crystallizer with seeds in inlet feed; equation (3-1) reduces to equation (3-14)

$$\frac{\partial}{\partial t} n(\zeta,t) + \frac{\partial}{\partial \zeta} [G(\zeta)n(\zeta,t)] = b(\zeta) + \frac{n_i}{\tau_i} - \frac{n}{\tau} \qquad (3\text{-}14)$$

where τ_i is the residence time of seed crystals in the feed.

Despite the fact that it is easier to start integration of equation (3-14) at t=0 and at ζ=0 because of initial and boundary conditions expressed by equations (3-15) and

(3-16), practical considerations dictate that we use the lowest experimentally measured time, t_w and size, L_w.

$$n(\zeta,0) = 0 \tag{3-15}$$

$$\left.\begin{aligned} n(0,t) &= 0 = \lim_{\zeta\to\infty} n(\zeta,t) \\ G(0) &= 0 \end{aligned}\right\} \tag{3-16}$$

First integrating with respect to time yields

$$n(\zeta,t_m) - n(\zeta,t_w) + \frac{\partial}{\partial\zeta}\left[G(\zeta)\int_{t_w}^{t_m} n(\zeta,\tau)d\tau\right] = (t_m-t_w)b(\zeta)$$

$$- \frac{1}{\tau}\int_{t_w}^{t_m} n(\zeta,\tau)d\tau + \frac{1}{\tau_i}\int_{t_w}^{t_m} n_i(\zeta,\tau)d\tau .$$

A second integration with respect to size results in the following expression:

$$\int_{L_w}^{L_k} n(\zeta,t_m)d\zeta - \int_{L_w}^{L_k} n(\zeta,t_w)d\zeta + G(L_k)\int_{t_w}^{t_m} n(L_k,\tau)d\tau$$

$$- G(L_w)\int_{t_w}^{t_m} n(L_w,\tau)d\tau = (t_m-t_w)\int_{L_w}^{L_k} b(\zeta)d\zeta$$

$$- \frac{1}{\tau}\int_{L_w}^{L_k}\int_{t_w}^{t_m} n(\zeta,\tau)d\tau d\zeta + \frac{1}{\tau_i}\int_{L_w}^{L_k} n_i(\zeta,\tau)d\tau d\zeta .$$

After rearrangement and denoting t_w and L_w by t_1 and L_1 respectively, the following equation is obtained:

$$\bar{N}(L_k, t_m) = -G(L_k)\bar{X}(L_k, t_m) + \bar{B}(L_k) \tag{3-17}$$

where

$$\bar{B} = \int_{L_1}^{L_k} b(\zeta)d\zeta \tag{3-17a}$$

$$\bar{X} = \frac{1}{t_m - t_1} \int_{t_1}^{t_m} n(L_k, \tau)d\tau \tag{3-17b}$$

$$\bar{N} = \frac{\int_{L_1}^{L_k} n(\zeta, t_m)d\zeta}{t_m - t_1} - \frac{\int_{L_1}^{L_k} n(\zeta, t_1)d\zeta}{t_m - t_1} - G(L_1)\int_{t_1}^{t_m} n(L_1, \tau)d\tau$$

$$+ \frac{1}{\tau(t_m - t_1)} \int_{L_1}^{L_k} \int_{t_1}^{t_m} n(\zeta, \tau)d\tau d\zeta$$

$$- \frac{1}{\tau_i(t_m - t_1)} \int_{L_1}^{L_k} \int_{t_1}^{t_m} n_i(\zeta, \tau)d\tau d\zeta. \tag{3-17c}$$

Cognizant of the discrete nature of experimental data, we let m = 2,3,...,M and k = 2,3,W. For each value of k, $\bar{N}$ and $\bar{X}$ are M-dimensional vectors. A plot of equation (3-17) in the form $\bar{N}(L_k, t_m)$ versus $X(L_k, t_m)$ for each value of k results in a straight line with a slope equal to $-G(L_k)$ and intercept, $\bar{B}(L_k)$, provided $\bar{N}(L_k, t_m)$ and $X(L_k, t_m)$ can be completely determined. Thus G and $\bar{B}$ can be generated at corresponding sizes, L_k's by repeating the above plot for various values of k. Finally, G and B can each be plotted against size.

If we had started the integration at zero size (that is $L_1=0$), $G(L_1)$ would be zero and $\bar{N}$ would be completely determined without much ado. Unfortunately $\bar{N}$ is yet undetermined because $G(L_1)\neq 0$. However, by following the procedure enumerated below, $\bar{N}$ and hence G and B can be determined.

Step 1. First fit particle size data via least squares regression to obtain a functional form for $n(\zeta,t)$. One does not need to perform a fitting for $n_i(\zeta,t)$ since this is usually given.

Step 2. Calculate the various integrals that make up $\bar{N}$ and $\bar{X}$ analytically, if possible.

Step 3. Because $\bar{N}$ cannot be calculated until $G(L_1)$ is known, guess a value for $G(L_1)$ and calculate $\bar{N}$ and $\bar{X}$. For each value of $k\geq 2$, plot $\bar{N}(L_k,t_m)$ versus $\bar{X}(L_k,t_m)$. For example, data for k=2 would be as shown below.

Data for k=2

$\bar{N}(L_2,t_2)$	$\bar{X}(L_2,t_2)$
$\bar{N}(L_2,t_3)$	$\bar{X}(L_2,t_3)$
$\bar{N}(L_2,t_4)$	$\bar{X}(L_2,t_4)$
$\bar{N}(L_2,t_5)$	$\bar{X}(L_2,t_5)$
$\vdots$	$\vdots$
$\bar{N}(L_2,t_M)$	$\bar{X}(L_2,t_M)$

A plot of $\bar{N}$ versus $\bar{X}$ data is illustrated in Figure 2 for the case k=2. The plot in Figure 3 is typical since every

value of k yields a straight line with negative slope and positive intercept. An alternative approach is performing a least squares linear regression on the data to determine the slope and the intercept. For a given $G(L_1)$ record the sum of square error or the chi-square error for each k and the total chi-square error for all k's. Total chi-square error = $\sum_{k=2}^{W} \chi_k^2$ where χ_k^2 is the chi-square error for a particular value of k. For perfect data the coefficient of determination of the fit for each k is one; in other words, the chi-square error is zero.

Step 4. Repeat step 3 for different guesses of $G(L_1)$.

Step 5. Plot total chi-square error against $G(L_1)$ values and record the $G(L_1)$ corresponding to the lowest chi-square error. The value of $G(L_1)$ so obtained is more accurate than other values of $G(L_1)$. A plot of total chi-square error versus $G(L_1)$ values might look like that in Figure 4.

Step 6. Using the value of $G(L_1)$ corresponding to the minimum error, plot $\bar{B}(\zeta)$ and $G(\zeta)$ each against ζ, where ζ takes discrete values, L_k, k = 2,3,...,W. Obtain $G(L_c)$ by extrapolation. Typical plots for $\bar{B}(\zeta)$ and $G(\zeta)$ might look like those in Figures 5 and 6.

The first guess in step 3 can be generated by minimizing equation (3-18), a rearranged version of equation (3-17), over unknowns, $G(L_1)$, $G(L_2)$ and $\bar{B}(L_2)$ when k=2.

$$\bar{N}(L_2,t_m) + G(L_2)\bar{X}(L_2,t_m) - \bar{B}(L_2) = 0, \quad m = 2,3,\ldots,M \tag{3-18}$$

For a crystallizer with no seeds in inlet feed equation (3-17) is still valid with $\overline{N}$ no longer containing the term in $n_i(\zeta,\tau)$. Similarly, for a batch crystallizer $\overline{N}$ no longer contains the term in n_i as well as the double integral of $n(\zeta,\tau)$. Thus for the batch crystallizer $\overline{N}$ is represented by equation (3-19):

$$\overline{N} = \frac{\int_{L_1}^{L_k} n(\zeta,t_m)d\zeta}{t_m-t_1} - \frac{\int_{L_1}^{L_k} n(\zeta,t_1)d\zeta}{t_m-t_1} - G(L_1)\int_{t_1}^{t_m} n(L_1,\tau)d\tau \qquad (3\text{-}19)$$

Every other term in equation (3-17) remains the same.

This concludes our analysis for the determination of growth and birth functions in an unsteady state crystallizer. It should be noted that no assumptions were made in the above analysis. The only approximations made were in the minimization procedure used for data treatment.

The methods treated above for the determination of growth and birth functions in steady and unsteady state crystallizers also allow for the determination of these functions to be made in terms of process conditions, such as supersaturation, crystallizer impeller speed, etcetera. The growth and birth functions are simply determined for each fixed value of a process condition, and correlations could be obtained, if desired. Good empirical correlations can only come after an accurate method of quantification of growth and birth rates has been established.

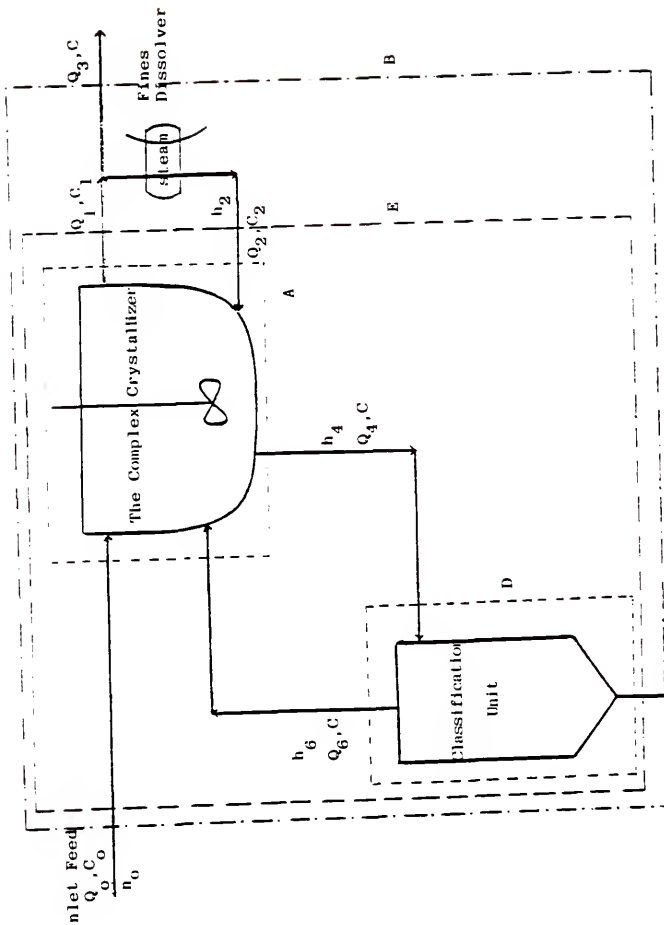

Figure 7. Schematic Diagram of the Complex Crystallizer.

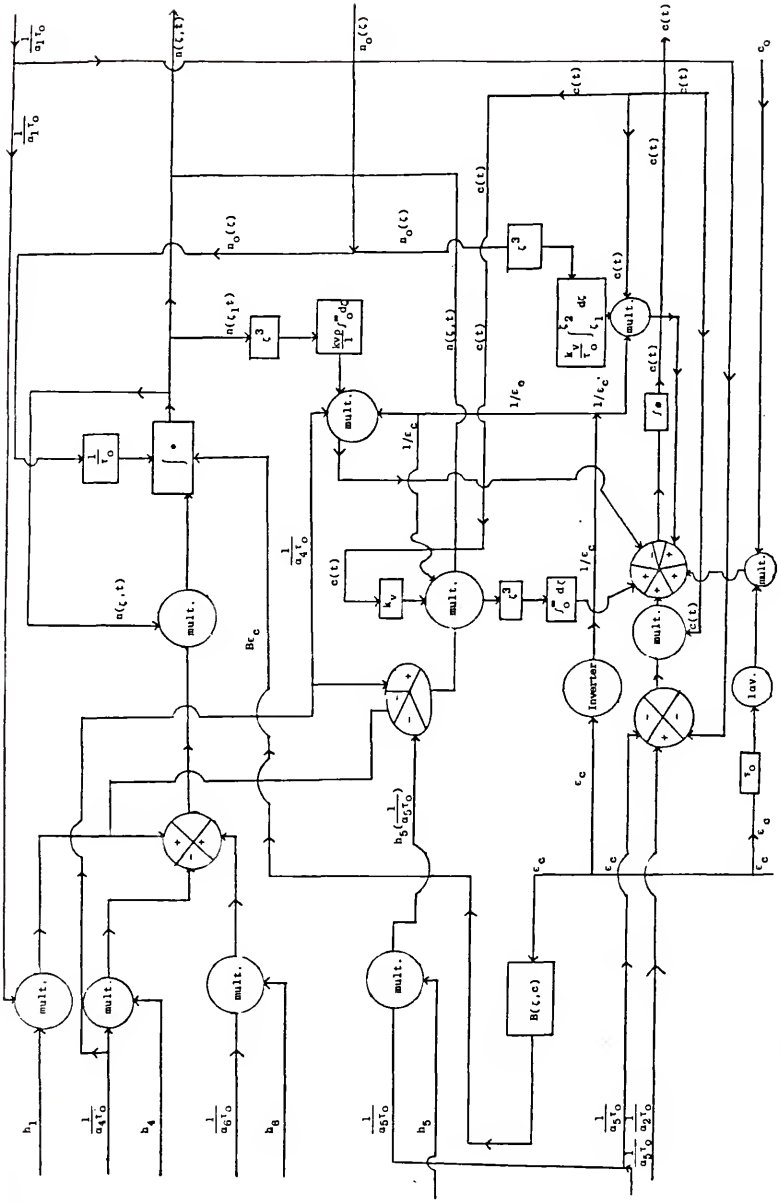

Figure 8. Information Flow Diagram for the Complex Crystallizer.

A stability criteria would not be very practical unless a method for the accurate quantification of growth and birth rates was available. This is so because the very equations from which stability criteria are derived contain the two fundamental quantities, growth and birth rates.

Dynamics and Stability of the Complex Crystallizer

The problem associated with obtaining a good stability criteria is much more complex mathematically than that associated with the quantification of growth and birth rates. Because of the associated mathematical intricacy of crystallizers' stability problems, previous researchers have oftentimes found it necessary to make oversimplifying assumptions, thereby making the criteria so obtained of less practical value.

The crystallizer under study is very similar to the R-Z crystallizer studied by Randolph, Beer and Keener (1973), and will be referred to as "the complex crystallizer." The complex crystallizer, the schematic diagram of which is shown in Figure 7, is that which is equipped with fines destruction and recycle, seeding, clear liquor advance, and product classification. It is obvious from Figure 7 that, in addition to the population balance equation, other material balance equations are required to completely establish the balance equations of the complex crystallizer. Because the conditions are isothermal and there is no

significant energy changes in the system, the balance equations do not include an energy balance equation.

Complex Crystallizer Balance Equations

The various system boundaries, A, B, D, E, in Figure 7 are those around which material balances are made. The flows P_i and Q_i ($i = 0,1,2,\ldots,6$) represent solid and liquid flow rates respectively. The classification functions, $h_i(\zeta)$, are size dependent removal functions representing the ratio of crystals removed in a certain size range during classification to that expected with ordinary mixed withdrawal. The classification functions, $h_i(\zeta)$, can also be viewed as removal probability functions. As an example, a classification function $h_1(\zeta)$ is defined by equation (3-20).

$$h_1(\zeta) = \begin{cases} R-1 , & (0,L_f) \\ 0 , & \text{other sizes} \end{cases} \qquad (3\text{-}20)$$

Equation (3-20) indicates that crystals in the size range $(0,L_f)$ have a probability of removal that is (R-1) times that in a mixed withdrawal case while the probability of removal of crystals larger than size L_f is zero. The functions $h_i(\zeta)$ are represented below:

$$h_1(\zeta) = \begin{matrix} R-1 , & [0,L_f] \\ 0 , & \text{otherwise} \end{matrix} \qquad (3\text{-}21)$$

$$h_2(\zeta) = 0 , \qquad \text{for all sizes} \qquad (3\text{-}22)$$

$$h_3(\zeta) = h_1(\zeta) \tag{3-23}$$

$$h_4(\zeta) = \begin{cases} 1 , & [0,L_f] \\ a , & (L_f,L_p] \\ z , & (L_p,\infty) \end{cases} \tag{3-24}$$

$$h_5(\zeta) = \begin{cases} 1-\theta , & [0,L_f] \\ a , & (L_f,L_p] \\ z(1-\beta) , & (L_p,\infty) \end{cases} \tag{3-25}$$

where $0 \leq \theta \leq 1$

$0 \leq \beta \leq 1$

$$h_6(\zeta) = \begin{cases} \theta , & [0,L_f] \\ 0 , & (L_f,L_p] \\ z\beta , & (L_p,\infty) \end{cases} . \tag{3-26}$$

In the above equations L_f and L_p represent maximum sizes for fines and intermediate size product. Sizes larger than L_p represent the oversize product. The advantage of the classification functions is that differences in crystal distribution are completely accounted for, thereby eliminating the need to separately indicate the different distributions, n_i's. It would be desirable that the volume on which the birth function and crystal size distribution (CSD) is based remains constant, even during transient operation. To achieve this it is necessary to define the void fraction

within the crystallizer, ε_c, in order to reexpress all volume based quatities on a slurry volume basis. The slurry volume remains constant during transient operations. The void fraction, ε_c, is defined as the ratio of clear liquor volume, V_L, to slurry volume, V_S.

$$\varepsilon_c = V_L/V_S \tag{3-27}$$

It suffices to specify four of the seven volumetric flow rates in Figure 7. From Figure 7 the following relationships among the various flow rates can be established:

$$Q_o = Q_3 + Q_5 \tag{3-28}$$

$$Q_1 = Q_3 + Q_2 \tag{3-29}$$

$$Q_o = Q_1 - Q_2 + Q_5 \tag{3-30}$$

$$Q_4 = Q_5 + Q_6 \tag{3-31}$$

$$Q_o = Q_1 - Q_2 + Q_4 - Q_6 \ . \tag{3-32}$$

The flow rates Q_o, Q_1, Q_2, and Q_5 are feed, fines removal, dissolved fines recycle and product volumetric flow rates, respectively. The clear liquor volumetric flow rate is represented by Q_3.

Applying the general population balance derived in the appendix to Figure 7, the following particle number balance equation results:

$$\frac{\partial}{\partial t}(V_s n) + \frac{\partial}{\partial \zeta}(GV_s n) = V_s B\varepsilon_c + \left[-Q_1 h_1(\zeta) - Q_4 h_4(\zeta) + Q_6 h(\zeta)\right] n(\zeta) + Q_o n_o(\zeta) \ .$$

Since V_s is constant the above equation reduces to

$$\frac{\partial n}{\partial t} + \frac{\partial}{\partial \zeta}(Gn) = B\varepsilon_c + \left[\frac{-Q_1}{V_s} h_1(\zeta) - \frac{Q_4}{V_s} h_4(\zeta) + \frac{Q_6}{V_s} h_6(\zeta)\right] n(\zeta,t) + \frac{Q_o}{V_s} n_o(\zeta) \quad . \tag{3-33}$$

Let

$$\tau_i = V_s/Q_i \tag{3-34}$$

$$\tau_i = \alpha_i \tau_5 . \tag{3-35}$$

By combining equations (3-33), (3-34) and (3-35), the following equation results:

$$\frac{\partial n}{\partial t} + \frac{\partial}{\partial \zeta}(Gn) = B\varepsilon_c + \left[\frac{-1}{\alpha_1 \tau_5} h_1(\zeta) - \frac{1}{\alpha_4 \tau_5} h_4(\zeta) + \frac{1}{\alpha_6 \tau_5} h_6(\zeta)\right] n(\zeta) + \frac{1}{\alpha_o \tau_5} n_o(\zeta) \quad . \tag{3-36}$$

The terms of equation (3-36) represent, in order, the accumulation of crystals at size ζ, the net flux of crystals away from size ζ due to growth, the input of particles due to nucleation, the input or withdrawal of particles as a result of classification, and the input of particles due to solids in feed.

Solute and Solid Balance

As mentioned earlier the solute and solid balance is required as it complements the crystal population balance equation, both of which, together, form the governing equation for the dynamics of the complex crystallizer. The solute and solid balance is derived by setting all inputs in both dissolved and solid form equal to all outputs plus accumulation.

A solute balance around boundary E of Figure 7 results in the following expression:

$$\frac{d}{dt}(V_s\varepsilon_c C) = Q_o C_o + Q_2 C_2 - [Q_1 C + Q_5 C] - (k_v\rho/\tau_4)V_s \int_o^\infty n(\zeta,t)\zeta^3 d\zeta \qquad (3\text{-}37)$$

where τ_4 is taken to be the average residence time of crystals in crystallizers. The quantities, C_i, $i = 0,2$, denote the supersaturation of the i-th stream. The volumetric shape factor, crystal density and the supersaturation of the well mixed suspension inside the crystallizer are denoted by k_v, ρ, and C, respectively.

Combining equations (3-35) and (3-37) yields the following equation after rearrangement:

$$\frac{d\varepsilon_c}{dt} = \frac{-\varepsilon_c}{C}\frac{dc}{dt} + \frac{C_o}{\tau_o C} + \frac{C_2}{C\tau_2} - \left[\frac{1}{\tau_1} + \frac{1}{\tau_5}\right] - \left(\frac{k_v\rho}{C\tau_4}\right)\int_0^\infty n(\zeta,t)\zeta^3 d\zeta \ . \qquad (3\text{-}38)$$

A solute plus solid balance around boundary E of Figure 7 yields

$$V_s\varepsilon_c \frac{dC}{dt} = -V_s(c-\rho) \frac{d\varepsilon_c}{dt} + Q_oC_o + Q_2C_2 + (k_vV_s\rho/\tau_o) \int_{\zeta_1}^{\zeta_2} n_o(\zeta)\zeta^3 d\zeta$$

$$-\left[Q_1C + Q_5C + (k_vV_s\rho/\tau_5)\int_0^{\infty} h_5(\zeta)n(\zeta,t)\zeta^3 f\zeta\right.$$

$$\left. + (k_vV_s\rho/\tau_1) \int_0^{\infty} h_1(\zeta)n(\zeta,t)\zeta^3 d\zeta\right]$$

where crystals in the feed have sizes in the range ζ_1 to ζ_2. Upon rearrangement the above equation yields

$$\frac{dc}{dt} = \frac{-(c-\rho)}{\varepsilon_c} \frac{d\varepsilon_c}{dt} + \frac{C_o}{\tau_o\varepsilon_c} + \frac{C_2}{\tau_2\varepsilon_c} + \frac{(k_v\rho/\tau_o)}{\varepsilon_c} \int_{\zeta_1}^{\zeta_2} n_o(\zeta)\zeta^2 d\zeta$$

$$- \left[\frac{C}{\tau_1\varepsilon_c} + \frac{C}{\tau_5\varepsilon_c} + \frac{(k_v\rho/\tau_5)}{\varepsilon_c} \int_0^{\infty} h_5(\zeta)n(\zeta,t)\zeta^3 d\zeta\right.$$

$$\left. + \frac{(k_v\rho/\tau_1)}{\varepsilon_c} \int_0^{\infty} h_1(\zeta)n(\zeta,t)\zeta^3 d\zeta\right] . \qquad (3\text{-}39)$$

Substituting the expression for $\frac{d\varepsilon_c}{dt}$ in $\frac{-(c-\rho)}{\varepsilon_c} \frac{d\varepsilon_c}{dt}$ results in the following equation:

$$\frac{-(c-\rho)}{\varepsilon_c} \frac{d\varepsilon_c}{dt} = \frac{-(c-\rho)}{\varepsilon_c} \left\{\frac{-\varepsilon_c}{C} \frac{dC}{dt} + \frac{C_o}{\tau_oC} + \frac{C_2}{C\tau_2} - \frac{1}{\tau_1} + \frac{1}{\tau_5}\right.$$

$$\left. - \left(\frac{k_v\rho}{C\tau_4}\right) \int_0^{\infty} n(\zeta,t)\zeta^3 d\zeta\right\} .$$

Upon rearrangement, the following equation results:

$$\frac{-c-\rho)}{\varepsilon_c} \frac{d\varepsilon_c}{dt} = \frac{(c-\rho)}{C} \frac{dC}{dt} - \frac{(c-\rho)C_o}{\varepsilon_cC\tau_o} - \frac{(c-\rho)C_2}{\varepsilon_cC\tau_2} + \frac{(c-\rho)}{\varepsilon_c} \left(\frac{1}{\tau_1} + \frac{1}{\tau_5}\right)$$

$$+ \frac{k_v\rho(c-\rho)}{\varepsilon_c\tau_4C} \int_0^{\infty} n(\zeta,t)\zeta^3 d\zeta .$$

Substituting the above equation into equation (3-39) yields

$$\frac{dC}{dt} = \frac{(c-\rho)}{c}\frac{dC}{dt} - \frac{(c-\rho)C_o}{\varepsilon_c C\tau_o} - \frac{(c-\rho)C_2}{\varepsilon_c C\tau_2} + \frac{(c-\rho)}{\varepsilon_c}\left[\frac{1}{\tau_1} + \frac{1}{\tau_5}\right]$$

$$+ \frac{k_v\rho(c-\rho)}{\varepsilon_c\tau_4 C}\int_0^\infty n(\zeta,t)\zeta^3 d\zeta + \frac{C_o}{\tau_o\tau_c} + \frac{C_2}{\tau_2\tau_c}$$

$$+ \frac{(k_v\rho/\tau_o)}{\varepsilon_c}\int_{\zeta_1}^{\zeta_2} n_o(\zeta)\zeta^3 d\zeta - \left[\frac{c}{\tau_1\varepsilon_c} + \frac{c}{\tau_5\varepsilon_c}\right.$$

$$\left. + \frac{(k_v\rho/\tau_5)}{\varepsilon_c}\int_0^\infty h_5(\zeta)n(\zeta,t)\zeta^3 d\zeta + \frac{(k_v\rho/\tau_1)}{\varepsilon_c}\int_0^\infty h_1(\zeta)n(\zeta,t)\zeta^3 d\zeta\right]$$

which after a slight algebraic manipulation becomes

$$\left(\frac{\rho}{c}\right)\frac{dC}{dt} = \frac{\rho C_o}{\varepsilon_c C\tau_o} + \frac{\rho C_2}{\varepsilon_c C\tau_2} - \frac{\rho}{\varepsilon_c}\left[\frac{1}{\tau_1} + \frac{1}{\tau_5}\right] + \frac{k_v\rho(c-\rho)}{\varepsilon_c\tau_4 C}\int_0^\infty n(\zeta,t)\zeta^3 d\zeta$$

$$+ \frac{(k_v\rho/\tau_o)}{\varepsilon_c}\int_{\zeta_1}^{\zeta_2} n_o(\zeta)\zeta^3 d\zeta - \frac{k_v\rho/\tau_5}{\varepsilon_c}\int_0^\infty h_5(\zeta)n(\zeta,t)\zeta^3 d\zeta$$

$$= \frac{k_v\rho/\tau_1}{\varepsilon_c}\int_0^\infty h_1(\zeta)n(\zeta,t)\zeta^3 d\zeta \ .$$

Solving the above equation for $\frac{dC}{dt}$ results in equation (3-40).

$$\frac{dC}{dt} = \frac{C_o}{\varepsilon_c\tau_o} + \frac{C_2}{\varepsilon_c\tau_2} - \frac{C}{\varepsilon_c}\left[\frac{1}{\tau_1} + \frac{1}{\tau_5}\right] + \frac{k_v(c-\rho)}{\varepsilon_c\tau_4}\int_0^\infty n(\zeta,t)\zeta^3 d\zeta$$

$$+ \frac{k_v C}{\varepsilon_c\tau_o}\int_{\zeta_1}^{\zeta_2} n_o(\zeta)\zeta^3 d\zeta - \frac{k_v C}{\varepsilon_c\tau_5}\int_0^\infty h_5(\zeta)n(\zeta,t)\zeta^3 d\zeta$$

$$- \frac{k_v C}{\varepsilon_c\tau_1}\int_0^\infty h_1(\zeta)n(\zeta,t)\zeta^3 d\zeta \ . \qquad (3\text{-}40)$$

Substituting equation (3-35) into (3-40) yields equation (3-41):

$$\frac{dC}{dt} = \frac{C_o}{\varepsilon_c \alpha_o \tau_5} + \frac{C_2}{\varepsilon_c \alpha_2 \tau_5} - \frac{C}{\varepsilon_c}\left[\frac{1}{\alpha_1 \tau_5} + \frac{1}{\tau_5}\right] + \frac{k_v(c-\rho)}{\varepsilon_c \alpha_4 \tau_5}\int_0^\infty n(\zeta,t)\zeta^3 d\zeta$$

$$+ \frac{k_v C}{\varepsilon_c \alpha_o \tau_o}\int_{\zeta_1}^{\zeta_2} n_o(\zeta)\zeta^3 d\zeta - \frac{k_v C}{\varepsilon_c \tau_5}\int_0^\infty h_5(\zeta) n(\zeta,t)\zeta^3 d\zeta$$

$$- \frac{k_v C}{\varepsilon_c \tau_1}\int_0^\infty h_1(\zeta) n(\zeta,t)\zeta^3 d\zeta \quad . \qquad (3\text{-}41)$$

Combining equations (3-33), (3-34) and (3-35) results in equation (3-42):

$$\frac{\partial n}{\partial t} + \frac{\partial}{\partial \zeta}(Gn) = B\varepsilon_c + \left[\frac{-1}{\alpha_1 \tau_5} h_1(\zeta) - \frac{1}{\alpha_4 \tau_5} h_4(\zeta) + \frac{1}{\alpha_6 \tau_5} h_6(\zeta)\right] n(\zeta,t)$$

$$+ \frac{1}{\alpha_o \tau_5} n_o(\zeta) \quad . \qquad (3\text{-}42)$$

This completes the derivation of the balance equations (3-41) and (3-42) of the complex crystallizer. It must be noted that there were no assumptions in the above derivation.

Dynamics and Stability

Most of the stability criteria for crystallizers have been derived by making oversimplifying assumptions in the balance equations because of the mathematical complexity. Previous authors have found it very difficult if not impossible to deal with the size dependence of the birth and

growth functions. For this reason, they often assume that birth occurs at one size and describe this as the "lumped birth function." Moreover, this size (at which birth occurs) is usually taken as the zero size. The criteria derived with these assumptions, therefore, have little or no practical value. In order to carry out a thorough analysis one must use more complete equations such as (3-41) and (3-42) as the basic equations to which stability methods are applied. We shall apply our stability method to equations (3-41a) and (3-42), which are recapitulated below for easy reference. Equation (3-41a) is a slightly modified version of equation (3-41).

$$\frac{dC}{dt} = \frac{C_o}{\varepsilon_c \alpha_o \tau_5} + \frac{C(1+r)}{\varepsilon_c \alpha_2 \tau_5} - \frac{C}{\varepsilon_c}\left(\frac{1}{\alpha_1 \tau_5} + \frac{1}{\tau_5}\right) + \frac{k_v(c-\rho)}{\varepsilon_c \alpha_4 \tau_5}\int_0^\infty n(\zeta,t)\zeta^3 d\zeta$$

$$+ \frac{k_v C}{\varepsilon_c \alpha_o \tau_5}\int_{\zeta_1}^{\zeta_2} n_o(\zeta)\zeta^3 d\zeta - \frac{k_v C}{\zeta_c \tau_5}\int_0^\infty h_5(\zeta) n(\zeta,t)\zeta^3 d\zeta$$

$$- \frac{k_v C}{\varepsilon_c \tau_1}\int_0^\infty h_1(\zeta) n(s,t)\zeta^3 d\zeta \qquad (3\text{-}41a)$$

$$\frac{\partial n}{\partial t} + \frac{\partial}{\partial \zeta}(Gn) = B\varepsilon_c + \left[-\frac{1}{\alpha_1 \tau_5} h_1(\zeta) - \frac{1}{\alpha_4 \tau_5} h_4(\zeta) + \frac{1}{\alpha_6 \tau_5} h_6(\zeta)\right]\frac{n(\zeta,t)}{\tau_5}$$

$$+ \frac{1}{\alpha_o \tau_5} n_o(\zeta) \; . \qquad (3\text{-}42)$$

Equation (3-41a) was obtained by combining equations (3-41) and (3-43).

$$C_2 = (1+r)C \ , \qquad 0 \leq r < 1 \tag{3-43}$$

Because the mass of dissolved fines is usually very small, C_2 is often approximated by C, in which case, r equals zero. However, the form of equation (3-43) above is chosen to allow for conditions under which mass of dissolved fines is not negligible.

The growth and birth functions not only depend on size but also depend on the crystallizer environment as represented by equations (3-44) and (3-45).

$$G = g(c)\phi(\zeta) \tag{3-44}$$

$$B = \sigma(c)b(\zeta) \tag{3-45}$$

where $g(c)$ and $\sigma(c)$ denote the environmental dependence of the growth and birth rates respectively, while $\phi(\zeta)$ and $b(\zeta)$ similarly represent the size dependence. The crystallizer environment has been taken to be the effective concentration that surrounds the various crystals. Incorporating equations (3-44) and (3-45) into equation (3-42) yields the following expression:

$$\frac{\partial n}{\partial t} + g(c)\frac{\partial}{\partial \zeta}(\phi n) = \varepsilon_c \sigma(c)b(\zeta) + \Gamma_1(\zeta)n + \frac{1}{\alpha_o \tau_5} n_o(\zeta) \tag{3-46}$$

where

$$\Gamma_1(\zeta) = \frac{-1}{\alpha_1} h_1(\zeta) - \frac{1}{\alpha_4} h_4(\zeta) + \frac{1}{\alpha_6} h_6(\zeta) \ . \tag{3-47}$$

With the appropriate definitions of Γ_2 and $\Gamma_3(\zeta)$, equation (3-41a) is rewritten as equation (3-48):

$$\frac{dC}{dt} = \frac{C_o}{\varepsilon_c \alpha_o \tau_5} + \frac{C\Gamma_2}{\varepsilon_c \tau_5} + \frac{k_v C}{\varepsilon_c \tau_5} \int_0^\infty \Gamma_3(\zeta) n \zeta^3 d\zeta - \frac{k_v \rho}{\varepsilon_c \alpha_4 \tau_5} \int_0^\infty n \zeta^3 d\zeta$$

$$+ \frac{k_v C}{\varepsilon_c \alpha_o \tau_5} \int_{\zeta_1}^{\zeta_2} n_o(\zeta) \zeta^3 d\zeta \qquad (3\text{-}48)$$

where

$$\Gamma_2 = \frac{1+r}{\alpha_2} - \frac{1}{\alpha_1} - 1 \qquad (3\text{-}49)$$

$$\Gamma_3(\zeta) = \frac{1}{\alpha_4} - h_5(\zeta) - \frac{1}{\alpha_1} h_1(\zeta) \ . \qquad (3\text{-}50)$$

Before applying our stability method equations (3-46) and (3-48) are made dimensionless by defining the following dimensionless variables:

$$y = \frac{c}{\bar{c}} \ ; \quad c^* = \frac{c_o}{\bar{c}} \ ; \quad \theta = \frac{t}{T} \ ; \quad \eta = \frac{n}{\bar{n}} \ ; \quad n_{in}(z) = \frac{n_o(\zeta)}{\bar{n}} \ ;$$

$$v(y) = \frac{g(c)}{\bar{g}} \ ; \quad u(y) = \frac{\sigma(c)}{\bar{\sigma}} \ ; \quad z = \frac{\zeta}{\bar{\zeta}} \ ; \quad W(z) = \frac{\phi(\zeta)}{\bar{\phi}} \ ;$$

$$R(z) = \frac{b(\zeta)}{\bar{b}} \ ; \quad \nu_5 = \frac{\tau_5}{T}$$

where the "bars" denote some reference variables. The variable, T, represents an appropriate reference time. Upon substitution of the above dimensionless variables, equations (3-46) and (3-49) can be transformed into the following equations:

$$\frac{d\eta}{d\theta} + \left[\frac{\bar{g}\bar{\phi}\bar{T}}{\bar{\zeta}}\right] v(y) \frac{d}{dz}(W\eta) = \left[\frac{\bar{b}\bar{\sigma}\bar{T}}{\bar{n}}\right]\varepsilon_c u(y)R(z) + \Gamma_1(\zeta)\frac{\eta}{\nu_5} + \frac{1}{\alpha_o}\frac{n_{in}}{\nu_5} \tag{3-51}$$

$$\frac{dy}{d\theta} = \frac{c^*}{\varepsilon_c\alpha_o\nu_5} + \frac{\Gamma_2 y}{\varepsilon_c\nu_5} + [k_v\bar{n}(\bar{\zeta})^4]\frac{y}{\varepsilon_c\nu_5}\int_0^\infty \Gamma_3(z)\eta z^3 dz - \left[\frac{k_v\rho\bar{n}(\bar{\zeta})^4}{\bar{c}}\right]\frac{1}{\varepsilon_c\alpha_4\nu_5}\int_0^\infty \eta z^3 dz + [k_v\bar{n}(\bar{\zeta})^4]\frac{y}{\varepsilon_c\alpha_o\nu_5}\int_{z_1}^{z_2} n_{in}(z)z^3 dz \; . \tag{3-52}$$

The terms in square brackets in equations (3-51) and (3-52) are dimensionless quantities defined below.

Let

$$a_1 = \frac{\bar{g}\bar{\phi}\bar{T}}{\bar{\zeta}}$$

$$a_2 = \frac{\bar{b}\bar{\sigma}\bar{T}}{\bar{n}}$$

$$a_3 = k_v\bar{n}(\bar{\zeta})^4$$

$$a_4 = \frac{k_v\rho\bar{n}(\bar{\zeta})^4}{\bar{c}} \; .$$

Using the above definitions, equations (3-51) and (3-52) are recasted into equations (3-53) and (3-54) respectively.

$$\frac{d\eta}{d\theta} + a_1 v(y)\frac{d}{dz}(W\eta) = a_2 u(y)R(z) + \Gamma_1(z)\frac{\eta}{\nu_5} + \frac{1}{\alpha_o}\frac{n_{in}}{\nu_5} \tag{3-53}$$

$$\frac{dy}{d\theta} = \frac{c^*}{\varepsilon_c \alpha_o \nu_5} + \frac{\Gamma_2 y}{\varepsilon_c \nu_5} + \frac{a_3 y}{\varepsilon_c \nu_5} \int_0^\infty \Gamma_3(z)\eta z^3 dz - \frac{a_4}{\varepsilon_c \alpha_4 \nu_5} \int_0^\infty \eta z^3 dz$$

$$+ \frac{a_3 y}{\varepsilon_c \alpha_o \nu_5} \int_{z_1}^{z_2} n_{in}(z) z^3 dz \qquad (3\text{-}54)$$

Without loss of generality the a_i's, i = 1,2,3,4, are set equal to one.

$$\frac{d\eta}{d\theta} + v(y) \frac{\partial(w\eta)}{\partial z} = \varepsilon_c u(y) R(z) + \frac{\Gamma_1(z)\eta}{\nu_5} + \frac{1}{\alpha_o \nu_5} n_{in} \qquad (3\text{-}55)$$

$$\frac{dy}{d\theta} = \frac{c^*}{\varepsilon_c \alpha_o \nu_5} + \frac{\Gamma_2}{\varepsilon_c \nu_5} y + \frac{1}{\varepsilon_c \nu_5} y \int_0^\infty \Gamma_3(z)\eta z^3 dz - \frac{1}{\varepsilon_c \alpha_4 \nu_5} \int_0^\infty \eta z^3 dz$$

$$+ \frac{1}{\varepsilon_c \alpha_o \nu_5} y \int_{z_1}^{z_2} n_{in}(z) z^3 dz \ . \qquad (3\text{-}56)$$

The boundary and initial conditions for equations (3-55) and (3-56) are given below:

$$\eta(z,0) = \eta_o(z) \qquad (3\text{-}57)$$

$$y(0) = y_o \qquad (3\text{-}58)$$

$$\lim_{z \to \infty} \eta(z,\theta) = 0 \qquad (3\text{-}59)$$

$$\eta(0,\theta) = 0 \ . \qquad (3\text{-}60)$$

As a reminder, we indicate below the change from the original variables to the dimensionless variables:

$n \rightarrow \eta$	# of particles
$g \rightarrow v$	concentration dependent part of growth rate
$\phi \rightarrow W$	size dependent part of growth rate
$\sigma \rightarrow u$	concentration dependent part of birth rate
$b \rightarrow R$	size dependent part of birth rate
$\zeta \rightarrow z$	particle size
$c \rightarrow y$	supersaturation
$c_o \rightarrow c^*$	inlet concentration
$t \rightarrow \theta$	time
$\tau_5 \rightarrow \nu_5$	residence time

Equations (3-55) through (3-60) constitute the final forms of the crystallizer governing equations to which our stability method will be applied.

We proceed by taking a Taylor's series expansion of some of the quantities in equations (3-55) and (3-56):

$$y(\theta) = y_o + \varepsilon y_1(\theta)$$

$$v(y) = v_o + \varepsilon v_o' y_1(\theta)$$

$$u(y) = u_o + \varepsilon u_o' y_1(\theta)$$

$$\eta(z,\theta) = \eta_o(z) + \varepsilon \eta_1(z,\theta)$$

where $\eta_o(z)$ is a time independent solution and ε is a small parameter. The quantities g_o' and σ_o' are defined below:

$$v_o' = \left.\frac{dv(y)}{dy}\right|_{y=y_o} \tag{3-61}$$

$$u_o' = \left.\frac{du(y)}{dy}\right|_{y=y_o} . \tag{3-62}$$

Upon substitution of the above Taylor expansions into equations (3-55) and (3-56), the following equations result:

$$\frac{\partial}{\partial\theta}(\eta_o+\varepsilon\eta_1) + (v_o+\varepsilon y_1 v_o')\frac{\partial}{\partial z}(W(\eta_o+\varepsilon\eta_1)) = \varepsilon_c R(z)(U_o+\varepsilon y_1 u_o') + \frac{\Gamma_1(z)}{\nu_5}(\eta_o+\varepsilon\eta_1) + \frac{1}{\alpha_o\nu_5} n_{in} \tag{3-63}$$

$$\frac{d}{d\theta}(y_o+\varepsilon y_1) = \frac{c^*}{\varepsilon_c\alpha_o\nu_5} + \frac{\Gamma_2}{\varepsilon_c\nu_5}(y_o+\varepsilon y_1) + \frac{1}{\varepsilon_c\nu_5}(y_o+\varepsilon y_1) \int_0^\infty \Gamma_3(z)(\eta_o+\varepsilon\eta_1)z^3dz - \frac{1}{\varepsilon_c\alpha_4\nu_5}\int_0^\infty(\eta_o+\varepsilon\eta_1)z^3dz + \frac{1}{\varepsilon_c\alpha_o\nu_5}(y_o+\varepsilon y_1)\int_{z_1}^{z_2} n_{in}(z)z^3dz \ . \tag{3-64}$$

Equating coefficients of equal powers of ε on both left and right hand sides of equations (3-63) and (3-64) results in the following equations:

$$v_o\frac{d}{dz}(W\eta_o) = \varepsilon_c R(z)u_o + \frac{\Gamma_1(z)}{\nu_5}\eta_o + \frac{1}{\alpha_o\nu_5} n_{in} \tag{3-65}$$

$$0 = \frac{c^*}{\varepsilon_c\alpha_o\nu_5} + \frac{\Gamma_2}{\varepsilon_c\nu_5} y_o + \frac{1}{\varepsilon_c\nu_5} y_o\int_0^\infty \Gamma_3(z)\eta_o z^3dz - \frac{1}{\varepsilon_c\alpha_4\nu_5}\int_0^\infty \eta_o z^3dz + \frac{1}{\varepsilon_c\alpha_o\nu_5} y_o\int_{z_1}^{z_2} n_{in}(z)z^3dz \tag{3-66}$$

$$\frac{\partial}{\partial\theta}\eta_1 + v_o\frac{\partial}{\partial z}(W\eta_1) + y_1 v_o\frac{d}{dz}(W\eta_o) = \varepsilon_c u_o' y_1 R(z) + \frac{\Gamma_1(z)}{\nu_5}\eta_1 \tag{3-67}$$

$$\frac{dy_1}{d\theta} = \frac{\Gamma_2 y_1}{\varepsilon_c \nu_5} + \frac{1}{\varepsilon_c \nu_5} \int_0^\infty \Gamma_3(z)(y_1\eta_o + y_o\eta_1)z^3 dz = \frac{1}{\varepsilon_c \alpha_4 \nu_5} \int_0^\infty \eta_1 z^3 dz$$

$$+ \frac{1}{\varepsilon_c \alpha_o \nu_5} \int_{z_1}^{z_2} n_{in}(z) z^3 dz \ . \qquad (3\text{-}68)$$

Rewriting equations (3-65) and (3-66) one obtains

$$\frac{d\eta_o}{dz} + h(z)\eta_o = \frac{\varepsilon_c R(z) u_o}{v_o W} + \frac{1}{\alpha_o \nu_5 v_o W} n_{in} \qquad (3\text{-}65a)$$

where

$$h(z) = \left(\frac{1}{W}\frac{dW}{dz} - \frac{\Gamma_1}{\nu_5 v_o W}\right)$$

$$y_o = \left(\frac{1}{\varepsilon_c \alpha_o \nu_5} \int_0^\infty \eta_o z^3 dz - \frac{c^*}{\varepsilon_c \alpha_o \nu_5}\right) \Big/ \left(\frac{\Gamma_2}{\varepsilon_c \nu_5} + \frac{1}{\varepsilon_c \nu_5} \int_0^\infty \Gamma_3(z)\eta_o z^3 dz\right.$$

$$\left. + \frac{1}{\varepsilon_c \alpha_o \nu_5} \int_{z_1}^{z_2} n_{in}(z) z^3 dz\right) . \qquad (3\text{-}66a)$$

It should be observed that y_o is simply a constant. The solution to equation (3-65a) is given by

$$\eta_o(z) = e^{-[F(z)-F(z_o)]} \eta_o(z_o) + e^{-F(z)} \int_{z_o}^{z} e^{-F(x)} \left[\frac{\varepsilon_c u_o R(x)}{v_o W}\right.$$

$$\left. + \frac{1}{\alpha_o \nu_5 v_o W} n_{in}(x)\right] dx \qquad (3\text{-}69)$$

where

$$F(z) = \int^{z} h(x)dx .$$

By choosing z_o equal to zero, equation (3-67) reduces to equation (3-69):

$$\eta_o(z) = e^{-F(z)} J(z) \qquad (3\text{-}69a)$$

where

$$J(z) = \int_0^z e^{-F(x)} \left[\frac{\varepsilon_c u_o R(x)}{v_o W} + \frac{1}{\alpha_o \nu_5 W} n_{in}(x)\right] dx.$$

Equations (3-66a) and (3-69a) constitute the pair of time independent solutions, (η_o, y_o).

Considering equations (3-67) and (3-68) we make the following substitutions to obtain equations (3-70) and (3-71),

$$\eta_1(z,\theta) = N(z)e^{-\lambda\theta}$$

$$y_1(\theta) = m_o e^{-\lambda\theta}$$

$$\frac{d}{d\theta}\left(N(z)e^{-\lambda\theta}\right) + v_o \frac{d}{dz}\left(WN(z)e^{-\lambda\theta}\right) + m_o e^{-\lambda\theta} v_o' \frac{d}{dz}\left(W\eta_o\right)$$
$$= \varepsilon_c u_o' m_o e^{-\lambda\theta} R(z) + \frac{\Gamma_1(z)}{\nu_5} N(z)e^{-\lambda\theta} \qquad (3\text{-}70)$$

$$\frac{d}{d\theta}\left(m_o e^{-\lambda\theta}\right) = \frac{\Gamma_2}{\varepsilon_c \nu_5} m_o e^{-\lambda\theta} + \frac{1}{\varepsilon_c \nu_5} \int_0^\infty \Gamma_3(z)[m_o\eta_o + y_o N(z)]e^{-\lambda\theta} z^3 dz$$
$$- \frac{1}{\varepsilon_c \alpha_4 \nu_5} \int_0^\infty N(z)e^{-\lambda\theta} z^3 dz + \frac{1}{\varepsilon_c \alpha_o \nu_5} m_{oe}^{-\lambda\theta}$$
$$\cdot \int_{z_1}^{z_2} n_{in}(z) z^3 dz. \qquad (3\text{-}71)$$

Equation (3-71) reduces to equation (3-72):

$$m_o = \frac{\frac{1}{\varepsilon_c \alpha_4 \nu_5} \int_0^\infty N(z) z^3 dz - \frac{1}{\varepsilon_c \nu_5} \int_0^\infty \Gamma_3(z) y_o N(z) z^3 dz}{\frac{\Gamma_2}{\varepsilon_c \nu_5} + \frac{1}{\varepsilon_c \nu_5} \int_0^\infty \Gamma_3(z) \eta_o z^3 dz + \frac{1}{\varepsilon_c \alpha_o \nu_5} \int_{z_1}^{z_2} n_{in}(z) z^3 dz} . \tag{3-72}$$

Substitution of equation (3-72) into (3-70) results in the following equation:

$$-\left(\lambda + \frac{\Gamma_1}{\nu_5}\right) N(z) + v_o \frac{d}{dz} (WN(z)) = \left[\frac{1}{\varepsilon_c \alpha_4 \nu_5} \int_0^\infty N(z) z^3 dz - \frac{1}{\varepsilon_c \nu_5} \int_0^\infty \Gamma_3(z) y_o N(z) z^3 dz\right] \frac{\Omega(z)}{(\lambda + Q^*)} \tag{3-73}$$

where

$$\Omega(z) = \varepsilon_c u_o' R(z) - v_o' \frac{d}{dz} (W\eta_o) \tag{3-74}$$

$$Q^* = \frac{\Gamma_2}{\varepsilon_c \nu_5} + \frac{1}{\varepsilon_c \nu_5} \int_0^\infty \Gamma_3(z) \eta_o z^3 dz + \frac{1}{\varepsilon_c \alpha_o \nu_5} \int_{z_1}^{z_2} n_{in}(z) z^3 dz . \tag{3-75}$$

Upon rearranging equation (3-73) one obtains equation

$$-\left[\lambda^2 + \lambda \frac{\Gamma_1}{\nu_5} + Q^*\right] + \frac{\Gamma_1}{\nu_5} Q^* N(z) + \lambda v_o \frac{d}{dz} (WN(z)) + Q^* v_o \frac{d}{dz} (WN(z)) = \left[\frac{1}{\varepsilon_c \alpha_4 \nu_5} \int_0^\infty N(z) z^3 dz - \frac{1}{\varepsilon_c \nu_5} \int_0^\infty \Gamma_3(z) y_o N(z) z^3 dz\right] \Omega(z). \tag{3-76}$$

Since any piecewise continuous function with finite left and right hand limits and with a square integrable first derivative may be expanded in terms of a complete set of functions, and since N(z) satisfies these restrictions, we choose to expand N(z) as in equation (3-77):

$$N(z) = \sum_{n=0}^{\infty} A_n f_n(z) \tag{3-77}$$

where $f_n(z)$ is a member of a complete and orthonomal set of functions. Combining equations (3-76) and (3-77) one obtains equation (3-78):

$$-\left[\lambda^2 + \lambda\left(\frac{\Gamma_1}{\nu_5} + Q^*\right) + \frac{\Gamma_1}{\nu_5} Q^*\right] \sum_{n=0}^{\infty} A_n f_n(z) + \lambda v_o \frac{d}{dz}\left(W \sum_{n=0}^{\infty} A_n f_n(z)\right)$$

$$+ Q^* v_o \frac{d}{dz}\left(W \sum_{n=0}^{\infty} A_n f_n(z)\right) = \left[\frac{1}{\varepsilon_c \alpha_4 \nu_5} \int_0^{\infty} \left(\sum_{n=0}^{\infty} A_n f_n(z)\right) z^3 dz\right.$$

$$\left. - \frac{1}{\varepsilon_c \nu_5} \int_0^{\infty} \Gamma_3(z) y_o\left(\sum A_n f_n(z)\right) z^3 dz\right] \Omega(z) \; . \tag{3-78}$$

Multiplying equation (3-78) by $f_m(z)$, integrating with respect to z from zero to infinity, and applying orthogonality principle, one obtains equation (3-79) after a slight algebraic manipulation.

$$-(\lambda^2 + \lambda Q^*)A_m - (\lambda+Q^*)\frac{1}{\nu_5}\sum_{n=0}^{\infty} A_n \alpha_{mn} + (\lambda+Q^*)v_o\sum_{n=0}^{\infty} A_n \beta_{mn}$$

$$- \frac{1}{\varepsilon_c \alpha_4 \nu_5}\delta_m \sum_{n=0}^{\infty} A_n \gamma_n + \frac{y_o}{\varepsilon_c \nu_5}\delta_m \sum_{n=0}^{\infty} A_n \chi_n = 0 \qquad (3\text{-}79)$$

where

$$\alpha_{mn} = \int_0^{\infty} \Gamma_1(z) f_n(z) f_m(z) dz$$

$$\beta_{mn} = \int_0^{\infty} (W'(z) f_n(z) + f_n'(z) W(z)) f_m(z) dz$$

$$\delta_m = \int_0^{\infty} f_m \, \Omega(z) dz$$

$$\gamma_n = \int_0^{\infty} f_n(z) z^3 dz$$

$$\chi_n = \int_0^{\infty} \Gamma_3(z) f_n(z) z^3 dz \; .$$

It should be noted that stability is guaranteed when the real part of λ is positive and the system is said to be asymptotically stable even if the imaginary part of λ is nonzero. A nonzero imaginary part of λ gives rise to an oscillatory system which may or may not be damped.

The expression represented by equation (3-79) is an infinite dimensional system for the A_n's and is representable in matrix form by

$$M\vec{A} = \vec{0} \ , \tag{3-80}$$

where M represents the matrix of coefficients, and $\vec{A}$ denotes a vector of A_n's. Obviously for nontriavial A_n's the determinant of M must be zero, that is,

$$\det M = 0 \ . \tag{3-81}$$

For a finite dimensional matrix, M equation (3-81) becomes the characteristic equation which is a polynomial equation in λ, and of the form,

$$a_n\lambda^n + a_{n-1}\lambda^{n-1} + \ldots + a_o = 0. \tag{3-82}$$

Suppose $A_o \neq 0$, then the resulting characteristic equation is a quadratic in λ and is denoted below by the a_n's.

$$a_2 = 1 \tag{3-83}$$

$$a_1 = Q^* + \alpha_{oo}/\nu_5 - v_o\beta_{oo} \tag{3-84}$$

$$a_o = \frac{Q^*}{\nu_5}(\alpha_{oo} - \nu_5 v_o \beta_{oo}) + \delta_o \frac{(\gamma_o - \alpha_4 y_o \chi_o)}{\varepsilon_c \alpha_4 \nu_5} \tag{3-85}$$

For A_o, $A_1 \neq 0$, the resulting fourth order polynomial equation is similarly denoted below.

$$a_4 = 1 \tag{3-86}$$

$$a_3 = 2Q^* + \psi_{oo} + \psi_{11} \tag{3-87}$$

$$a_2 = Q^* + 2Q^*(\psi_{oo} + \psi_{11}) + \Lambda_{oo} + \Lambda_{11} + \psi_{oo}\psi_{11} - \psi_{01}\psi_{10} \tag{3-88}$$

$$a_1 = Q^{*2}(\psi_{oo}+\psi_{11}) + Q^*(\Lambda_{oo}+\Lambda_{11}) + 2Q^*(\psi_{oo}\psi_{11}-\psi_{01}\psi_{10}) + \psi_{11}\Lambda_{oo} + \psi_{oo}\Lambda_{11} - \psi_{01}\Lambda_{10} - \psi_{10}\Lambda_{01} \quad (3\text{-}89)$$

$$a_o = Q^{*2}(\psi_{oo}\psi_{11}-\psi_{01}\psi_{10}) + Q^*(\psi_{11}\Lambda_{oo}+\psi_{oo}\Lambda_{11}-\psi_{01}\Lambda_{10}-\psi_{10}\Lambda_{01}) + \Lambda_{oo}\Lambda_{11} - \Lambda_{01}\Lambda_{10} \quad (3\text{-}90)$$

where

$$\psi_{mn} = \frac{\alpha_{mn}}{\nu_5} - v_o\beta_{mn}$$

$$\Lambda_{mn} = \delta_m P_n$$

$$P_n = (\gamma_n-\alpha_4 y_o\chi_n)/(\varepsilon_c\alpha_4\nu_5)$$

$$\delta_m = u_o'I_m - v_o'L_m$$

$$I_m = \varepsilon_c \int_0^\infty f_m R(z)dz$$

$$L_m = \int_0^\infty f_m(z)\,\frac{d}{dz}[\eta_o(z)W(z)]dz\,.$$

For stability purposes, the quadratic equation usually suffices. However, one can also utilize the quartic equation, which will show similar behavior as does the quadratic, since higher and lower order characteristic equations show similar trends with regard to stability.

By judiciously choosing $f_m(z)$ to closely resemble $N(z)$ and by satisfying the boundary conditions of the system, the similarity behavior mentioned above is made even better. Applying Routh-Hurwitz criterion to the polynomial equation (3-82) reveals that, in general, a necessary condition for stability is for the a_n's to have alternating signs. An additional equation relating the various a_n's is usually required to obtain a sufficiency condition. However, for the quadratic case, the alternating signs are both a necessary and sufficient condition. Illustrating this for the quadratic case, one obtains $a_2>0$, $a_1<0$, $a_o>0$. Since equation (3-82) is in such a form that $a_n=1$ always, a_n is therefore always positive. The stability criteria for the quadratic case are

$$a_2 = 1>0 \tag{3-83a}$$

$$a_1 = [Q^* + \alpha_{oo}/\nu_5 - v_o\beta_{oo}] < 0 \tag{3-84a}$$

$$a_o = \left[\frac{Q^*}{\nu_5}(\alpha_{oo}-\nu_5 v_o\beta_{oo}) + \delta_o \frac{(\gamma_o-\alpha_4 y_o\chi_o)}{\varepsilon_c\alpha_4\nu_5}\right] > 0. \tag{3-85a}$$

Similarly for the quartic case the stability criteria are given by

$$a_4 > 0 \tag{3-86a}$$

$$a_3 < 0 \tag{3-87a}$$

$$a_2 > 0 \tag{3-88a}$$

$$a_1 < 0 \tag{3-89a}$$

$$a_o > 0 \tag{3-90a}$$

$$-a_1(-a_3a_2+a_1) - a_3^2a_o > 0 \ . \tag{3-99}$$

It should be noted, however, that embedded in the a_n's are all the parameters of the complex crystallizer. As a result the effects of the parameters on the stability of the crystallizer can be monitored efficiently. It is possible that for some of the parameters, the effects are reflective of the degree of positivity or negativity of the expressions in the stability criteria. In other words, if an increasing value of such a parameter shows an increasing stabilizing trend on the system, this effect will be reflected by a corresponding increase in the positivity or negativity of the expressions. A better way to monitor the stabilizing or destabilizing effect of a parameter is to apply the Root-Locus method directly to the characteristic polynomial equation (3-82).

The usual data available in the literature are not suitable for a stability analysis such as that described above. In addition to the time dependent number-size distribution, one needs to obtain the growth and birth functions in the separable forms shown in equation (3-44) and (3-45).

$$G = g(c)\phi(\zeta) \tag{3-44}$$

$$B = \sigma(c)b(\zeta). \tag{3-45}$$

How one might obtain these separable functions is discussed in the appendix. It should be noted that the above method of analysis does not presume the existence of nucleation models. Instead it requires that the analyst experimentally determine b(c) and g(c). It accommodates the total size dependent functions $\phi(\zeta)$ and $b(\zeta)$ and the complex crystallizer operating parameters. The only assumption is that, like its predecessors, it approximates g(c) and b(c) up to first order in concentration, c. Therefore, in comparison with others, this method is more thorough and is based on very practical considerations. This ends the discussion of our stability analysis. In Chapter IV we devise example data that closely approximate reality to illustrate how to utilize this method. Before proceeding to Chapter IV some discussion about nucleation models is appropriate inasmuch as these models form an integral part of other stability methods.

Nucleation Models

The three main nucleation models that have been used extensively are the (i) Volmer's model, (ii) Mier's model, and (iii) power-law model.

(i) The Volmer's model, based on thermodynamic considerations, has an Arrehenius type of concentration dependence as evidenced by equation (1-3) which is recapitulated below for easy reference:

$$B(c) = K_2 \exp(-K_3/(\ell_n c/c_s)^2) \quad . \qquad (1\text{-}3)$$

The concentration dependent part of the birth function, B(c) represented by equation (1-3), decreases to zero exponentially as the concentration decreases. In general, the birth function depends both on particle size as well as the environment which is represented by concentration. Oftentimes researchers would simply ignore the size dependence and represent the complete birth function by B(c). Volmer's model was based on clear solution and should, therefore, apply only to homogeneous nucleation. To this effect Sherwin et al. (1967) mentioned that the use of such a model in the design of continuous crystallizers might seem questionable. However, they used the same model in their study entitled "Dynamic Behavior of the Well-Mixed Isothermal Crystallizer" because they felt that in a bed of large amounts of crystals the dependence of nucleation on total crystal surface is small compared to the nonlinear dependence on saturation. To support the use of the model they cited the work of Rumford and Bain (1960) who claimed the dependence of nucleation on supersaturation in a bed of large crystals of sodium

chloride was similar to that of homogeneous nucleation, Rumford and Bain found the lower metastable concentration, c_m, for sodium chloride system to be 1.5 gm/liter. The metastable concentration, c_m, is that higher than the saturation concentration, c_s, and below which all secondary nucleation ceases but above which nucleation increases rapidly. Another verion of equation (1-3) often used consists of a one-term Taylor series expansion of $\ell n(c/c_s)$ and is represented by equation (3-92):

$$B(c) = K_2 \exp(-K_3/(c/cs-1)^2) \quad . \tag{3-92}$$

The above equation assumes (c/c_s-1) is small.

(ii) Mier's metastable model is represented by equation (3-93):

$$B(c) = \begin{cases} K_n(c-c_m)^P, & c>c_m \\ 0 & c\leq c_m \end{cases} \quad . \tag{3-93}$$

Mier's model shows the same discontinuity as Volmer's model. Beckman (1976) claimed that both models are qualitatively the same for small deviations about c_m, that both are valid for the lower metastable region and that Mier's model is essentially a one-term Taylor expansion of Volmer's model. It would be interesting to see some justification for this claim.

(iii) The power-law model was obtained when Randolph and Larson (1962) approximated c_m by c_s in equation (3-93),

thereby obtaining equation (3-94), by virtue of which B can be expressed as a function of G defined in equation (2-13) .

$$B = K_n(c-c_s)^P \tag{3-94}$$

$$G = K_1(c-c_s) \tag{2-13}$$

Combining equations (3-94) and (2-13), one obtains equation (3-95):

$$B(G) = K_N G^P = k_c(c-c_s)^P \ . \tag{3-95}$$

In support of the power law model, they argued that c_m is very close to c_s for most inorganic systems. On the contrary, however, Rumford and Bain (1960) argued that the approximation, that (c_m-c_s) is very small compared to $(c-c_s)$ might be valid only for precipitation of insoluble compounds but hardly for crystallizers which, in most cases, operate close to the metastable range. Equation (3- 95) thus leads to a significant simplification of the mathematics that would be involved in any analysis involving B and G.

Another version of the power law model is represented by equation (3-96) in which M_T denotes the suspension density,

$$B(c) = K_c(c-c_s)^P \ M_T^j = K_c' G^P M_T^j \ . \tag{3-96}$$

The incorporation of M_T accounts for the fact that nucleation is by secondary mechanism. Unlike Mier's model and Volmer's model, the power-law model is nicely behaved and does not possess any discontinuity.

Researchers often use these models in defining steady state dimensionless parameters, b* and g* used in stability analysis. The quantities b* and g* are defined essentially to be the steady state first derivatives with respect to concentration of the birth and growth rates with appropriate dimensionalizing quantities as follows:

$$b^* = \frac{(c_o-\bar{c})}{\bar{B}} \frac{dB(c)}{dc}\Big|_{\bar{c}} \tag{3-97}$$

$$g^* = \frac{(c_o-\bar{c})}{\bar{G}} \frac{dG(c)}{dc}\Big|_{\bar{c}} . \tag{3-98}$$

Hence b*/g* is defined by equation (2-12) :

$$b^*/g = \frac{\bar{G} \frac{dB(c)}{dc}|_{\bar{c}}}{\bar{B} \frac{dG(c)}{dc}|_{\bar{c}}} = i . \tag{2-12}$$

The quantity, c_o, is inlet concentration as defined earlier. However, any other appropriate concentration parameter could be used in place of c_o. The quantities, b*/g*, for the various models are represented by the expressions below.

Volmer's model (second version):

$$b^*/g^* = \frac{2k_3}{\left(\frac{\bar{c}}{c_s} - 1\right)^2} = i \qquad (2\text{-}14)$$

Mier's model:

$$b^*/g^* = P \frac{(\bar{c}-c_s)}{(\bar{c}-c_m)}, \qquad c>c_m \qquad (3\text{-}99)$$

Power-law model (both versions):

$$b^*/g^* = P = \frac{d\ell n\ B(c)\big|_{\bar{c}}}{d\ell n\ G(c)\big|_{\bar{c}}} . \qquad (3\text{-}100)$$

Randolph and Larson (1971) indicated that a value of 21 for the nucleation to growth sensitivity parameter, i, would represent such an extreme kinetic order causing discontinuity in nucleation rate, that the corresponding higher concentration could be described as an upper metastable threshold of homogeneous nucleation. Such a value has never been observed in most kinetic studies. Of the three nucleation models above Beckman (1976) claimed that the power-law model is the most versatile inasmuch as it is the only model good for both class I and class II systems. However, attempts by Song and Douglas (1975) to explain their cyclic data with this model failed, thus contradicting Beckman's claim. They were able to explain

the same data with Volmer's model by using long retention times thereby approaching very low supersaturations. Similarly Lei et al. (1971a) claimed that Mier's model is capable of approximating the behavior of crystallizers with fine traps with either low or high b*/g* values.

A look at the above models reveals some striking differences in the expressions for b*/g* as we let $\bar{c}$ approach c_s.

Volmer's model (second version): $\lim_{\bar{c}\to c_s} b^*/g^* \to \infty$ (3-101)

Mier's model: $\lim_{\bar{c}\to c_s} b^*/g^* = 0$ (3-102)

Power-law model (both versions): $\lim_{\bar{c}\to c_s} b^*/g^* = P.$ (3-103)

The resulting b*/g* values show inconsistencies and hence the models are not equivalent for all crystallizer conditions. Researchers usually show the region of stability on the graphs of the steady state parameters, g* and b*/g*. Yu and Douglas (1975) showed plots with g* and b*/g* taking values in the intervals $(0,\infty)$ and $(11,\infty)$ respectively. In practice, of course, one operates at one fixed point (g*, b*/g*) which one hopes is in the stable region. Because the parameters, g* and b*/g*, in theory, can only be controlled inferentially and cannot easily be set to some desired values, especially via the models discussed above,

their usefulness as stability parameters is very limited. As a result of the inconsistencies arising in b*/g* for the various models, it is not surprising that one model can explain cyclic data while another cannot. It would be useful to establish stability criteria which depend on more readily accessible parameters. In addition, there are some algebraic errors in the derivations of the stability equations in the studies by Sherwin et al. (1967) and Yu and Douglas (1975) which might invalidate their results.

CHAPTER IV
RESULTS

Steady State Determination of Growth and Birth Functions

One of the purposes of this study is to devise a method for accurately quantifying growth and birth rates in a steady state crystallizer. This method developed in the first section of Chapter III will be illustrated with data taken from the literature. Kambaty and Larson (1978) showed plots of particle number size distribution for magnesium sulphate heptahydrate ($MgSO_4 \cdot 7H_2O$) crystals as depicted in figures 9 and 10 . Some of the plots were for nuclei generation from the faces or the edges of the crystals, while other plots were for different impurity concentration, equivalent to different solute concentration. In all these plots nuclei generation was by contact. Repetitive contacting was carried out for an interval of approximately ten residence times after reaching steady state and sampling was done at one residence time intervals (one residence time is 9 minutes). The size distribution of the various samples was measured with a model TA II Coulter Counter. The concentration of each experimental run was fixed. Since the purpose of this study is simply to use these data in exemplifying the

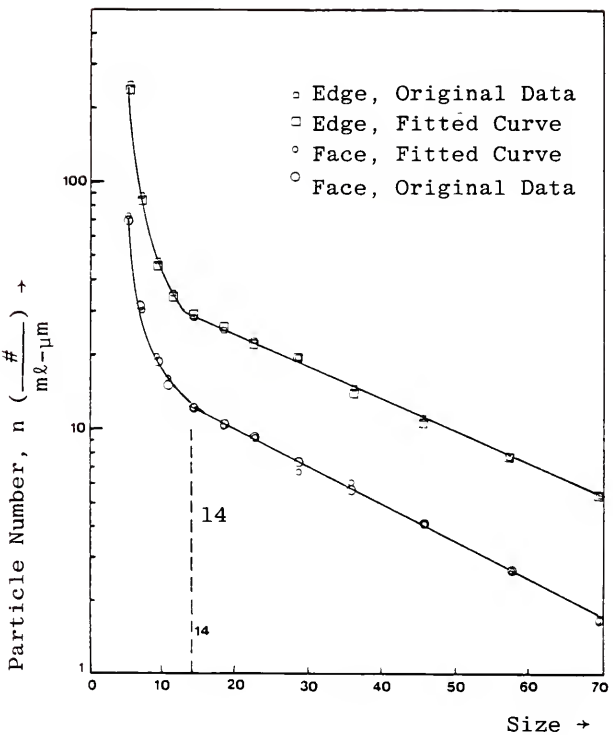

Figure 9. Experimental and Fitted Curves for Particle Number Versus Size for Both Edge and Face of Magnesium Sulfate.

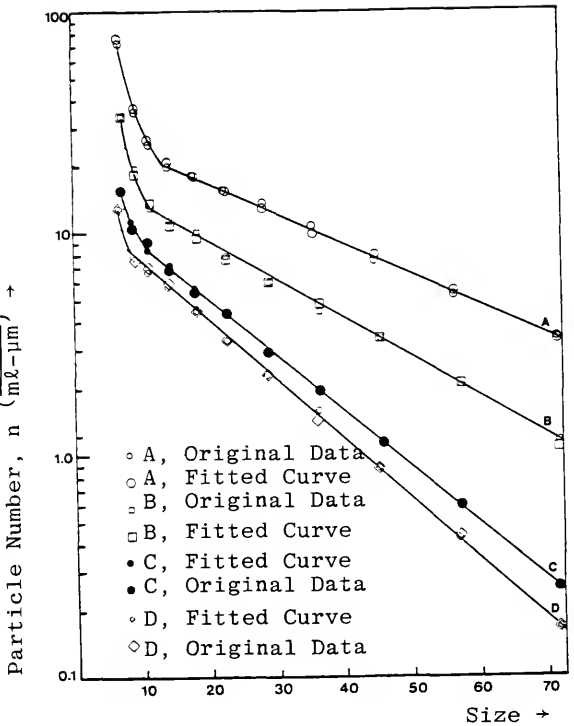

Figure 10. Experimental and Fitted Curves for Crystal Size Distribution for Magnesium Sulfate at Four Different Concentrations. A,B,C,D Have Concentration in Descending Order of Magnitude.

Table 1

Data for Plot E in Figure 10
C_1=5407.625 C_2=0.6569098
γ_1=45.79739 γ_2=0.03146495

Size	Original Data	Fitted Date
5.0	0.250000E 03	0.241687E 03
7.0	0.850000E 02	0.911892E 02
10.0	0.470000E 02	0.410214E 02
11.5	0.350000E 02	0.347251E 02
14.0	0.280000E 02	0.300283E 02
18.0	0.250000E 02	0.260334E 02
22.5	0.230000E 02	0.225640E 02
27.8	0.190000E 02	0.190965E 02
36.5	0.150000E 02	0.145233E 02
45.0	0.115000E 02	0.111151E 02
57.0	0.750000E 01	0.761961E 01
70.0	0.500000E 01	0.506159E 01

Data for Plot F in Figure 10
C_1=890.0442 C_2=0.5652139
γ_1=20.33548 γ_2=0.03509961

5.0	0.735000E 02	0.697932E 02
7.0	0.300000E 02	0.329321E 02
10.0	0.185000E 02	0.174400E 02
11.5	0.169500E 02	0.149199E 02
14.0	0.129000E 02	0.127664E 02
18.0	0.105000E 02	0.108451E 02
22.5	0.940000E 01	0.923421E 01
27.8	0.664000E 01	0.766462E 01
36.5	0.600000E 01	0.564760E 01
45.0	0.422000E 01	0.419077E 01
57.0	0.277000E 01	0.275024E 01
70.0	0.177000E 01	0.174263E 01

Table 2

Data for Plot A in Figure 11
C_1=26044.52 C_2=0.8731303
γ_1=34.03978 γ_2=0.03112719

Size	Original Data	Fitted Data
7.2	0.750000E 02	0.756792E 02
9.2	0.370000E 02	0.340184E 02
10.09	0.265000E 02	0.287520E 02
14.2	0.214300E 02	0.219863E 02
18.3	0.191700E 02	0.192605E 02
23.3	0.166700E 02	0.164820E 02
28.8	0.150000E 02	0.138886E 02
36.2	0.118500E 02	0.110312E 02
44.4	0.800000E 01	0.854617E 01
56.8	0.567000E 01	0.580956E 01
71.7	0.370000E 01	0.365359E 01

Data for Plot B in Figure 11
C_1=5378.973 C_2=0.7708762
γ_1=19.04890 γ_2=0.03808283

7.2	0.350000E 02	0.353847E 02
9.2	0.200000E 02	0.178923E 02
10.09	0.137500E 02	0.152241E 02
14.2	0.118800E 02	0.111869E 02
18.3	0.106000E 02	0.949264E 01
23.3	0.800000E 01	0.784354E 01
28.8	0.625000E 01	0.636124E 01
36.2	0.413000E 01	0.479902E 01
44.4	0.350000E 01	0.351181E 01
56.8	0.229000E 01	0.219001E 01
71.7	0.129000E 01	0.124169E 01

Table 3

Data for Plot C in Figure 11
C_1=1621.810 C_2=0.7644494
γ_1=15.34124 γ_2=0.05621562

Size	Original Data	Fitted Data
7.2	0.166700E 02	0.168360E 02
9.2	0.118800E 02	0.105774E 02
10.09	0.850000E 01	0.942475E 01
14.2	0.700000E 01	0.693656E 01
18.3	0.567000E 01	0.548517E 01
23.3	0.413000E 01	0.414013E 01
28.8	0.300000E 01	0.303902E 01
36.2	0.200000E 01	0.200479E 01
44.4	0.129000E 01	0.129437E 01
56.8	0.330000E 00	0.329706E 00
71.7	0.270000E 00	0.272500E 00

Data for Plot D in Figure 11
C_1=6608237. C_2=1.955293
γ_1=13.46922 γ_2=0.06041371

7.2	0.138000E 02	0.138004E 02
9.2	0.800000E 01	0.782786E 01
10.09	0.680000E 01	0.733949E 01
14.2	0.583000E 01	0.571179E 01
18.3	0.430000E 01	0.445860E 01
23.3	0.336000E 01	0.329619E 01
28.8	0.236000E 01	0.236432E 01
36.2	0.174000E 01	0.151200E 01
44.4	0.930000E 00	0.901307E 00
56.8	0.430000E 00	0.435574E 00
71.7	0.170000E 00	0.177062E 00

method described in Chapter III, we shall not concern ourselves any further with minute details of the experiment.

The data were first fitted with equation (3-9),

$$n(\zeta) = c_1 \exp(-\gamma_1 \zeta) + c_2 \exp(-\gamma_2 \zeta) \qquad (3\text{-}9)$$

and the constants c_1, c_2, γ_1 and γ_2 for each plot are shown in tables 1, 2, and 3. Neither the nonlinear regression routine, nlin, described in Helwing and Council (1979) in the Statistical Analysis System (SAS) User's Guide 1979 edition nor the ZxSSQ, a nonlinear regression routine of the International Mathematical and Statistical Libraries (IMSL) gave good fit, the former being the worse. These two routines were discarded and a subroutine, Simple, developed by Doctor Bob Coldwell of the Physics Department, University of Florida, was used. The listing for the subroutine Simple, a geometric search method, which is slow but gives good fit is included in the appendix as part of one of the programs used in this study. Computer programs utilizing the simple subroutine were run interactively on the McGill University System for Interactive Computing (music-mvs) available to University of Florida students at no cost. Because it was free of charge, and is good, the Fortran coded subroutine Simple was used for almost all the nonlinear regression analyses of this study. The fits were good as evident from both figures 9 and 10 and tables 1, 2 and 3. For most of the fits the estimated uncertainty in the data is less than 10% to within a confidence level of 0.90. Each fit was then used

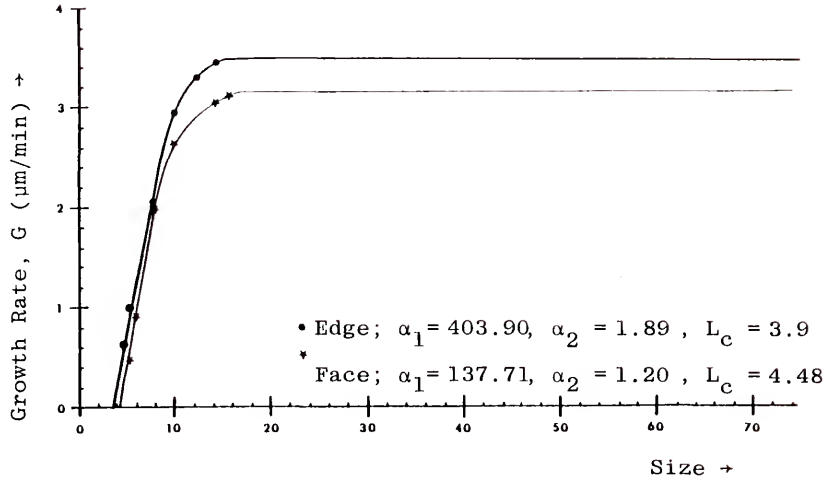

Figure 11. Growth Rate Versus Size for Magnesium Sulphate.

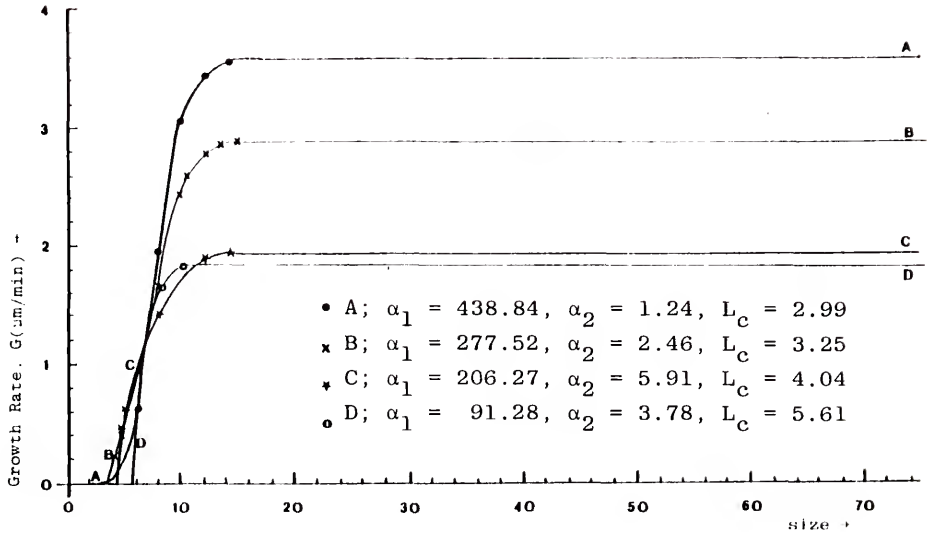

Figure 12. Plot of Growth Rate Versus Size for Various Concentrations. A,B,C,D have concentrations in descending order of magnitude.

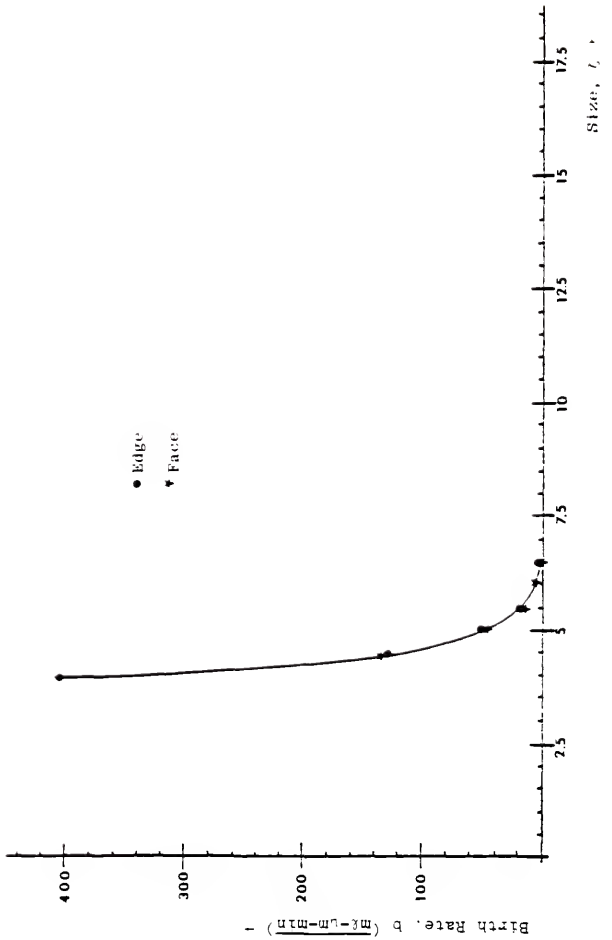

Figure 13. Plot of Birth Rate Versus Size.

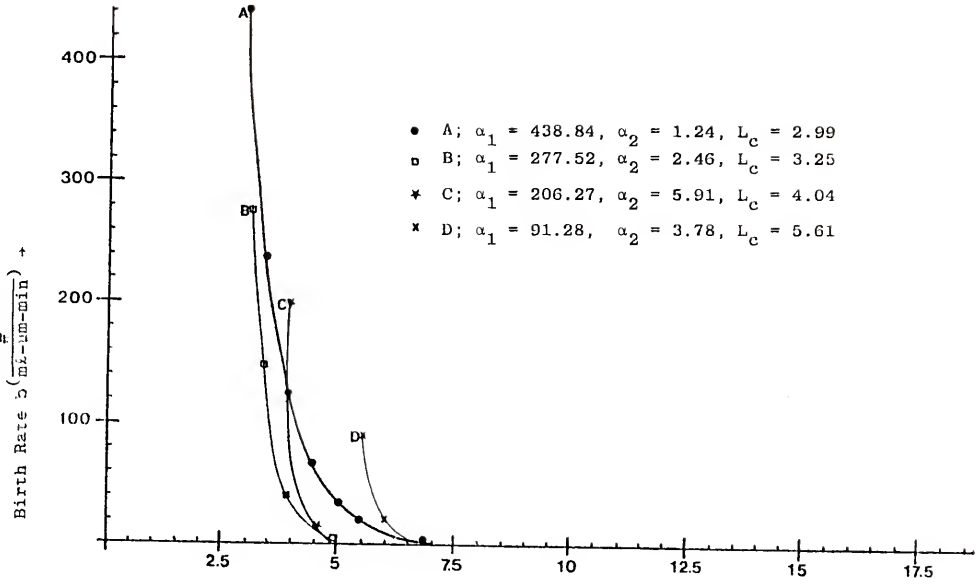

Figure 14. Plot of Birth Rate Versus Size for Various Concentrations; A, B, C, D Have Concentrations in Descending Order of Magnitude.

to generate more values, $n(\zeta_i)$ via equation 3-11 within the interval I_2 which constitutes the straight line portion of each plot of figures 9 and 10, and in which $G(\zeta_i)$ is constant. Thus several values (over 130) of F_i for each plot were generated:

$$F_i = G(\zeta_i)n(\zeta_i) \ , \qquad i = 1,2,\ldots,n \tag{3-11}$$

The unknown parameters α_1, α_2, and L_c were then obtained by minimizing the percent error sum of squares, s, defined by equation (3-13):

$$S = \sum_{i=1}^{N} [(F_i - F_{A1})/F_i]^2 \tag{3-13}$$

where F_{A1} is defined by equation (3-12). This approach constitutes the second version of the minimization procedure. The chi-square error obtained from minimizing over α_1, α_2, and L_c for each fit was much smaller than the corresponding error in the fit expressed by equation (3-9), and lay in the interval $(10^{-2}, 10^{-4})$. The functions $b(\zeta)$ and $G(\zeta)$ were calculated from equations (3-8) and (3-10) and plotted for each set of data in figures 11 through 14. The uncertainty in the value of $G(\zeta)$ and $b(\zeta)$ for most of the different data is less than 10% to within a confidence level of 0.90. Both the error analyses pertaining to the determination of the uncertainty in $G(\zeta)$ and $b(\zeta)$ and those pertaining to the data are included in the appendix. This concludes the quantification of growth and birth rates in a steady state crystallizer.

Unsteady State Determination of Growth and Birth Functions

Another purpose of the study is to device a method for accurately quantifying growth and birth functions in an unsteady state crystallizer. This method developed in a general sense in the second section of Chapter III will be exemplified with literature data. The illustration about to be described is for a batch crystallizer and hence the two terms n_i/τ_i and n/τ in equation (3-14) vanish. As a result equation (3-14) becomes

$$\frac{\partial}{\partial t} n(\zeta,t) + \frac{\partial}{\partial \zeta} [G(\zeta)n(\zeta,t)] = b(\zeta) \ . \qquad (4-1)$$

Transient data were very scanty and the little available in the literature were not suitable because of the conditions under which they were taken. They were taken under conditions of step input in flow rate or some other disturbance to the crystallizer. The only data, though extremely small but suitable for illustrative purposes, were that of P.D.B. Bujac (1976) of ICI Corporate Laboratory, Cheshire, England. The data reported by Bujac were for commercial grade pentaerythritol (PE) crystals. This particular substance is of interest inasmuch as published data on secondary nucleation for organic substances are almost nonexistent.

The experimental work of Bujac involved preparation of pentaerythritol seed crystals by washing with 8% aqueous PE solution to remove dust and placed in 1-liter vessel

containing 800 mℓ of the solution. The mechanism of nucleation was by fluid shear via agitation by baffles. After two minutes, agitation was stopped; seeds were allowed to settle and 2 mℓ sample taken. This sample was mixed with 150 mℓ of 8% PE-nitric acid (nitric acid used as an electrolyte) and size analyzed with a model TA Coulter Counter. Agitation was restarted and the sampling procedure repeated for different times. The cummulative distribution obtained was converted to particle number size distribution and reported in the form of figure 15, from which the data for this analysis were taken.

In order to obtain a functional form for $n(\zeta,t)$, step 1 of the procedure described in the second section of Chapter III was carried out. A combination of the subroutine, Simple, and a Harwell subroutine, VA05AD, obtainable from the Theoretical Physics Division, Atomic Energy Research Establishment, Harwell, Berkshire, England, was used for the nonlinear regression analysis. The functional form chosen for the data is shown below:

$$\begin{aligned} n(\zeta,t) = {} & \tilde{a}_1 \exp(-\tilde{a}_2\zeta)(2 - \exp(-\tilde{a}_3 t) - \exp(-\tilde{a}_{10} t^2)) \\ & + \tilde{a}_4 \exp(-\tilde{a}_5\zeta)(2 - \exp(-\tilde{a}_6 t) - \exp(-\tilde{a}_{11} t^2)) \\ & + \tilde{a}_7 \exp(-\tilde{a}_8\zeta)(2 - \exp(-\tilde{a}_9 t) - \exp(-\tilde{a}_{12} t^2)) \end{aligned} \quad (4\text{-}2)$$

where $\tilde{a}_i$, $i = 1,2,\ldots,12$ are regression parameters over which the minimization procedure is done. The functional

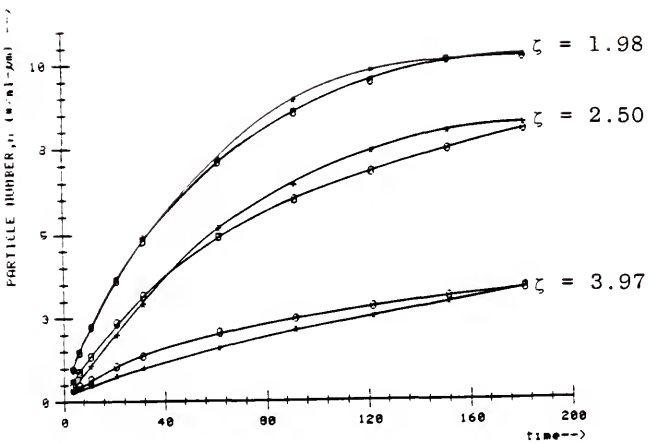

Figure 15. Transient Particle Number Versus Time for Each Fixed Size, ζ.

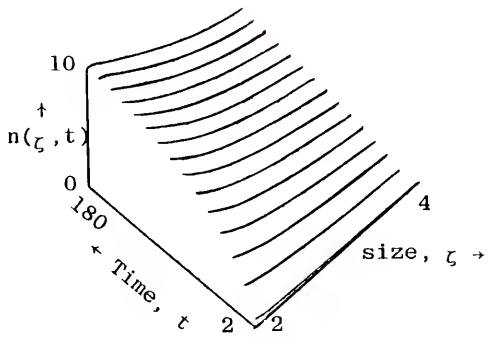

Figure 16a.

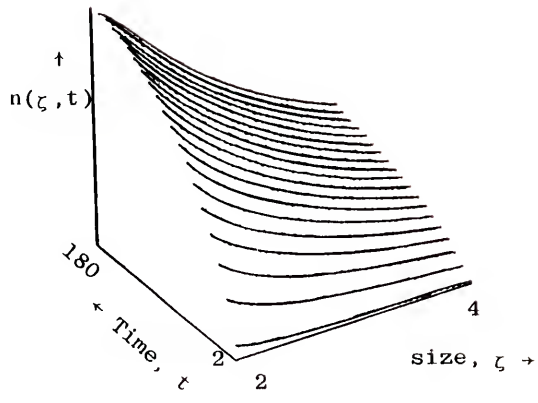

Figure 16b.

Figure 16. Two Different Rotations of 3-D Plot of the Fit for the Transient Crystal Size Distribution.

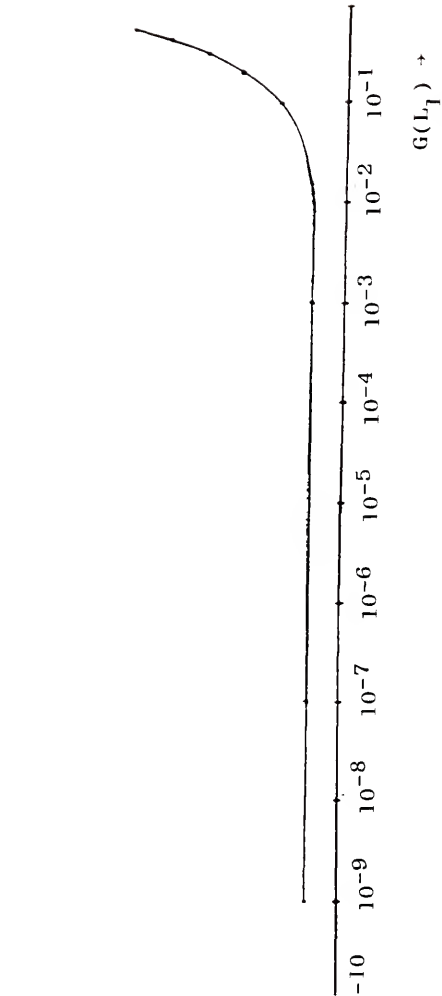

Figure 17. Plot of Total Chi-Square Error Versus $G(L_1)$ Guesses.

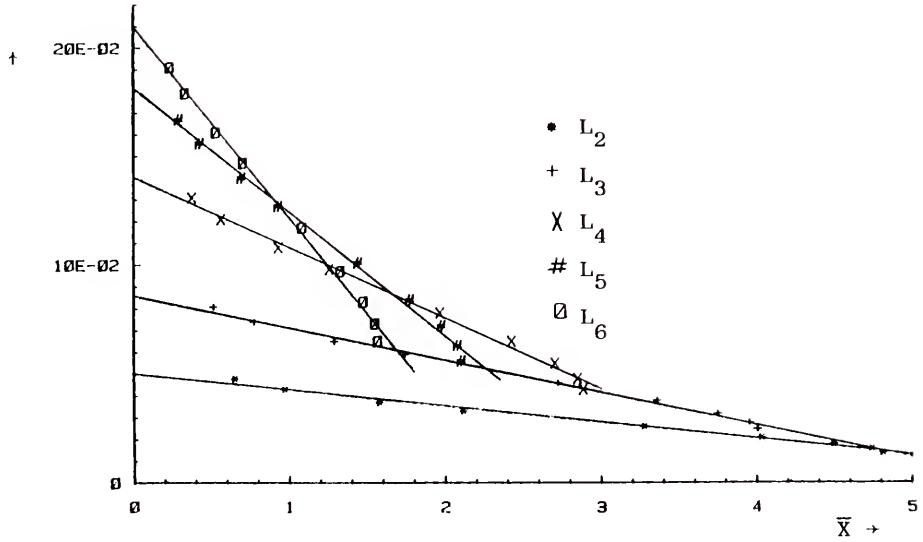

Figure 18. Plot of $\overline{N}$ Versus $\overline{X}$ for Various Sizes, L_k, k=2,3,4,5,6.

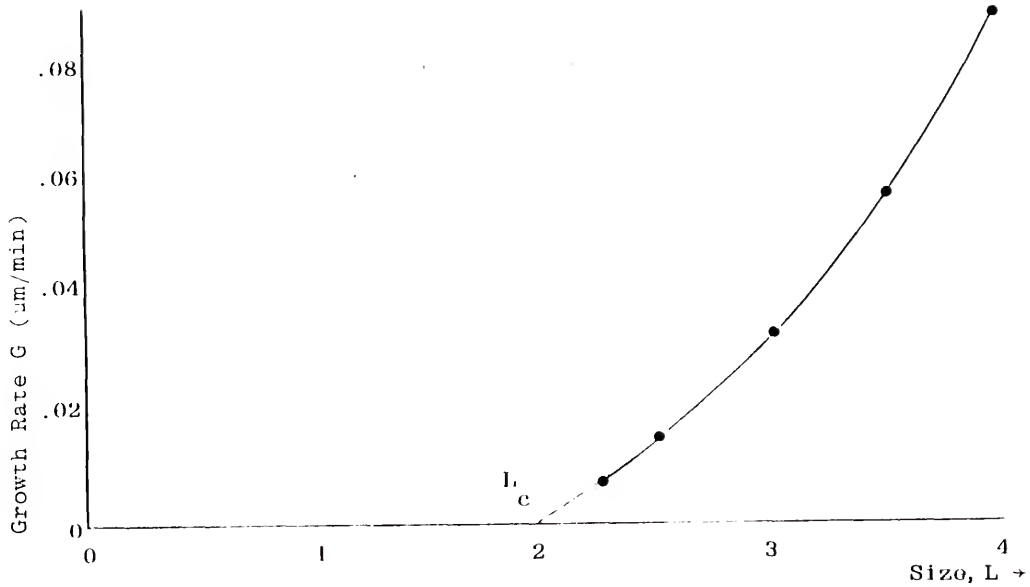

Figure 19. Growth Rate Versus Size for Transient Data.

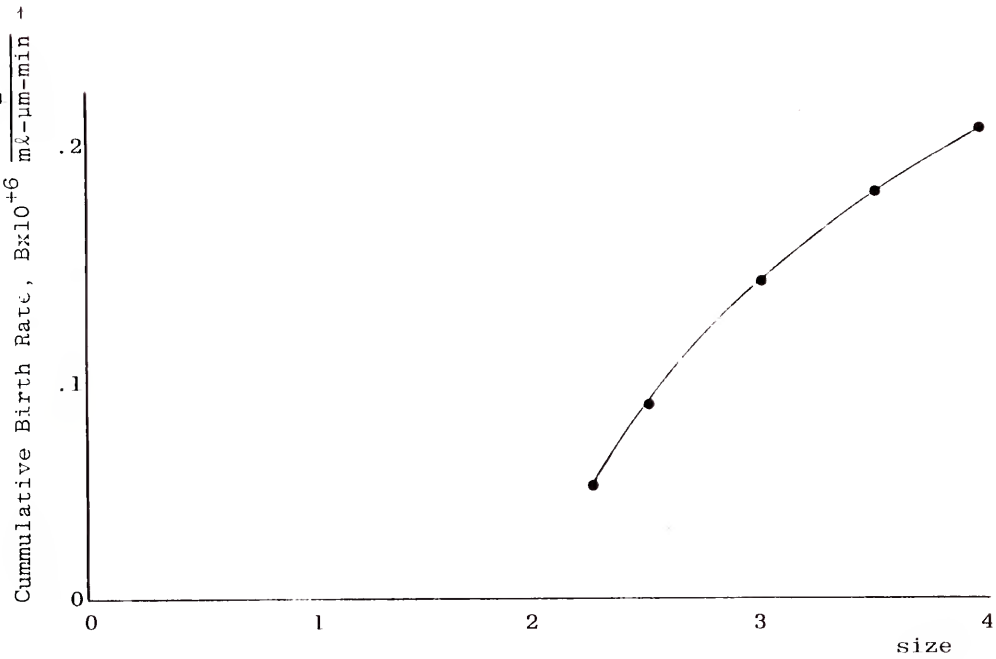

Figure 20. Cummulative Birth Rate Versus Size for Transient Data.

Table 4

Transient Data for Figure 16

Size	Time	Original $N(\zeta,t)$	Fitted $N(\zeta,t)$
1.98	2.33	0.770000E 00	0.756810E 00
1.98	4.65	0.128000E 01	0.125480E 01
1.98	9.30	0.206000E 01	0.203400E 01
1.98	19.53	0.346000E 01	0.340140E 01
1.98	30.0	0.466000E 01	0.454830E 01
1.98	60.0	0.698000E 01	0.688730E 01
1.98	90.0	0.872000E 01	0.833760E 01
1.98	120.0	0.956000E 01	0.927380E 01
1.98	150.0	0.984000E 01	0.987510E 01
1.98	180.0	0.100000E 02	0.998050E 01
2.50	2.33	0.350000E 00	0.374830E 00
2.50	4.65	0.530000E 00	0.651380E 00
2.50	9.30	0.900000E 00	0.116010E 01
2.50	19.53	0.179000E 01	0.213040E 01
2.50	30.0	0.272000E 01	0.295690E 01
2.50	60.0	0.495000E 01	0.466970E 01
2.50	90.0	0.620000E 01	0.578740E 01
2.50	120.0	0.720000E 01	0.659900E 01
2.50	150.0	0.776000E 01	0.725560E 01
2.50	180.0	0.800000E 01	0.782000E 01
3.97	2.33	0.180000E 00	0.140510E 00
3.97	4.65	0.200000E 00	0.282610E 00
3.97	9.30	0.320000E 00	0.477100E 00
3.97	19.53	0.570000E 00	0.851790E 00
3.97	30.0	0.800000E 00	0.117170E 01
3.97	60.0	0.140000E 01	0.183670E 01
3.97	90.0	0.190000E 01	0.227440E 01
3.97	120.0	0.230000E 01	0.259770E 01
3.97	150.0	0.272000E 01	0.286560E 01
3.97	180.0	0.324000E 01	0.310710E 01

Table 5

Values of Chi-Square Error and $G(L_1)$

$G(L_1)$	Chi-Square Error
0.0	.0125
10^{-9}	.0125
10^{-7}	.0124
.001	.0126
.01	.0139
.1	.0267
.2	.0412
.3	.0557
.4	.0701
.5	.0846

Table 6

Values of $\overline{N}$ and $\overline{X}$ for Various Sizes

	$\overline{N}$	$\overline{X}$
Size = L_2	0.048	0.650
	0.043	0.969
	0.037	1.579
	0.033	2.115
	0.026	3.277
	0.021	4.032
	0.018	4.496
	0.016	4.742
	0.014	4.813
Size = L_3	0.081	0.513
	0.074	0.773
	0.065	1.286
	0.059	1.738
	0.046	2.722
	0.038	3.359
	0.032	3.749
	0.028	3.952
	0.025	4.006
Size = L_4	0.131	0.374
	0.121	0.559
	0.108	0.928
	0.098	1.254
	0.078	1.965
	0.065	2.424
	0.055	2.703
	0.048	2.848
	0.043	2.884
Size = L_5	0.167	0.288
	0.156	0.422
	0.140	0.689
	0.127	0.925
	0.101	1.439
	0.084	1.770
	0.072	1.972
	0.063	2.075
	0.056	2.100
Size = L_6	0.191	0.231
	0.179	0.329
	0.161	0.526
	0.147	0.700
	0.117	1.079
	0.097	1.323
	0.083	1.471
	0.073	1.547
	0.065	1.564

Table 7

Results for Transient Data

INTERCEPT= 0.50303E-01 SLOPE=-0.73832E-02
COED= 0.988E 00 ERR-INT= 0.101E-02 ERR-SL= 0.302E-03

INTERCEPT= 0.85839E-01 SLOPE= 0.14658E-01
COED= 0.992E 00 ERR-INT= 0.136E-02 ERR-SL= 0.488E-03

INTERCEPT= 0.14068E 00 SLOPE=-0.32494E-01
COED= 0.995E 00 ERR-INT= 0.179E-02 ERR-SL= 0.893E-03

INTERCEPT= 0.18102E 00 SLOPE=-0.56929E-01
COED= 0.995E 00 ERR-INT= 0.219E-02 ERR-SL= 0.149E-02

INTERCEPT= 0.20976E 00 SLOPE=-0.88393E-01
COED= 0.995E 00 ERR-INT= 0.252E-02 ERR-SL= 0.230E-02

Table 8

Calculated Values of $\bar{B}$ and G
for Different Sizes

L_k	$\bar{B}x10^{-6}$	G
2.25	.050303	.0073832
2.50	.085839	.014658
3.00	.14068	.032494
3.50	.18102	.056929
3.97	.20976	.088393

form expressed by equation (4-2) is good as evident from figure 15 and table 4. The uncertainty of this fit is less than 10% to within a confidence level of 0.90. Step 2 of the procedure was carried out by analytically calculating all integrals in equation (4-2) except those involving terms of the form $\exp(-\tilde{a}_i t^2)$, i = 10, 11, 12. The remaining steps of the procedure were carried out displaying the plot of total chi-square error versus $G(L_1)$ values in figure 17 and table 5. The minimum error occurred at a value of $G(L_1)$ equal to 10^{-7}. For this value of $G(L_1)$ the quantities $\bar{N}$ and $\bar{X}$ were calculated and displayed in table 6, after which plots of $\bar{N}$ versus $\bar{X}$ were made for the various sizes as depicted in figure 18. It is evident from these plots that the data set for each size fits a straight line very closely. The parameters of interest from the plots that relate to $G(L_K)$ and $\bar{B}(L_K)$ are the slopes and intercept respectively. A linear regression of each $\bar{N}$-$\bar{X}$ data set was carried out to determine the corresponding slope and intercept. The fit for each data set was very good as manifested by the values for the coefficient of determination and other error estimates depicted in table 7. It should be noted that the negative of the slope is $G(L_K)$ while the intercept is equivalent to $\bar{B}(L_K)$. The resulting $G(L_K)$ and $\bar{B}(L_K)$ values displayed in table 8 were then plotted in figures 19 and 20. The uncertainty of the values of $G(L_K)$ and $\bar{B}(L_K)$ determined was less than 10% to within a confidence level of 0.90. The error

analysis pertaining to the determination of $G(L_K)$ and $\overline{B}(L_K)$ is included in the appendix. This concludes the exemplification for the quantification of growth and birth rates in an unsteady state crystallizer.

Stability Criteria for the Complex Crystallizer

Last but not least of the purposes of this study is the establishment of a stability criteria for the complex crystallizer. The work pertaining to the quantification of growth and birth rates in an unsteady state crystallizer described previously is very important in this study inasmuch as it is useful in obtaining the functions $v(y)$, $w(z)$, $u(y)$, $R(z)$ which are dimensionless forms of $g(c)$, $\phi(\zeta)$, $\sigma(c)$ and $b(\zeta)$ respectively. These dimensionless functions are used in the stability analysis. In other words, this study culminates in the establishment of the stability criteria. It should be noted, however, that the quantification of growth and birth rates is useful in other types of studies, such as formulating nucleation mechanisms, besides stability analysis.

The set of orthonormal functions $L_n^m(z)$ used for this analysis is a modified form of the associated Laguerre polynomials with a weighing function equal to 1, and is defined as follows:

$$\mathcal{L}_n^m(z) = \hat{a}_n Z^{m/2} e^{-z/2} L_n^m(z) , \qquad \begin{matrix} m=2, \\ n\geq 2 \end{matrix} \qquad (4\text{-}3)$$

$$L_n^m(z) = \frac{d^m}{dz^m} L_n(z) \tag{4-4}$$

where $L_n(z)$ is the n-th order Laguerre polynomial and

$$\hat{a}_n = \sqrt{\frac{(n-m)!}{(n!)^3}} \tag{4-5}$$

The orthonomality relationship is defined by equation (4-6):

$$\int_0^\infty \hat{a}_n \mathcal{L}_n^m(z) \quad \hat{a}_p \mathcal{L}_p^m(z) = \delta_{np} \tag{4-6}$$

where δ_{np} is the Kronecker delta function. The first four functions denoted f_o, f_1, f_2, f_3 respectively are given below together with some of their derivatives:

$$f_o(z) = \frac{1}{\sqrt{2}} z\, e^{-z/2} \tag{4-7}$$

$$f_1(z) = \sqrt{\frac{1}{216}} z\, e^{-z/2} (-6z+18) \tag{4-8}$$

$$f_2(z) = \sqrt{\frac{2}{(24)^3}} z\, e^{-z/2} (12z^2-96z+144) \tag{4-9}$$

$$f_3(z) = \sqrt{\frac{6}{(120)^3}} z\, e^{-z/2} (-20z^3+300z^2-1200z+1200) \tag{4-10}$$

$$f_o'(z) = e^{-z/2} (1 - \frac{z}{2})/\sqrt{2} \tag{4-11}$$

$$f_1'(z) = e^{-z/2} (z^2-7z+6)/(2\sqrt{6}) \tag{4-12}$$

$$f_2'(z) = e^{-z/2}\left(\frac{-z^3}{2} + 7z^2 + 22z + 12\right)/(4\sqrt{3}) \quad . \qquad (4\text{-}13)$$

The functions, $f_n(z)$, n = 0,1,... is defined below:

$$f_n(z) = \overset{2}{n+2}(z) \quad . \qquad (4\text{-}14)$$

It can be seen by inspection that each of the functions, $f_n(z)$, satisfies the boundary conditions of equations (3-59) and (3-60):

$$\lim_{z\to\infty} \eta(z) = 0 \qquad (3\text{-}59)$$

$$\eta(0,\theta) = 0 \qquad (3\text{-}60)$$

and hence those of equations (4-15) and (4-16) are

$$\lim_{z\to\infty} N(z) = 0 \qquad (4\text{-}15)$$

$$N(0) = 0 \quad . \qquad (4\text{-}16)$$

Because this study has to be very practical example data was chosen to closely resemble real data as much as possible. These example data were formulated in functional forms as follows:

$$W(z) = \frac{EM}{1 + A1\ e^{-(B1)z}} \quad , \qquad EM<<A \qquad (4\text{-}17)$$

where

$$EM = 1, \qquad A1 = 10^3, \qquad B1 = 0.3$$

$$\frac{d}{dz} W(z) = \frac{(EM)(B1)A1\ e^{-(B1)z}}{(1 + A1\ e^{-(B1)z})^2} \tag{4-18}$$

$$R(z) = EM2\ e^{-A3(z-2)} \tag{4-19}$$

where

$$EM2 = 10^6 , \qquad A3 = 0.5$$

$$\eta_o(z) = (EMH)e^{-A2(z-2)} \tag{4-20}$$

where

$$EMH = 10^3 , \qquad A2 = 0.21$$

$$\frac{d}{dz} \eta_o(z) = -(EMH)A2\ e^{-A2(z-2)} \tag{4-21}$$

The functions, $h_i(\zeta)$, defined in equations (3-20) through (3-26) are continuous and possess different values in different intervals. Due to the fact that $\Gamma_1(z)$ and $\Gamma_3(z)$ defined in equations (3-47) and (3-50) respectively are different combinations of the h_i's, they also share the same property. In other words, $\Gamma_1(z)$ and $\Gamma_3(z)$ are each continuous and also piecewisely differentiable. It was, therefore, deemed necessary to represent $\Gamma_1(z)$ and $\Gamma_3(z)$ as shown below:

$$\Gamma_1(z) = \begin{cases} CS1 = -(R/1)/AL1 - 1/AL4 + theta/AL6 , & (2, L_f] \\ CS2 = -A/AL4 , & (L_f, L_p] \\ CS3 = -ZS/AL4 + (ZS)B/AL6 , & (L_p, \infty) \end{cases} \tag{4-22}$$

$$\Gamma_3(z) = \begin{cases} C1 = 1/AL4 - (1-theta) - (R-1)/AL1 , & (2, L_f] \\ C_2 = 1/AL4 - A , & (L_f, L_p] \\ C_3 = 1/AL4 - ZS(1-B) , & (L_p, \infty). \end{cases} \tag{4-23}$$

The following changes in the original variables have been made:

$\alpha i \rightarrow$ Ali , $\quad i = 0,1,2,\ldots,6$

$\theta \rightarrow$ theta

$\beta \rightarrow$ B

$z^* \rightarrow$ ZS

$\nu_5 \rightarrow$ NU5

$r \rightarrow$ R2

$u_o \rightarrow$ UO

$v_o \rightarrow$ VO

$u_o' \rightarrow$ UOP

$v_o' \rightarrow$ VOP

$\varepsilon_c \rightarrow$ EC

$y_o \rightarrow$ YO

$L_f \rightarrow$ LF

$L_p \rightarrow$ LP

$Q^* \rightarrow$ QSTAR

$\Gamma_2 \rightarrow$ GAM2 .

Other information pertinent to the example data is

$$AL0 = 1/4 \tag{4-24}$$

$$AL1 = 1/9 \tag{4-25}$$

$$AL2 = 1/6 \tag{4-26}$$

$$AL3 = 1/3 \tag{4-27}$$

$$AL4 = 1/3 \tag{4-28}$$

$$AL5 = 1 \tag{4-29}$$

$$AL6 = 1/2 \tag{4-30}$$

$$UOP = 0.1 \tag{4-31}$$

$$VOP = 4.67 \tag{4-32}$$

$$UO = 0.01 \tag{4-33}$$

$$VO = 4.51 \tag{4-34}$$

$$YO = 1.01 \tag{4-35}$$

$$ENINT = \int_{z_1}^{z_2} n_{in}(z)\, z^3 dz\,. \tag{4-36}$$

Since there is no such thing as particle of zero size, the lowest size in the data is taken to be 2μm. This fact is reflected in the lower limit of integration being fixed at 2μm for each integral computed. The various integrals were computed via Gauss-Legendre and Gauss-Laguerre six and ten point quadrature formula. Though the six and ten point quadrature formula agree very closely, in all cases, calculations of the polynomial coefficients were based on the ten point formula. The integrals containing $\Gamma_1(z)$ or $\Gamma_3(z)$ had three different intervals of integration. The quadratic and quartic criteria described by equations (3-83a) through (3-85a), and equations (3-86a) through (3-100) respectively, were applied to the data. In addition the Root-locus method utilizing the quadratic and quartic versions of the polynomial equation (3-82) was also applied to

the data. The quadratic and quartic versions of equation (3-82) are denoted by equations (3-83) through (3-85) and equations (3-86) through (3-90) respectively. The effects of the various crystallizer operating parameters on the stability of the system were monitored both by the equations described in the stability criteria and by the Root-locus method.

A comprehensive stability program used for this analysis is included in the appendix. This program consists of (i) a subroutine, Gleg for computing Gauss-Legendre type integrals, (ii) a subroutine, Glag for computing Gauss-Laguerre type integrals, (iii) a main program that defines the various constants and parameters of the system, computes the various polynomial coefficients and their respective zeroes, and tests the stability criteria, and (iv) a function subprogram in which the functions to be integrated are defined. The main program calls ZPOLR, an IMSL subroutine for computing zeroes of an n-th order polynomial ($n \leq 101$), and the two subroutines, which in turn calls the function subprogram.

The format of the example data, which are described by equations (4-17) through (4-36), was chosen to facilitate the readability of the self-contained program. The comments in the program add to the clarity of the program. This program which uses a double precision version of Fortran-77 was run on the vax-11/780 mini-computer available to the University of Florida students at no cost. It could also

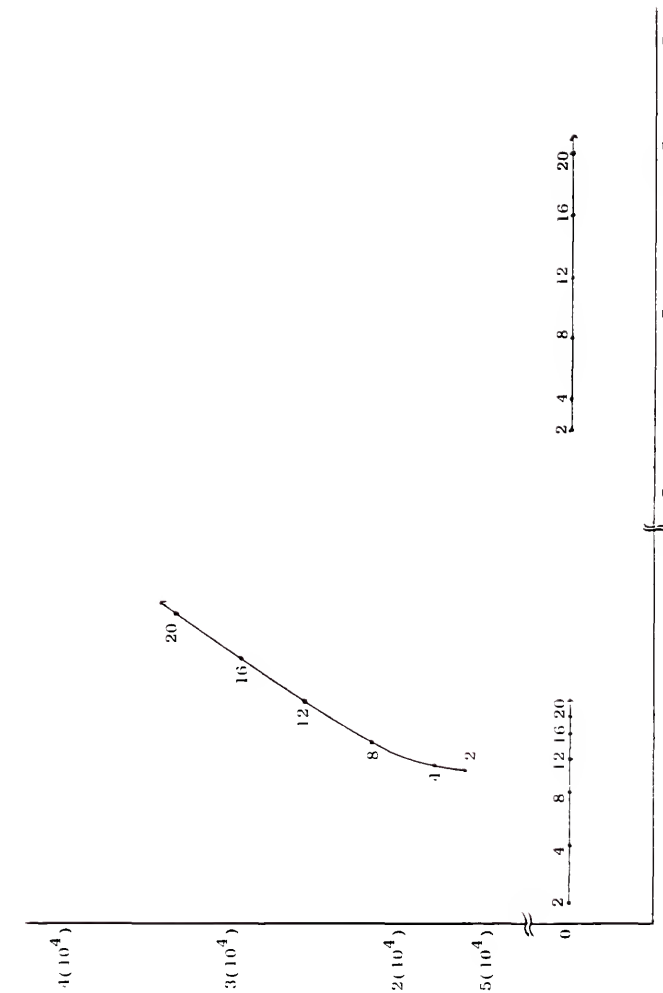

Figure 21. Root Locus Plot of the Effect of Recycle Rate of Dissolved Fines, R., on the Crystallizer Stability.

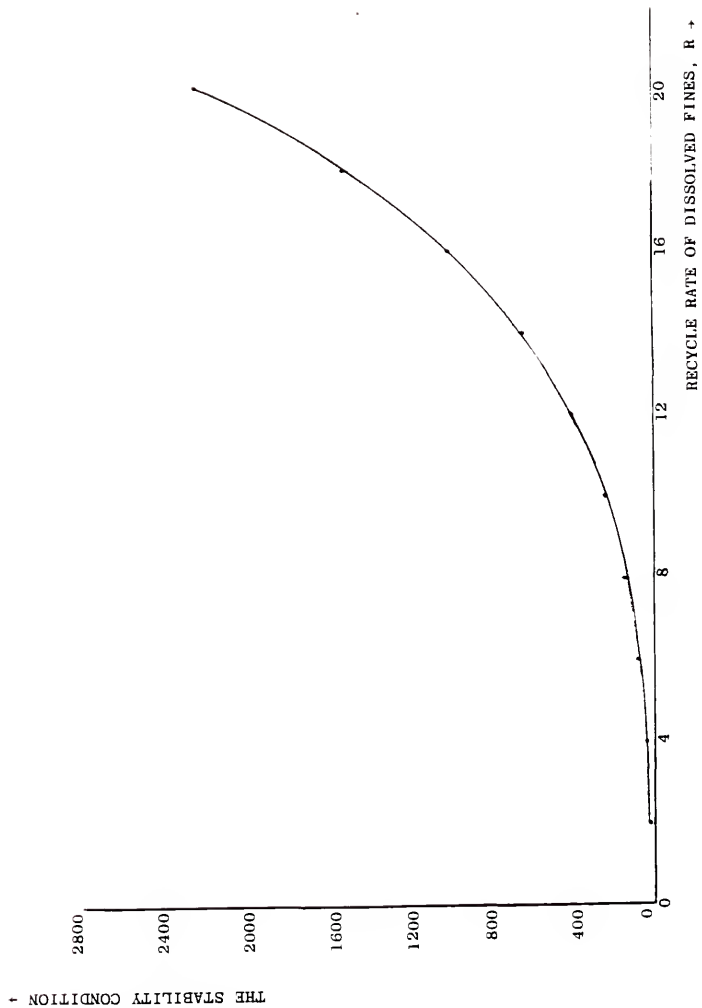

Figure 22. Effect of Recycle Rate of Dissolved Fines on the Stability Condition.

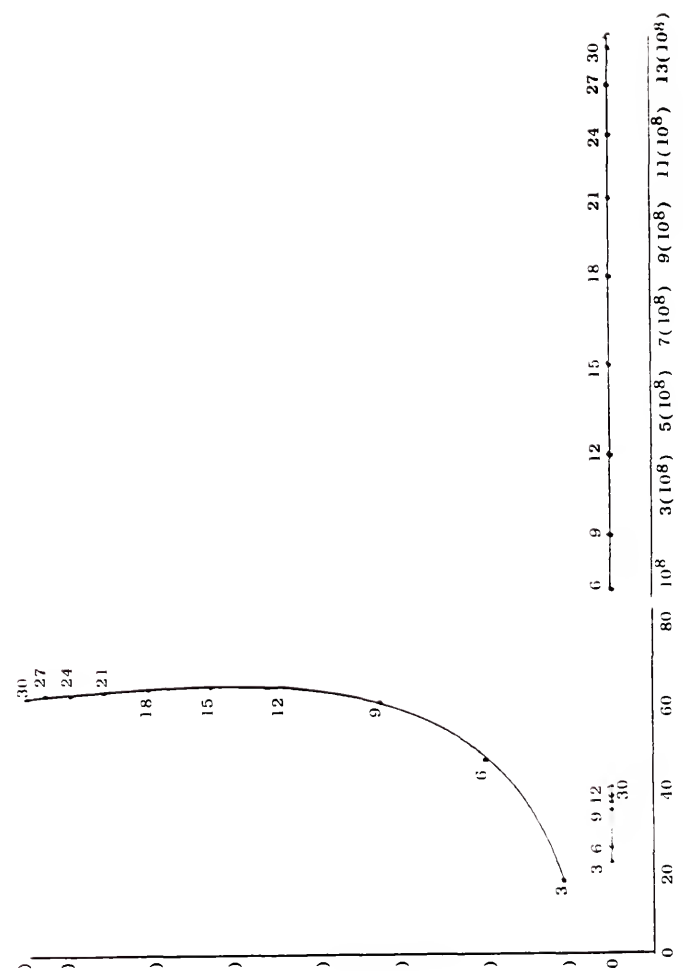

Figure 23. Root Locus Plot of the Effect of Maximum Fines Size, L_f on the Crystallizer's Stability.

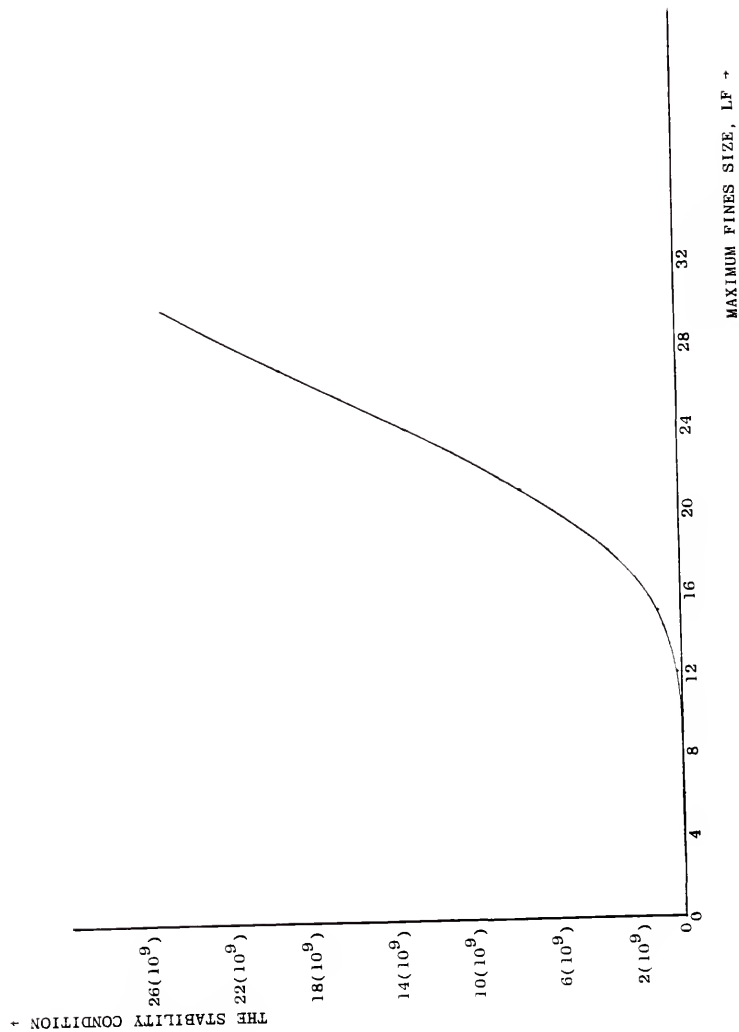

Figure 24. Effect of Maximum Fines Size on the Stability Condition.

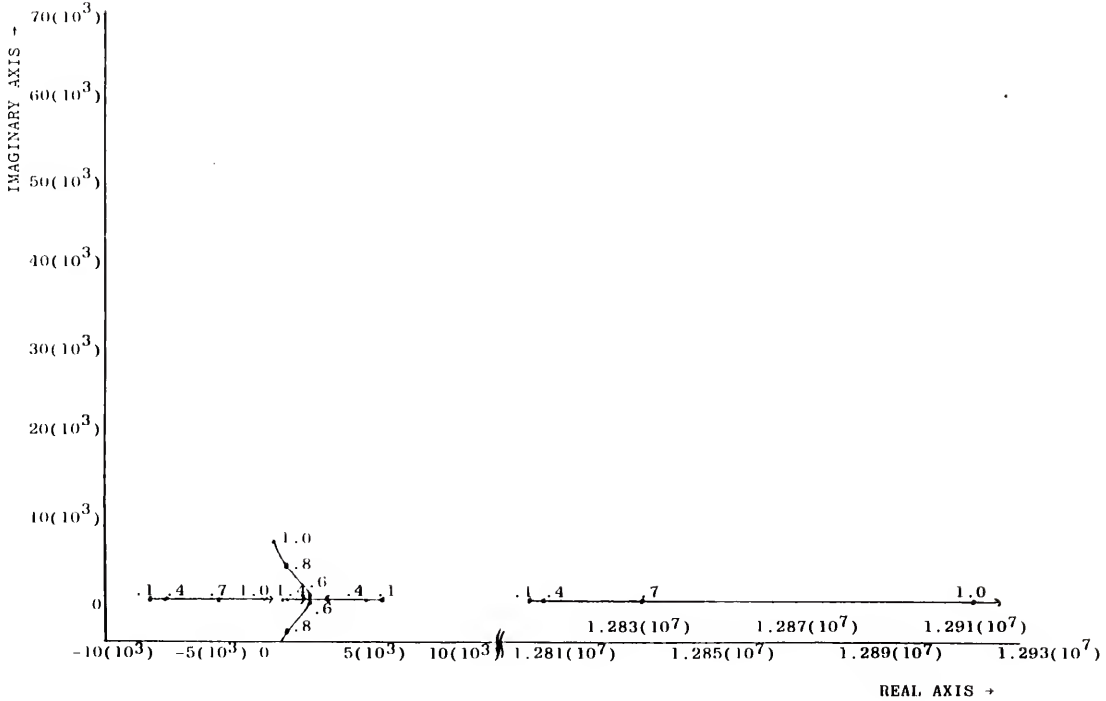

Figure 25. Root Locus Plot of the Effect of Maximum Fines Size, LF, on the Crystallyzer's Stability.

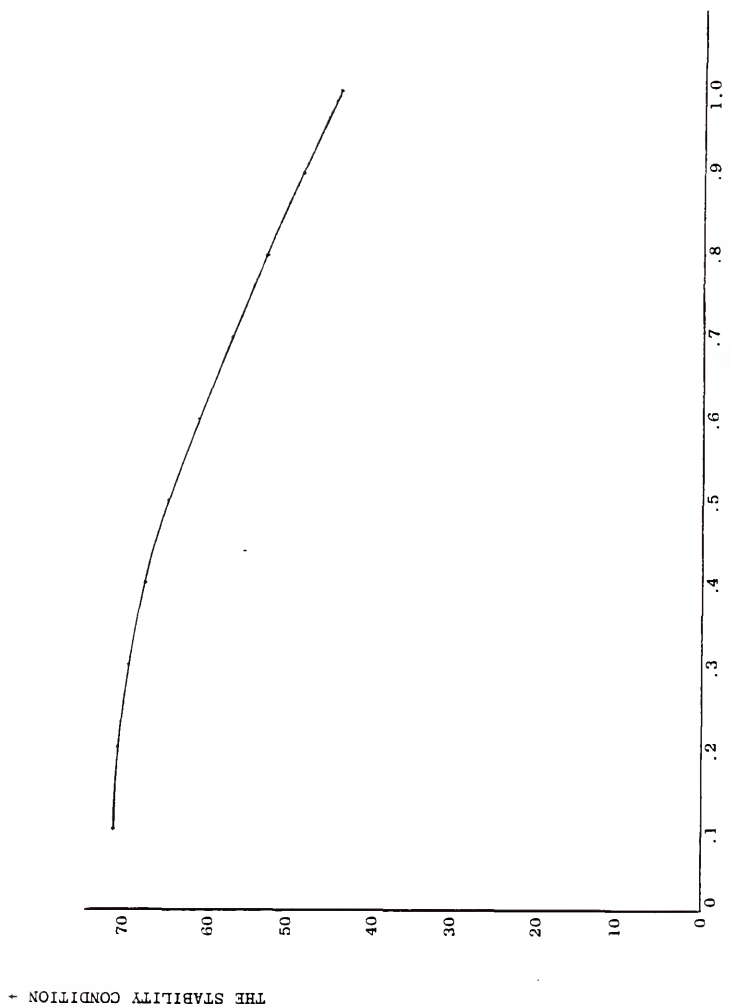

Figure 26. Effect of Maximum Fines Size on the Stability Condition.

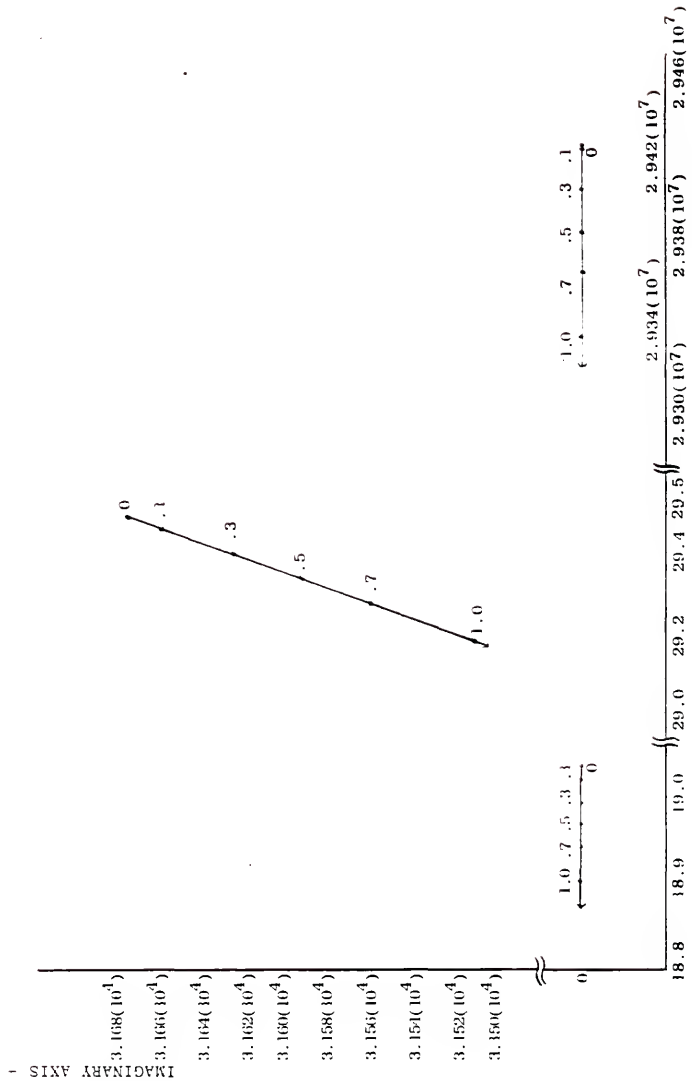

Figure 27. Root Locus Plot of the Effect of Recycle Rate of Undissolved Fines, theta, on the Crystallizer's Stability.

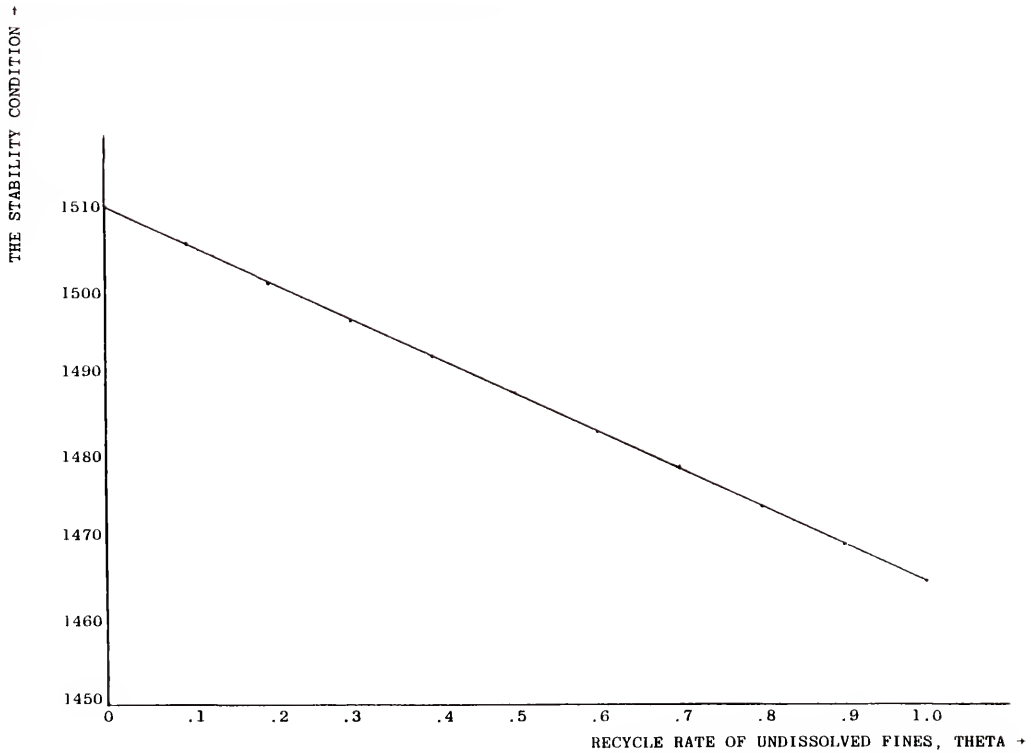

Figure 28. Effect of Recycle Rate of Undissolved Fines on the Stability Condition.

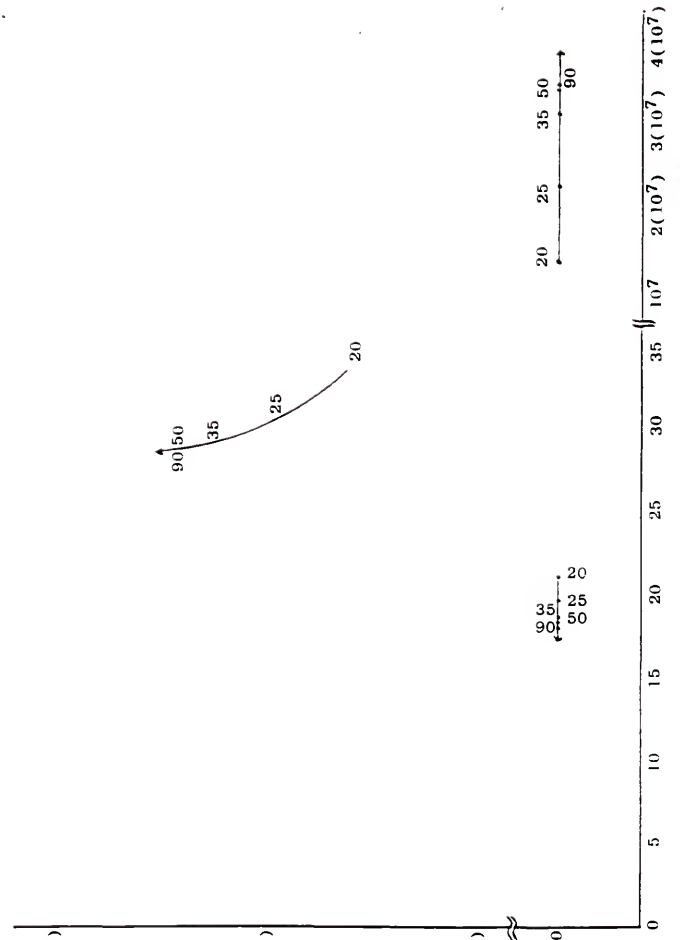

Figure 29. Root Locus Plot of the Effect of Product Classification, L_p, on the Crystallizer's Stability.

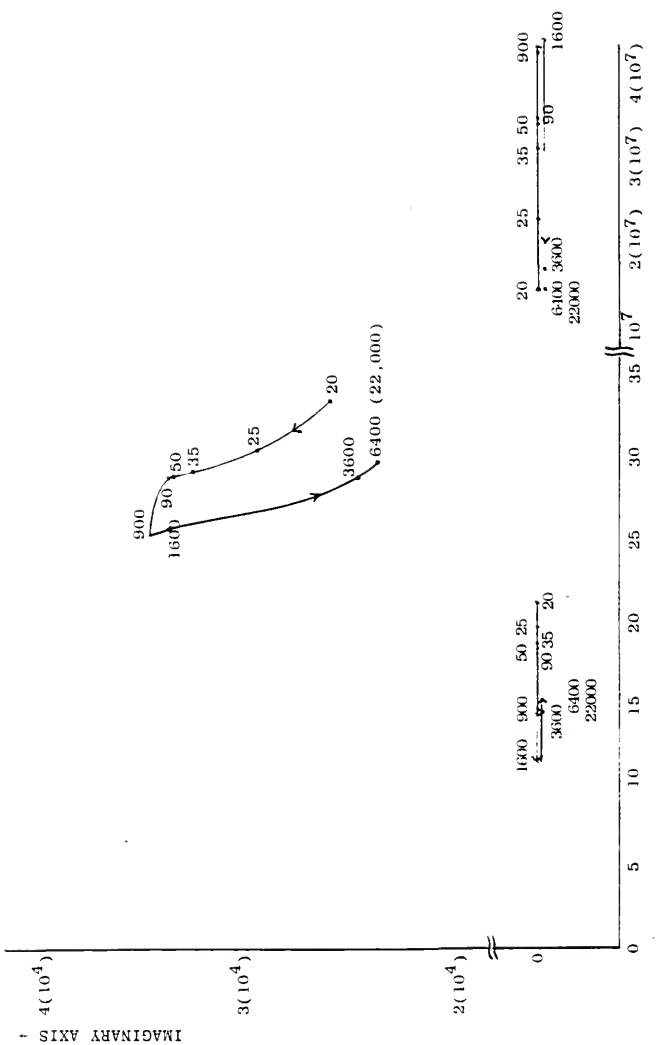

Figure 30. Root Locus Plot of the Effect of Product Classification, L_p, on the Crystallizer Stability.

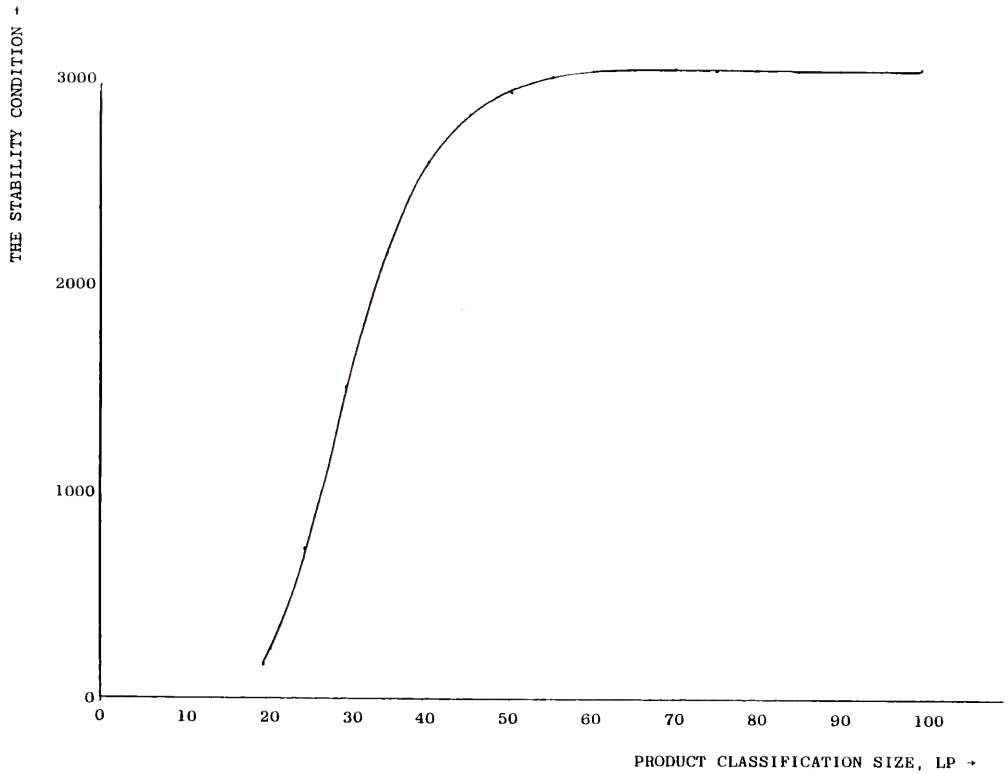

Figure 31. Effect of Product Classification Size on the Stability Condition.

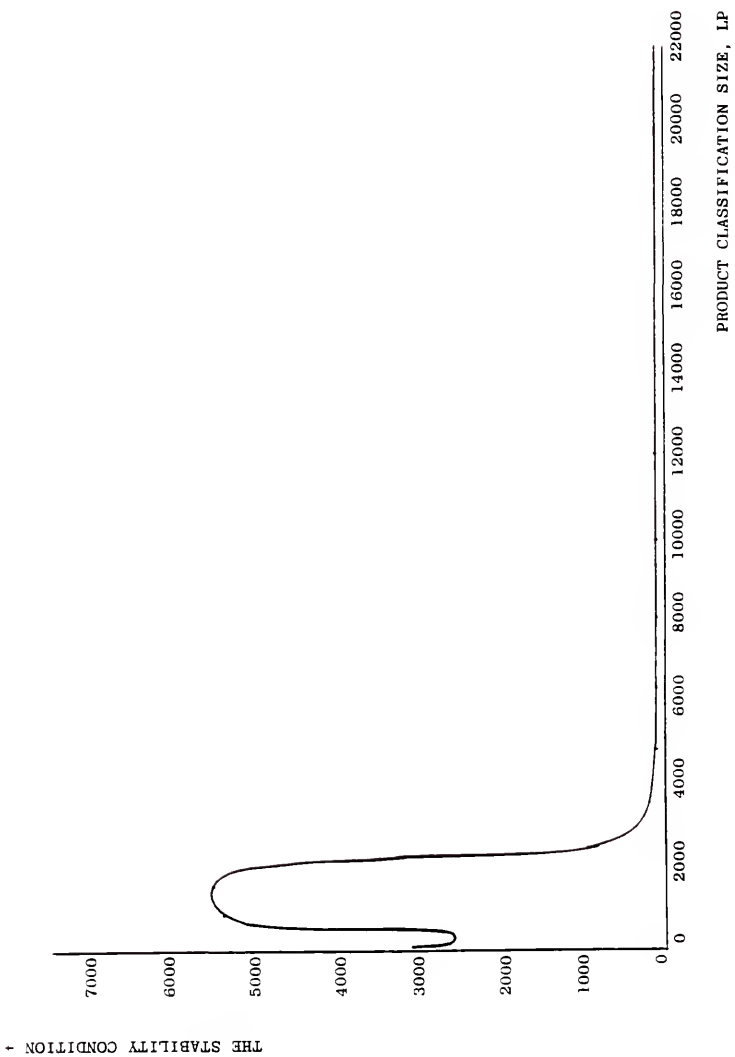

Figure 32. Effect of Product Classification Size on the Stability Condition.

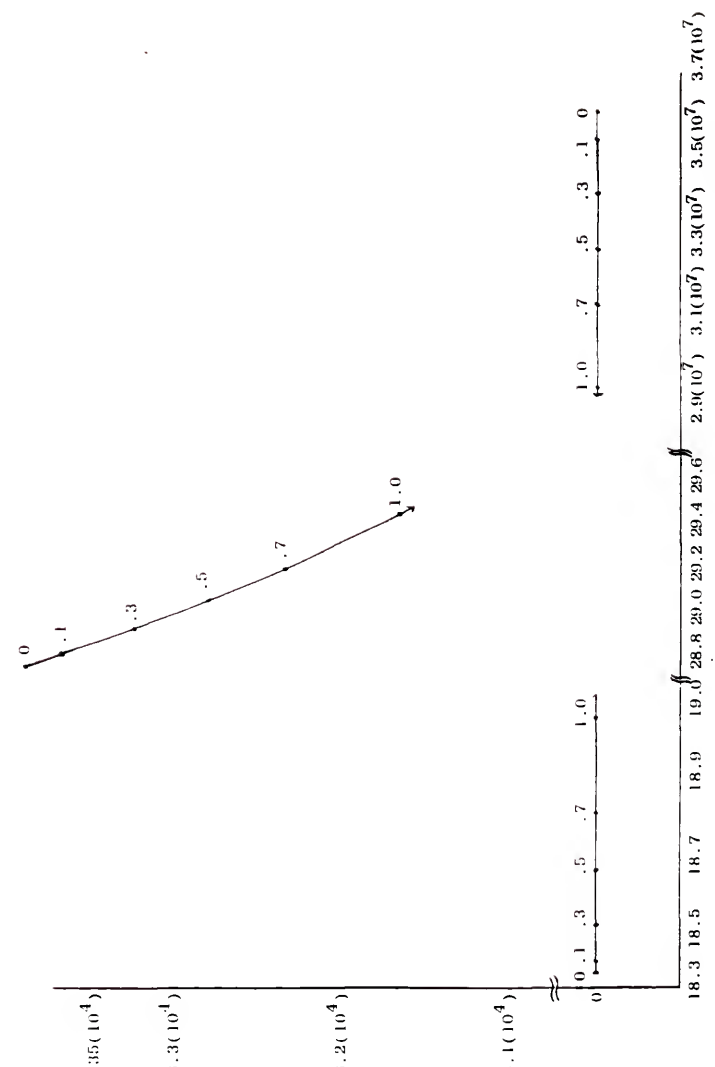

Figure 33. Root Locus Plot of the Effect of Product Recycle Rate, B, on the Crystallizer's stability.

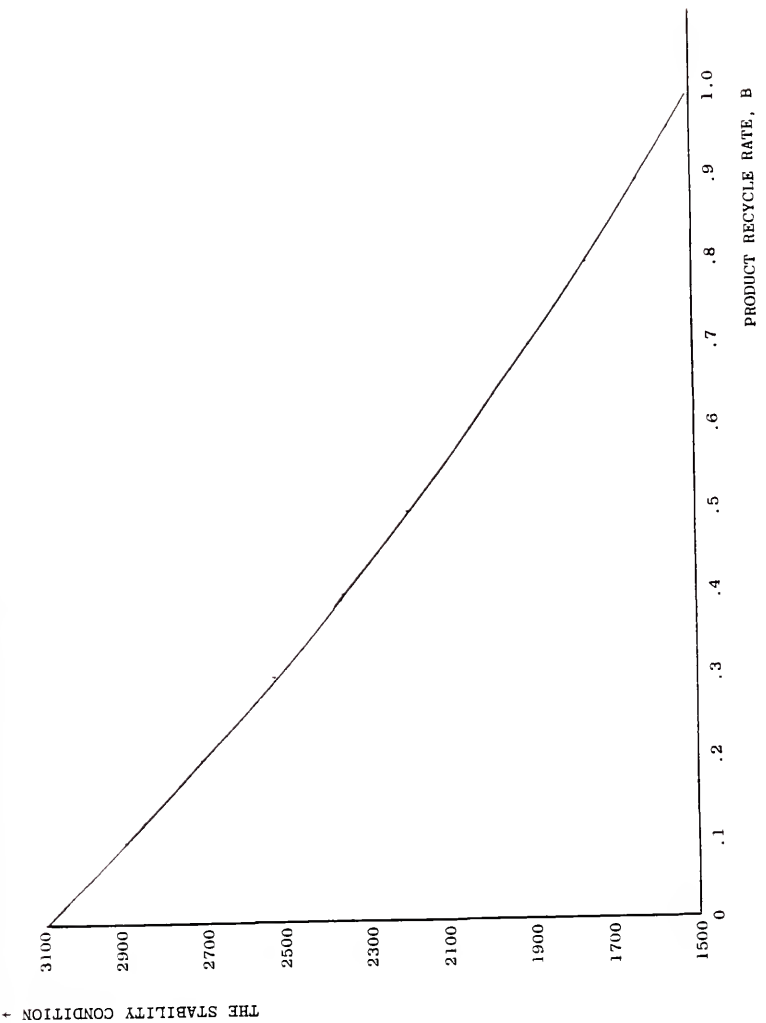

Figure 34. Effect of Product Recycle Rate on the Stability Condition.

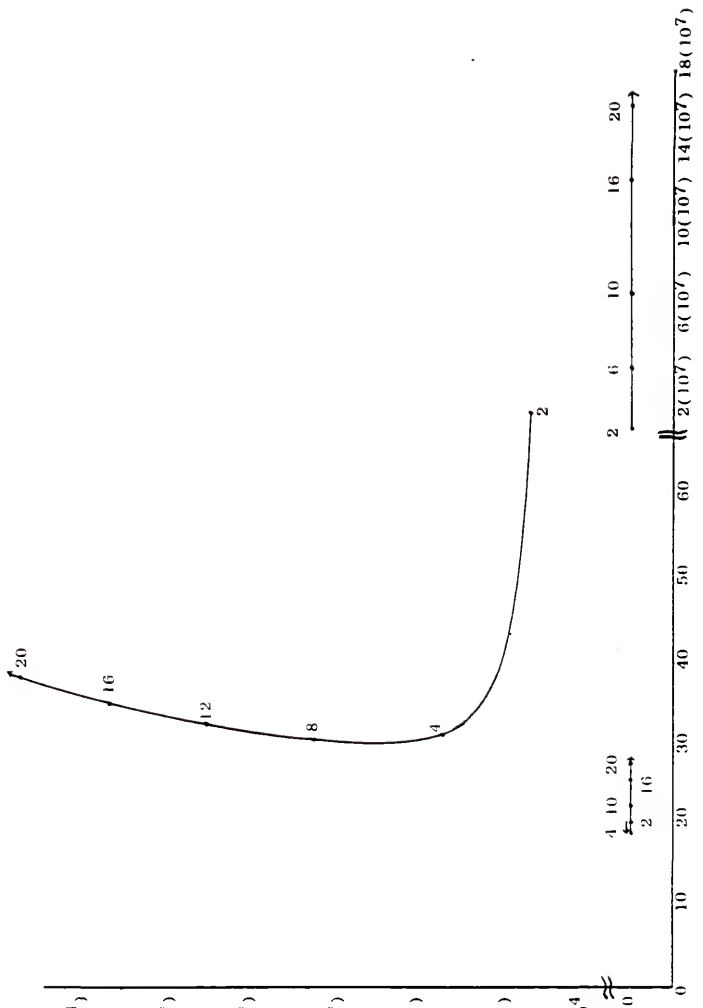

Figure 35. Root Locus Plot of the Effect of Intermediate Crystal Withdrawal Rate, A, on the Crystallizer's Stability.

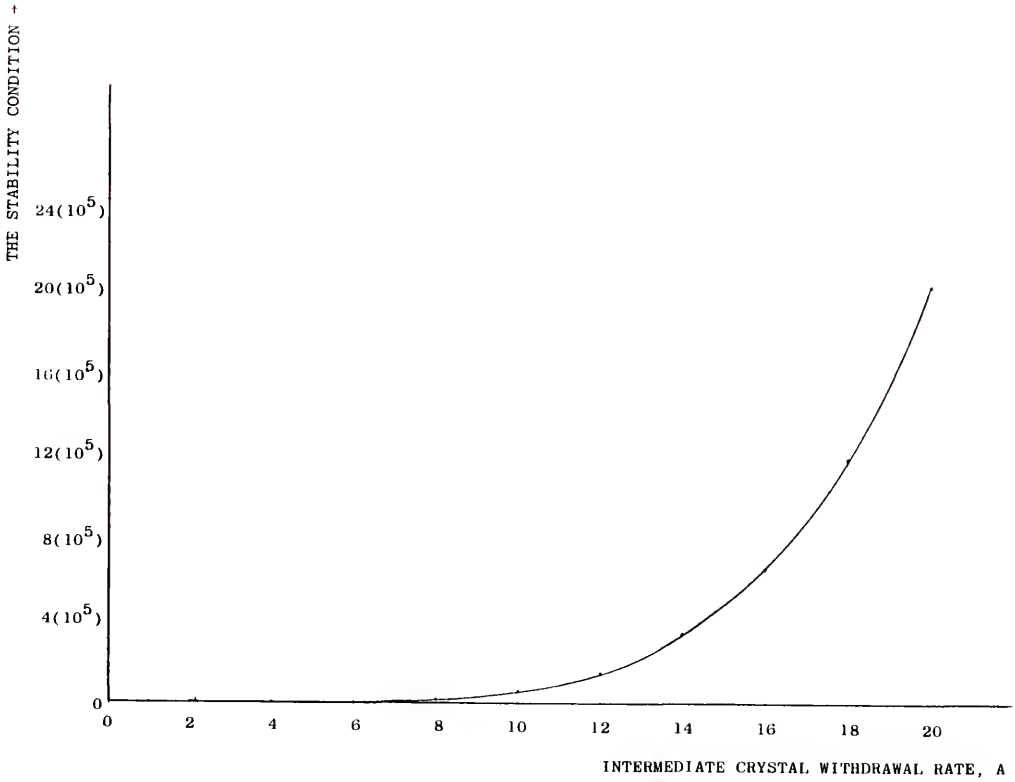

Figure 36. Effect of Intermediate Crystal Withdrawal Rate on the Stability Condition.

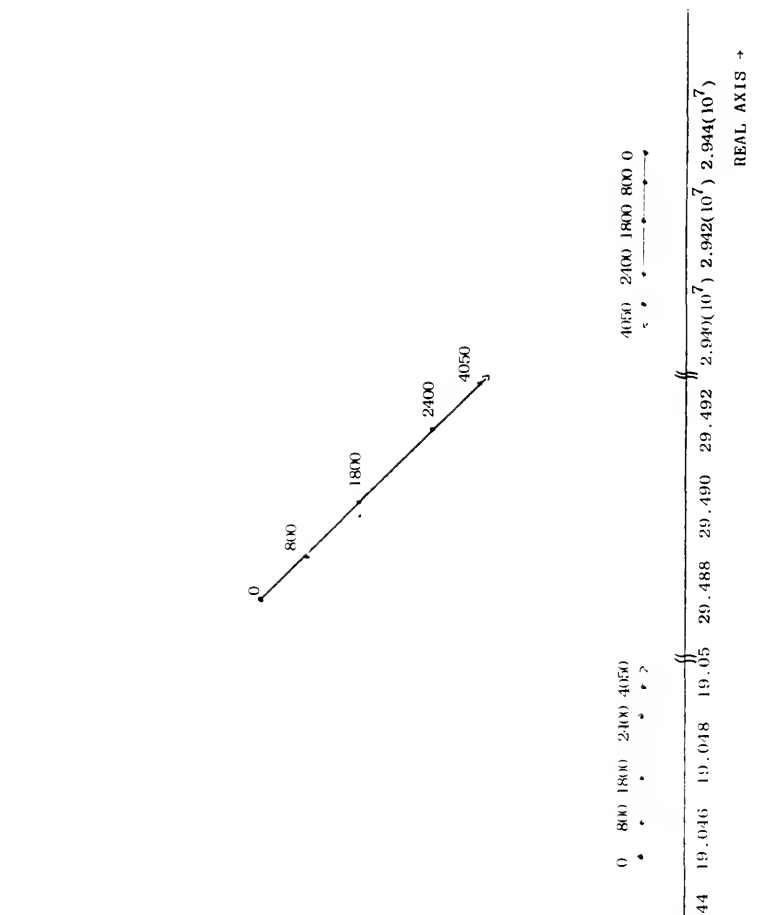

Figure 37. Root Locus Plot of the Effect of Feed Seeding and Seed Size, ENINT, on the Crystallizer's Stability.

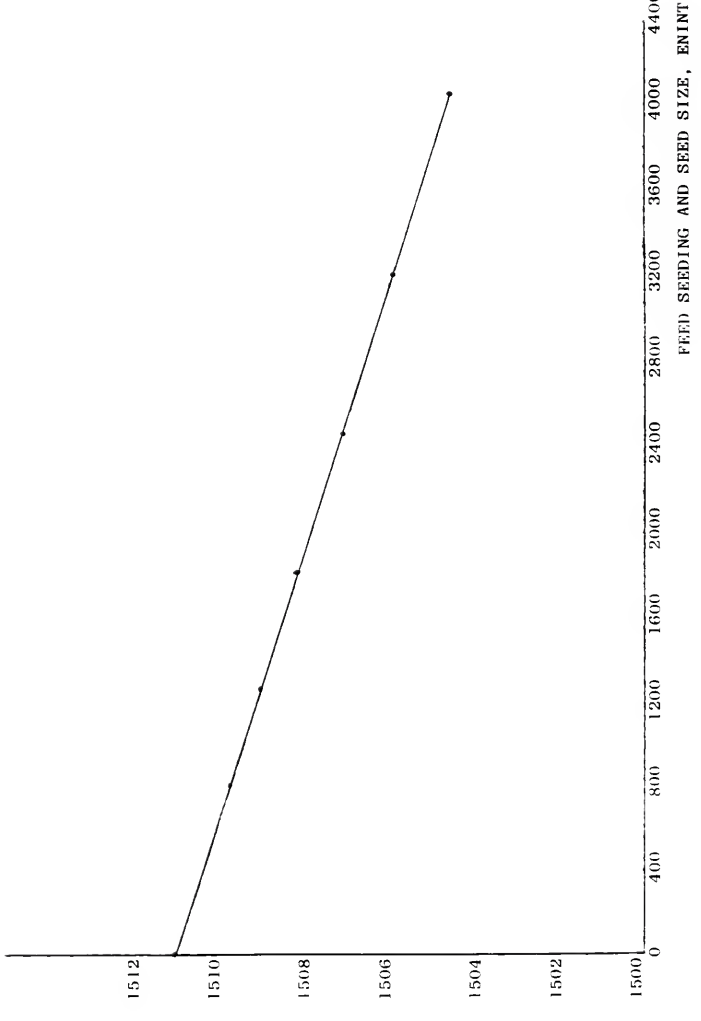

Figure 38. Effect of Feed Seeding and Seed Size on the Stability Condition.

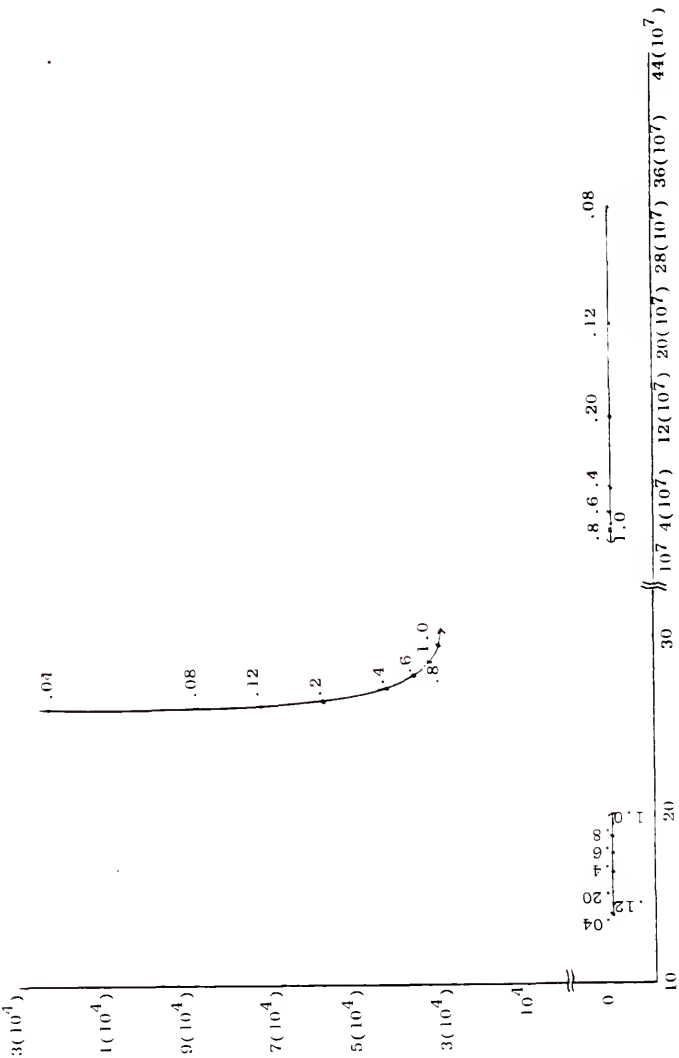

Figure 39. Root Locus Plot of the Effect of Void Fraction, ε_c, on the Crystallizer's Stability.

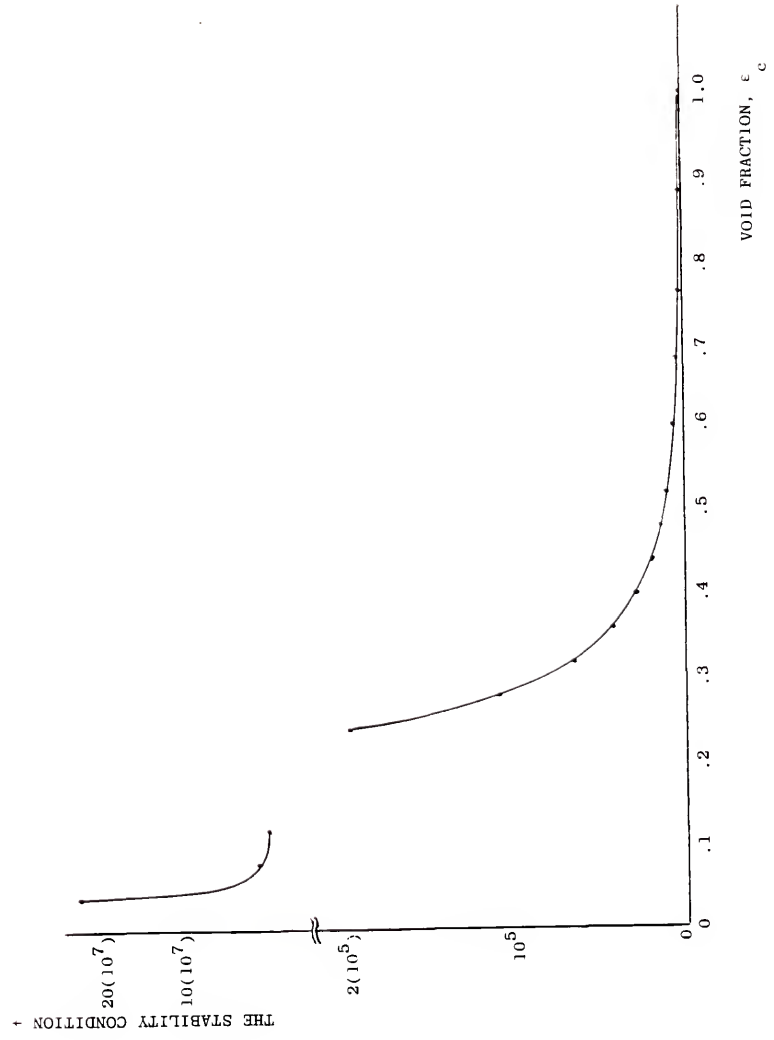

Figure 40. Void Fraction on the Stability Condition.

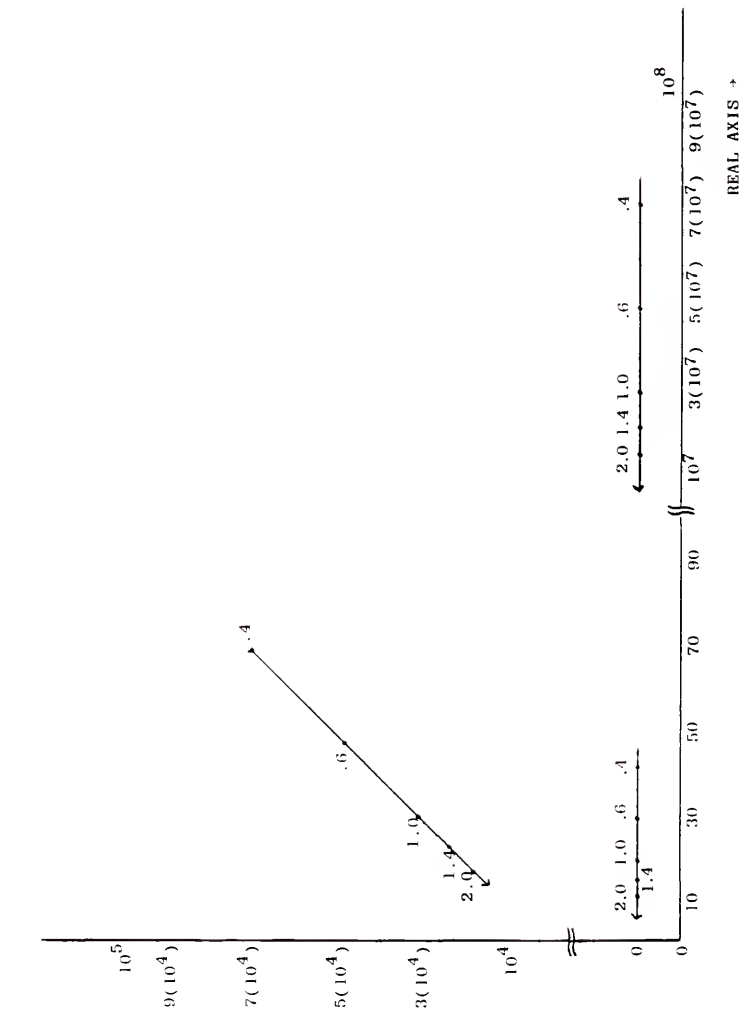

Figure 41. Root Locus Plot of the Effect of Residence Time on the Crystallizer's Stability.

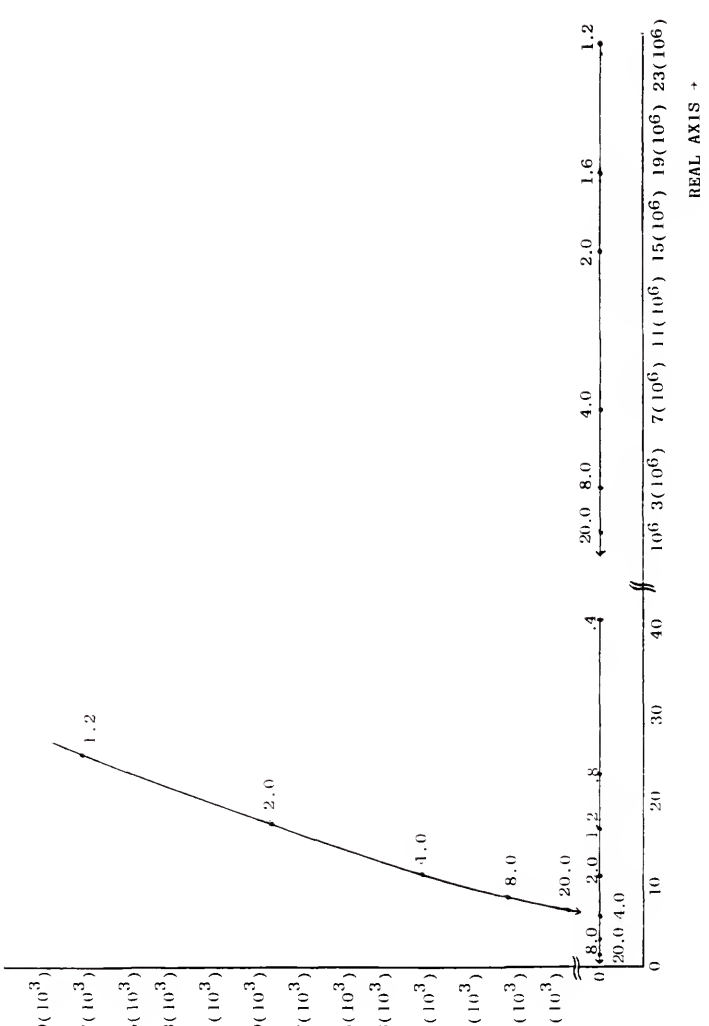

Figure 42. Root Locus Plot of the Effect of Residence Time on the Crystallizer's Stability.

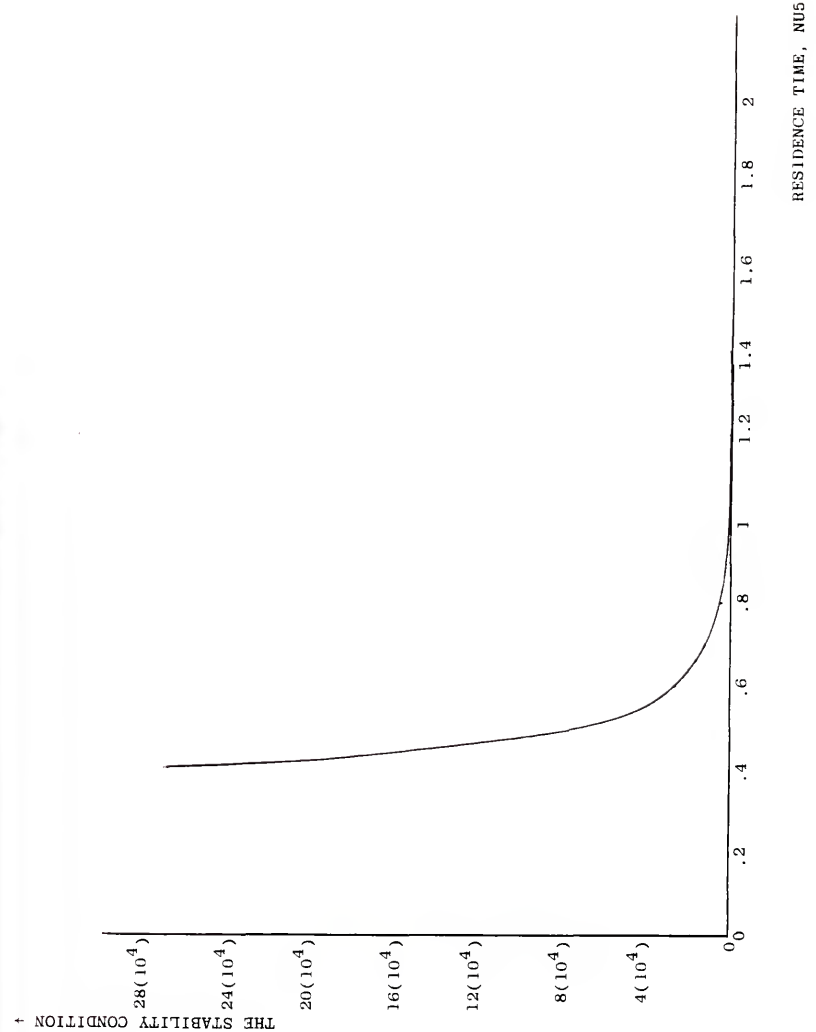

Figure 43. Effect of Residence Time on the Stability Condition.

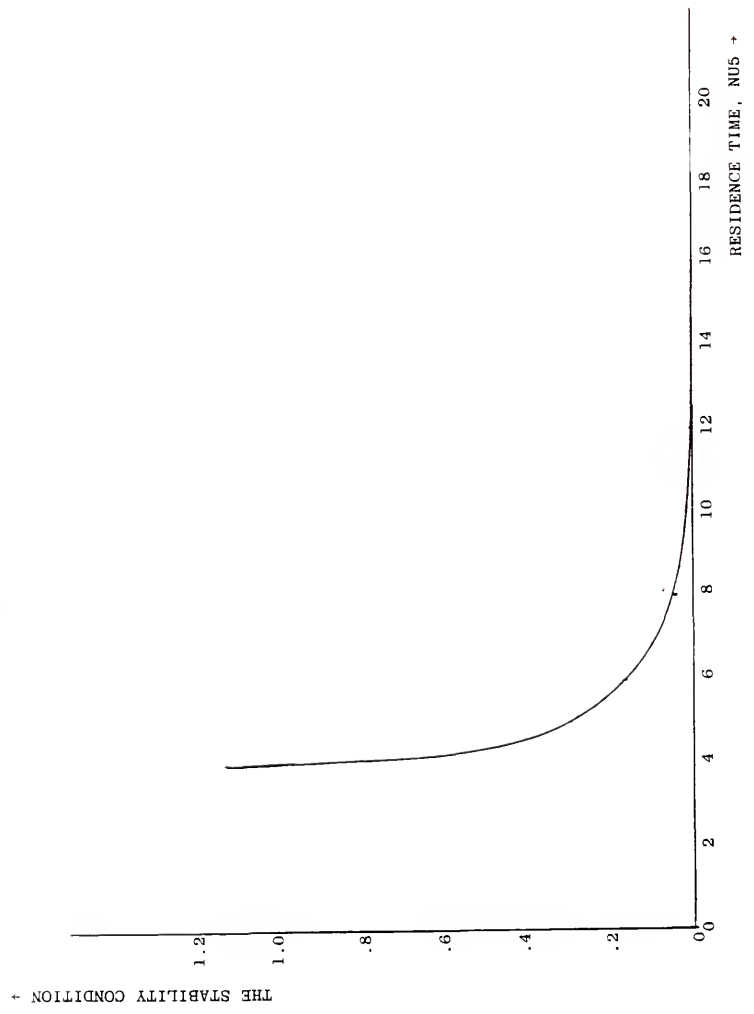

Figure 44. Effect of Residence Time on the Stability Condition.

be run without any modifications on the IBM Fortran-G compiler.

Root-locus plots have been made to show the effects of the various system parameters on the stability of the system. In addition, plots have been made to show the effects of system's parameters on the fourth order stability condition defined by equation (3-9) henceforth referred to as "the stability condition." The various plots are shown in figures 22 through 44 . When complex roots are involved in the Root-locus plots only those above the real axis are shown, since those below the axis are simply mirror images of those above. In this system, all roots lie to the right of the complex plane when the system is stable, and a crossover to the left-hand side implies that the system is exhibiting instability. The effects of parameters discussed below are for such a condition in which dissolved fines cause a proportionate increase of 0.5% (r=.005) in the concentration. The following cases are of particular interest:

Effects of recycling dissolved fines, R, and fines size L_f. The cases investigated are

$$2 \leq R \leq 18$$

$$0.1 \leq L_f \leq 30 \ .$$

Figure 21 shows that the systems stability increases with recycle rate of dissolved fines, R. This increase is greater for small values of R than for larger values.
For R<2.36 the system is unstable. Figure 22

shows that the stability condition is more positive for increasing R values, thereby complementing the trend shown by the system's stability. Figure 23 reveals that dissolving fines at larger sizes enhances the system's stability. This trend is complemented by the stability condition in figure 24 which becomes more positive for increasing L_f values. For the range $.1 \leq L_f \leq 1$ the system exhibits instability as shown in figure 25.
However the trend of the stability condition in figure 26 is in the opposite direction for this range, thus remaining decreasingly positive.

Effect of recycling undissolved fines, $(0 \leq \theta \leq 1)$.
Recycling solid undissolved fines decreases the stability region as revealed by the plot in figure 27 . This trend is supported by the increasing negativity of the stability condition in figure 28.

Effect of product withdrawal and or recycling.
The cases studied are

$$20 \leq L_p \leq 100 , \qquad 100 < L_p \leq 40{,}000$$
$$2 \leq z^* \leq 20$$
$$0 \leq \beta \leq 1 .$$

Withdrawing product in the size ranges $20 \leq L_p \leq 100$ and $400 \leq L_p < 1600$ decreases the stability region while withdrawing in the ranges $100 < L_p < 400$, $1600 < L_p$ increases the stability region as depicted in figures 29 and 30 . Beyond about $L_p = 5000$ the increasing effect of L_p on the

system's stability saturates. Values of L_p beyond this point do not stabilize the system as do some other lesser values of L_p. In other words, the effect of L_p shows some minimum and maximum in the range $20 \leq L_p \leq 40000$. Figures 31 and 32 show almost the opposite trend for the stability condition with some minimum and maximum in the range $20 \leq L_p \leq 40000$. Figure 31 is an enlargement of the plot of the effect of L_p on the stability condition. Whether or not L_p has an increasing or decreasing effect on the system's stability depends on the size range of product removal. For the range of values of z* above there is no effect of this variable on either the system's stability or the stability condition. No plot is shown for this case. Figure 33 shows that increasing the parameter, β, increases the system's stability while figure 34 reveals that the opposite trend prevails for the stability condition. The parameters, z* and β, are important inasmuch as they are involved in the quantities z*(1-β) and z*β. The quantity z*(1-β) reflects the accelerated product removal rate while z*β reflects the recycling rate of some of the oversize crystals into the crystallizer. The stability region is enlarged when the product is withdrawn at a slow rate and some of the oversize crystals recycled into the crystallizer at a fast rate.

Effect of withdrawing intermediate size crystals ($2 \leq a \leq 20$). Figure 35 shows that withdrawing intermediate size crystals (crystals in the size range, $L_f \leq z \leq L_p$) may either increase or decrease the system's stability for small

values of intermediate size crystal withdrawal rate, a. For higher values of a, ($8<a\leq 20$) the system's stability maintains an increasing trend. Figure 36 shows an increasing trend for the stability condition for all values of a in the range ($2\leq a\leq 20$).

Effect of feed seeding ($0 \leq \int_{z_1}^{z_2} n_o(z)\, z^3 dz \leq 4050$). Increasing values of feed seeding increases the system's stability for the range of values of feed seeding investigated as shown in figure 37. Similarly, figure 38 shows that the stability condition increases with increasing feed seeding.

Effect of crystallizer void volume ($.04<\varepsilon_c<1$). The system's stability increases with increasing values of the parameter, ε_c, as shown in figure 39. On the contrary, the stability condition shows the opposite trend, decreasing with increasing values of ε_c as depicted in figure 40.

Effect of crystal's residence time ($.4\leq \nu_5 \leq 20$). Figures 41 and 42 show that increasing residence time decreases the stability region for the above range of values. A similar trend is shown by figures 43 and 44 for the stability condition.

Discussion

The results of the first part of this study indicate that it is quite possible to accurately quantify nucleation and growth rates from only crystal size distribution measurements in a steady state crystallizer. It also indicates that invoking the "zero size" assumption and

ignoring the birth function arising from nuclei generation are no longer necessary. Khambaty and Larson (1978) had speculated that the curvature in the population density plots of figures 9 and 10 could be due to the size dependence of the growth rate in the small size range. They also speculated that the curvature could be explained if only a few of the nuclei survived from the enormous number produced in the small size range. From these speculations they postulated what the shape of the birth function should be. The results shown in figures 11 and 14 support these speculations indicating that the majority of the nuclei were born into a size range smaller than the lowest measured size and later grew to populate the curved part of the population density in a size dependent fashion. This occurrence of the majority of the nuclei being born into a size range smaller than the lowest measured size has been confirmed by direct observation and measurement by Garside and Larson (1978) and Garside, Rusli, and Larson (1979). The results are also in accord with parts of the survival theory of Strickland-Constable (1972). The survival theory was originally stated to describe collision breeding. It states that particles are generated in a size range close to the size of the critical nucleus at a given supersaturation and that only a fraction of these particles survive according to the supersaturation that the particles are exposed to. It states that particles smaller than the critical size redissolve while those that are larger survive. The theory

further assumes that the number and size of the nuclei generated are independent of supersaturation, an assumption proven wrong by Sung et al. (1973) who observed otherwise. The results indicated in figure 14 show higher nucleation rates correspond to conditions of higher supersaturation and vice versa and is, therefore, in agreement with the findings of Sung et al. (1973), and with the review by Garside and Davey (1980) who indicated several researchers to have made similar observations. Among these researchers were Garside, Rusli and Larson (1979) who similarly observed increase in nucleation rates of potash alum with supersaturation.

Another result obtained in this study is the ability to estimate the quantity, L_c, defined in equation (3-6) as the size at which the growth rate is zero ($G(L_c) = 0$). The plots in figure 12 reveal that lower L_c values correspond to higher concentration, a result which is in agreement with part of the survival theory. By comparison, L_c would then be the critical size and as shown by the plots in figure 12 $G(\zeta)>0$ if $\zeta>L_c$ indicating survival and growth of nuclei having size greater than the critical size. Another work that lends credence to the results of this study is that of Rousseau and Parks (1981) who obtained size dependent growth rate for magnesium sulfate heptahydrate crystals under different conditions and for different size range. Sidkar and Randolph (1976) using the MSMPR technique were unable to determine size dependent growth rate for

magnesium sulfate heptahydrate system with data covering size range 5μm to 70μm under different conditions. They reported size independent growth rate of 2.12μm/min for the large size range to which the MSMPR technique applies, and suggested that the curvature in the population density plot was due size dependent growth rate. Garside and Jancic (1979) required a separate experiment to determine surface integration and mass transfer rates of potash-alum and combined these with the population balance to estimate the size dependent growth rate. However, attempts by these authors to use the size dependent growth rate, $G(\zeta)$, in equation (2-9) in calculating size dependent birth rate, $b(\zeta)$, resulted in negative birth function. Rather than interprete these as death rates, they suggested that the results were insufficiently accurate to determine $b(\zeta)$ by their method. Also evident from the plots in figures 11 and 12 is the possible occurrence of growth dispersion, a phenomenon that has been addressed by some researchers, a few of whom are Bennema (1976), Janse and de Jong (1976), Burton, Cabrera, and Frank (1951), Rousseau (1980), and Garside and Jancic (1979). Growth dispersion, as defined by Rousseau (1980) is the occurrence of different growth rates for crystals of the same size under identical conditions. As explained by Janse and de Jong (1976), it affects the crystal size distribution in the same manner as does the size dependent growth, because during growth dispersion the average growth rate of all

crystals with size, ζ, increases with size. As a result curvature in the semi-log plot of population density might be due in part to size dependent growth rate and growth dispersion. To tell which one predominates requires a separate experiment.

Very few researchers have tried to address the problem of obtaining nucleation and growth rates in unsteady state crystallizers. Garside and Jancic (1976) using separate surface integration and mass transfer rates experiment in addition to the population balance equation applied a very crude differential method to potash alum-water system. Their results show very large scatter such that their differential method holds very little or no promise for transient data. Randolph and Cise (1972), who had thought it was patently impossible to uniquely specify both size dependent nucleation and growth rates using only the single size dependent measurement $n(\zeta)$, had to assume zero birth to calculate the growth of potassium sulfate crystals and vice versa. They admitted that their technique gives the upper bound to the two quantities, nucleation and growth rates. In fact, their technique gives a gross overestimation of these quantities. Because these two quantities (nucleation and growth rates) are very fundamental in nature, their determination requires an accurate method, and by virtue of this requirement renders their method totally inadequate for transient data.

There were no assumptions whatsoever in the method described in this study. The only approximation was in the minimization procedure. Despite the fact that the data for pentaerythritol were very few and covered a very limited size range, the results were as expected. The $\overline{N}$ versus $\overline{X}$ plots were expected to be linear and indeed they were as shown by figure 18 , and the high coefficient of determination (greater than 0.98) obtained for each plot. The results indicate very small growth rate for pentaerythritol crystals in the small size range measured. Bujac (1976) who had separately carried out small particle growth studies of the same substance for a wide range of supersaturation (5-30%) concluded that the growth rates of the small crystals were very small, less than .01μm/min. Bujac did not indicate whether the growth rates were size dependent or not and neither did he indicate the method by which he arrived at his estimate. The fact that he could not obtain better values of the growth rates than a mere estimate of the upper bound suggests that his method is not accurate enough to handle transient data.

Errors arising from using minimization procedures can be kept very low by trying different, but adequate functional forms for the data and by using good regression subroutines. Because the only source of error in the method described in this study is the regression subroutine, it is not surprising that the results show the nucleation and growth rates to be determined to a high degree of accuracy (less than

10% error to within a confidence level of .90). The results are practically insensitive to values of $G(L_1)$ on the straight part of the curve in figure 17. Hence the results demonstrate that this method is not only more powerful than those previously existing in the literature but also very adequate for transient data.

Before discussing the results of the stability study some possible explanations of why certain parameters may affect the crystallizer the way they do are appropriate. It is well established that classification often reduces the stability region of the crystallizer. One might explain this by considering an MSMPR crystallizer operating at steady state. Now suppose that crystals in a certain size range are removed at a more accelerated rate than the MSMPR rate and that this removal is such that it reduces the total crystal area, A_T, significantly. During this removal the supersaturation remains unaffected so that the remaining crystals are now exposed to a relatively higher supersaturation. As a result new crystals are formed and the crystals remaining in the crystallizer continue to grow. The simultaneous formation of crystals and growth of the remaining crystals reach a state where the supersaturation becomes depleted so that nucleation and growth stop. The resultant area is now greater. However, since crystal removal is still going on we imagine that more crystals are removed so that a resultant total area results. Again the remaining crystals in the crystallizer are exposed to a relatively higher supersaturation which causes further

nucleation and growth of already existing crystals. As we continue to remove crystals in this fashion the crystal size distribution in the crystallizer oscillates. This oscillation is termed cycling. In the terminology of this study the phrase "decreasing the stability region" is used in place of cycling. In the above explanation it is assumed that the system exhibits time delay.

One can similarly explain why removal, dissolution, and recycling of fines often stabilizes a crystallizer, that is, enlarges the stability region. Removal of large quantities of fines results in a significant reduction of the total crystal area while recycling of the dissolved fines causes appreciable increase in supersaturation. As a result, nucleation and growth of existing crystals occur. However, fines are still being removed so that these newly formed crystals are removed almost as they formed. Only growth of existing crystals is emphasized and the tendency to retain large showers of the newly formed crystals is thereby eliminated. Continuing this process has a stabilizing effect on the crystallizer.

Feed seeding tends to damp out perturbations arising from cycling of nuclei when the seeds are introduced in the feed continuously, thereby stabilizing the crystallizer. There is practically no effect if all the seeds are introduced at the same time.

At low ε_c the suspension is dense. As a result secondary nucleation becomes the dominant mechanism of nuclei formation and hence the system's stability is reduced.

The results of the section dealing with stability indicate that the trend shown by the stability condition with respect to the various parameters cannot predict the trend of the system's stability. In other words, whether the stability condition is increasingly positive or decreasingly positive has no effect on the system's stability. These results are as expected since all that is required of the stability condition is that it be positive. The results show that recycling of dissolved fines at higher rates and at larger fines size increasingly stabilize the system. These results are also true for the case in which dissolved fines cause a proportionate increase in concentration of 30% (r=.3). Plots for this case are not shown. The above results are in agreement with the works of Sherwin, Shinnar and Katz (1967), Lei et al. (1971a), Randolph, Beer and Keener (1973), who all worked with point fines trap. By point fines trap it is meant that the operation is such that the dissolved fines recycled are of negligible mass. Randolph, Beer and Keener also examined the case where the amount of dissolved and recycled fines is not negligible. This case is designated by $r \geq .2$ in this study. Sherwin et al. (1967) studied a class I system while Lei et al. (1971a) and Randolph et al. both studied class II systems. However, by changing the parameter, y_o, from 1.01 to 1.3 or above one would obtain a class I system. The explanation of why recycling dissolved fines at larger fines size has already been given above.

The results show that recycling undissolved fines decreases the system's stability while recycling product size crystals increases it. A possible explanation is that recycling product size crystals must affect the system in a manner analogous to feed seeding at increasing feed size. In other words, recycling product size particles or feed seeding tends to deplete the system supersaturation by competing for the solute resources, thereby reducing the net nucleation rate. This stabilization is reflected in the increasing positivity of the eigen value, λ. On the contracy, the opposite is true for recycling undissolved fines. Neither the recycling of undissolved fines nor that of product size crystals has been studied before. Recycling some of the product size crystals could provide a way of operating a crystallizer stably. Further, the results indicate that product classification can stabilize or destabilize a crystallizer depending on the classification size. Thus the trend shown by the system's stability contains some minimum and maximum. Beyond very large L_p values the system's stability increases to an asymptotic value much lower than the stability exhibited at L_p=20. Randolph et al. (1973) showed that beyond a certain classification size, L_p, the system becomes destabilized. It seems they must have examined a range of classification sizes smaller than those examined here, in which case, their range would correspond to the range $20 \leq L_p \leq 100$ in this study. Classifying the product at very high rates destabilizes the

system, a result which is in agreement with Randolph et al. (1973). That the crystallizer is stabilized by either feed seeding and/or seed size is in agreement with the results obtained by Randolph et al. (1973) and Hulburt and Stefango (1969).

The above results indicate that the accelerated removal rate, a, of intermediate size crystals may stabilize or destabilize the crystallizer. However, higher values of a increases the system's stability. Thus removing crystals of intermediate size at higher values of a might provide a way of stably operating a crystallizer that is unstable under a given condition. Values of a other than a=1 have not been investigated. Increasing crystallizer void volume, ε_c, especially in the range $.7 \leq \varepsilon_c \leq .95$ results in a slight increase in crystallizer's stability in agreement with Sherwin, Shinnar and Katz (1967) and Yu and Douglas (1975).

The results further show that long retention times decreases the system's stability. These findings are in agreement with those of Song and Douglas (1975) who experimentally observed oscillations. The effects of size dependent nucleation and growth rates on crystallizer's stability were simulated. Because both the birth and growth functions contain exponential terms, size independent growth and birth functions were obtained by setting each exponent in the exponential terms of these functions equal to zero. Plots were not shown for this. The results of the computer simulation indicate that size dependent growth rate does not

affect the system's stability while size dependent birth rate decreases it. Sherwin, Shinnar and Katz (1967) by using a growth rate that is linear in size concluded that size dependent growth rate stabilizes the system, and hence, there is no need to include size dependent growth rate in stability analysis. The results here show that the stability remains constant whether the growth rate is size dependent or not. The effect of size dependent birth rate has neven been studied until now. The usual practice adopted by researchers is to assume that the birth function is size independent, due to the fact that it simplifies the mathematical analysis. The result here indicates that constant birth function would result in greater system's stability, and therefore, may indicate that an unstable system is stable. The claim about size dependent growth and nucleation rates made in this study may not be very general since it is derived from example data that were not obtained from experiment.

It is important to note that the computer simulation and the stability criteria agree in all cases.

CHAPTER V
SUMMARY, IMPLICATIONS, CONCLUSIONS, AND RECOMMENDATIONS FOR FUTURE RESEARCH

Summary

Emphasis was placed on industrial interests and application throughout this study. The derivations of the various relationships and the whole study took into account the fact that certain quantities might not be readily accessible. It was necessary to utilize some data so that the reader would know how to apply the methods developed in this study. The general methods prevented here for the determination of nucleation and growth rates for the small size range in both steady and unsteady state crystallizers were not explored fully by previous investigators. In fact, researchers thought that it was impossible to determine nucleation and growth rates using only the crystal size distribution measurement. Though stability criteria have been developed for very simple and idealized crystallizer models by previous investigators, none has been developed for a crystallizer as complex as that examined in this study. The purposes of this study are to devise methods for quantifying nucleation and growth rates in steady and unsteady state crystallizers, and establish genuine stability criteria for complex crystallizers

such as that studied here. Chapter I dealt with the introduction of the subject, statement of the problem, purpose and need for the study, definition of terms, and organization of the remainder of the study. Pertinent literature was reviewed in Chapter II. The topics treated in Chapter II range from primary and secondary nucleation to dynamics, stability and control of crystallizers. Both class I and class II crystallizers were addressed in Chapter II. The methodology used in this study was described in Chapter III. A description of the theory and some procedure to be followed, when applying the methods developed in this study, are included in this chapter. The data and the results of this study were reported in Chapter IV followed by a discussion of those results. The results indicated that the techniques for obtaining nucleation and growth rates in steady and unsteady state crystallizers are effective and that the dynamics of a crystallizer with respect to its parameters can be monitored with the criteria developed here.

Implications

Implications of this study are reflected throughout crystallization theory and practice. Hardly is there any measurement in crystallization that does not directly or indirectly involve nucleation and growth rates. Even measurements of the effects of crystallizer parameters,

such as impact energy, impeller speed, and concentration of impurities involve nucleation and growth rates. Improper estimation of the nucleation and growth rates may lead to wrong conclusions about the effects of the various system parameters. Also fundamental studies such as that involving the development of nucleation and growth mechanisms require the estimation of nucleation and growth rates in the testing of the mechanisms. Again, improper estimation of nucleation and growth rates may lead to the selection of incorrect nucleation and growth mechanisms. In addition, nucleation and growth rates are very important in determining whether a crystallizer is stable or not. Thus the importance of these two fundamental quantities, nucleation and growth rate cannot be overemphasized. Obtaining very good stability criteria, such as that described in this study, is the most important step towards designing and operating a crystallizer to ultimately control the crystal size distribution in order to meet some product specification requirement. Embedded in the criteria described in this study are many crystallizer's parameters. The effects of these parameters on the crystallization can be monitored efficiently. In addition, the computer simulation reveals new ways of stably operating a crystallizer.

Conclusions

It has been shown that time dependent crystal size distribution can be represented by a functional form that is separable. An adequate method for calculating the critical size, L_c, in both steady and unsteady state crystallizers has been developed. The growth rate or the average growth rate and birth rate are size dependent in the small size range and most nuclei are formed in a range of size below the lowest measured size. Most importantly, new accurate methods have been developed for accurately quantifying growth and birth rates in steady and unsteady state crystallizers.

The stability analysis in this study reveals that recycling crystals of product size and withdrawing crystals of intermediate size at highly accelerated rates stabilizes the crystallizer. Also a classified crystallizer can be stable or unstable depending upon the size and the rate at which the classification occurs. The computer simulation of the stability criteria shows that size dependent growth does not affect crystallizer's stability while size dependent birth decreases it. Because the computer simulation was based on an example data, which was not obtained from experiment, this claim may not be general. Based on the results of this study it is concluded that a novel method for investigating the stability of a crystallizer has been established in this study. This method is capable of predicting stability in both class I and class II systems,

and in systems where the mass of dissolved fines may or may not be negligible. The computer simulation and the stability criteria agree in all cases.

Recommendations for Further Research

The following recommendations for further research stem from the results of this study.

1. Different expressions that preserve the physical behavior should be fitted to steady state and transient size distribution data to choose the expression that best represents the data. Experiments are to be carried out with both batch and continuous crystallizers to provide more complete transient data.
2. Numerical study of the complete set of the nonlinear equations be carried out to simulate the effects of the crystallizer parameters. Then some special transformation should be used to cast the equations into a closed set of nonlinear moment equations to which the second method of Lyapunov is applied. The second method of Lyapunov, which may be applied numerically, and then analytically, will provide a way to study the crystallizer's stability.
3. Bifurcation theory coupled with multiple time scale perturbation methods should be applied to the complete set of equations to predict oscillations with time dependent amplitude. Then a comparison of all the methods should be made.

4. Because there are many possible results embedded in the criteria developed in this study, it should be explored further, and a three-dimensional stability plot made to display the results. In addition, the effects of size dependent nucleation and growth rates should be studied in detail, and preferably with data obtained from industry.
5. Further research is required to determine the optimal set of classification functions for a desired product size distribution. This is a problem of distributed parameter control theory, and the classification functions are the control variables.

APPENDIX A
DERIVATION OF THE CRYSTALLIZER POPULATION BALANCE

Let ψ represent some entities in some volume in space. The entities ψ have two types of coordinates associated with them, namely, internal and external coordinates. The external coordinates are mainly spatial coordinates describing the position of the entities, ψ, and are designated as x,y,z. On the other hand, internal coordinates are intrinsic property such as age, color, size, activity, etc., and are designated $\zeta_1,\ldots,\zeta_m$. Thus the entities, ψ, are a function of both the external and internal coordinates,

$$\psi = \psi(x,y,z,\zeta,\ldots,\zeta_m)$$

Suppose some entities, ψ, are enclosed in a geometric volume element, $\Delta v = \Delta x\Delta y\Delta z$, then the fraction of entities enclosed is given by $\psi\Delta x\Delta y\Delta z\Delta\zeta,\Delta\zeta_2\ldots\Delta\zeta_m$. Since all of the entities must be in some region and must have a property value, the probability of this occurring is 1,

$$\int \psi(x,y,z,\zeta\ldots,\zeta_m)dxdydzd\zeta_1\ldots d\zeta_m = 1 \qquad \text{(A-1)}$$

$$B = \frac{\text{\# of entities born}}{(\text{unit time})(\text{unit geometric volume})(\text{unit property change})}$$

$$D = \frac{\#\text{ of entities dead}}{(\text{unit time})(\text{unit geometric volume})(\text{unit property change})} .$$

A material balance for an arbitrary small volume element in space R is given by,

Accumulation = net generation .

That is,

$$\frac{d}{dt}\int_R \psi dR = \int_R b_n dR \qquad \text{(A-2)}$$

where b_n = net birth (net generation) = B-D

$$dR = dxdydzd\zeta_1 \ldots d_{\zeta m}$$

$$\int_R = \int_x \int_y \int_z \int_{\zeta_1} \cdots \int_{\zeta_m} . \qquad \text{(A-3)}$$

Recalling Liebnitz rule,

$$\frac{d}{dt}\int_{a(t)}^{b(t)} f(x,t)dx = \int_{a(t)}^{b(t)} \left\{\frac{\partial}{\partial t} f(x,t)\right\}dx + [f(b(t),t)]\frac{db(t)}{dt} - [f(a(t),t)]\frac{da(t)}{dt}$$

$$= \int_{a(t)}^{b(t)} \left\{\frac{\partial}{\partial t} f(x,t) + \frac{d}{dx}\left[\frac{dx}{dt} f(x,t)\right]\right\}dx . \qquad \text{(A-4)}$$

Similarly,

$$\frac{d}{dt}\int_{R(t)} \psi dR = \int_R \left[\frac{\partial \psi}{\partial t} + \sum_{\ell} \frac{\partial}{\partial \ell}\left(\frac{\partial \ell}{\partial t}\psi\right)\right] dR$$

where

$$\ell = \{x, y, z, \zeta_1, \ldots, \zeta_m\} \ . \tag{A-5}$$

when $\ell = x$, $\frac{d\ell}{dt} = \frac{dx}{dt} \triangleq v_x$

when $\ell = \zeta_i$, $\frac{d\ell}{dt} = \frac{d\zeta_i}{dt} \triangleq v_i$.

Thus external and internal velocities, which are respectively $\vec{v}_e$ and $\vec{v}_i$, are represented as shown below,

$$\vec{v}_e = \begin{pmatrix} v_x \\ v_y \\ v_z \end{pmatrix} \ ; \qquad v_i = \begin{pmatrix} v_1 \\ v_2 \\ \vdots \\ v_m \end{pmatrix} \ . \tag{A-6}$$

The expression in equation (A-5) implies

$$\frac{d}{dt} \int_{R(t)} \psi dR = \int_R \left\{ \frac{\partial \psi}{\partial t} + \frac{\partial}{\partial x} (v_x \psi) + \frac{\partial}{\partial y} (v_y \psi) + \frac{\partial}{\partial z} (v_z \psi) \right\} dR$$

$$+ \int_R \left[\sum_{i=1}^{m} \frac{\partial}{\partial \zeta_i} (v_i \psi) \right] dR$$

$$= \int_R \left[\frac{\partial \psi}{\partial t} + \nabla \cdot (\vec{v}_\ell \psi) + \nabla \cdot (\vec{v}_i \psi) \right] dR$$

$$= \int_R \left[\frac{\partial \psi}{\partial t} + \nabla \cdot (\vec{v} \psi) \right] dR$$

where

$$\vec{v} = \vec{v}_e + \vec{v}_i \ .$$

Thus equation (A-3) becomes,

$$\int_R \left[\frac{\partial \psi}{\partial t} + \nabla \cdot (\vec{v}\psi)\right] dR = \int_{b_n} dR$$

$$\Rightarrow \int_R \left[\frac{\partial \psi}{\partial t} + \nabla \cdot (\vec{v}\psi) - b_n\right] dR = 0 \qquad \text{(A-7)}$$

Since region, R, was arbitrary, a necessary condition is for the integrand of equation (A-7) to be zero,

$$\frac{\partial \psi}{\partial t} + \nabla \cdot (\vec{v}\psi) - b_n = 0 \ . \qquad \text{(A-8)}$$

While R is a more general space of internal and external coordinates, the geometric volume, V, of the vessel, is a function only of the external coordinates, x,y,z. Integrating (A-8) over V gives,

$$\int_V \frac{\partial \psi}{\partial t}\, dV + \int_V \nabla \cdot [(\vec{v}_e + \vec{v}_i)\psi] dV - \int_V b_n dV = 0$$

$$\int_V \frac{\partial \psi}{\partial t}\, dV = \frac{d}{dt} \int_V \psi dV - \int_V \nabla \cdot (\vec{v}_s \psi) dV$$

$\vec{v}_s$ = velocity of any part of surface S enclosing volume, V . (A-9)

Using Gauss' divergence theorem the above equation becomes,

$$\frac{d}{dt} \int_V \psi dV + \int_s n \cdot (\vec{v}_e - \vec{v}_s)\psi ds + \int_V [\nabla \cdot (\vec{v}_i \psi) - b_n] dV = 0$$

$$\text{i.e., } \frac{d}{dt}(V\bar{\psi}) + \int_s n \cdot (\vec{v}_e - v_s)\psi ds + [\nabla \cdot (\vec{v}_i \psi) - b_n]V = 0$$

$\bar{\psi} = \frac{1}{V}\int_V \psi dV$ and $[\nabla\cdot(\vec{v}_i\psi)-b_n]$ is constant with respect to integration over external coordinate volume, V, due to its being a function of intrinsic coordinates only. Dividing through by V,

$$\frac{1}{V}\frac{d}{dt}(V\bar{\psi}) + \frac{1}{V}\int_s n\cdot(\vec{v}_e-\vec{v}_s)\psi d_s + \nabla\cdot(\bar{v}_i\psi) - b_n = 0 \ . \quad \text{(A-10)}$$

For a vessel with several inlets and outlets,

$$\int_s n\cdot(\vec{v}_e-\vec{v}_s)\psi d_s = \sum_k Q\ \psi_k \quad \text{(A-11)}$$

K designates inlet or outlet flow. For an inlet flow,

$$n\cdot(\vec{v}_e-\vec{v}_s) = -v_{in}\ , \qquad \psi = \psi_{in}\ . \quad \text{(A-12)}$$

For an outlet flow

$$n\cdot(\vec{v}_e-\vec{v}_s) = +v_{out}\ , \qquad \psi = \psi_{out}\ . \quad \text{(A-13)}$$

If it is also assumed that ψ is constant over the inlet and outlet surfaces, then

$$\int_{s_{in}} v_{in}\ \psi_{in}\ d\ s_{in} = \psi_{in}\int_{s_{in}} v_{in}\ d\ s_{in} = \psi_{in}Q_{in}\ . \quad \text{(A-14)}$$

Similarly,

$$\int_{s_{out}} v_{out}\ \psi_{out}\ d\ s_{out} = \psi_{out}\ Q_{out} \quad \text{(A-15)}$$

Thus equation (A-10) becomes

$$\frac{1}{V}\frac{d}{dt}(V\bar{\psi}) + \sum_{k}\frac{Q_k\psi_k}{V} + \sum_{i=1}^{m}\frac{\partial}{\partial\zeta_i}(v_i\psi) - b_n = 0 \quad . \tag{A-16}$$

For a crystallizer with one inlet and one outlet flow,

$$\sum_{k}\frac{Q_k\psi_k}{V} = \frac{1}{V}(-n_{in}Q_{in} + n_oQ_o)$$

where

$$\bar{\psi} = n = \text{number of crystals that have size, at time, } t \quad . \tag{A-17}$$

Subscripts "in" and "o" indicate inlet and outlet respectively. Also, when there is just a single internal property or co-ordinate that is of interest, such as the crystal size in a crystallizer, then the following is true,

$$i = 1 \quad , \qquad v_1 = G = \frac{d\zeta_1}{dt} = d\zeta \tag{A-18}$$

The single subscript, "1", in the above equation has been dropped. The term, G, denotes the crystal growth rate. Combining equations (A-16), (A-17), and (A-18), results in the following expression,

$$\frac{1}{V}\frac{\partial}{\partial t}(Vn) + \frac{\partial}{\partial\zeta}(Gn) = b_n + \frac{1}{V}(n_{in}Q_{in} - n_oQ_o) \quad . \tag{A-19}$$

Furthermore, for a well-mixed crystallizer equation (A-19) reduces to

$$\frac{1}{V}\frac{\partial}{\partial t}(Vn) + \frac{\partial}{\partial\zeta}(Gn) = b + \frac{1}{V}(n_{in}Q_{in} - nQ_o) \quad , \tag{A-20}$$

where the subscript "n" on b has been dropped. This concludes the derivation of the population balance equation.

APPENDIX B
ERROR ANALYSIS FOR THE DETERMINATION OF GROWTH AND BIRTH FUNCTIONS

The error analyses for the determination of growth and birth functions in steady and unsteady state crystallizers are shown below. These error analyses represent gross overestimation of the actual error because we do not consider the possibility of cancellation of errors. The errors alternate in signs and some of them may actually cancel out.

Steady state case. Consider the following equations

$$G(\zeta)n(\zeta) = \int_{L_c}^{\zeta} b(\Lambda)d\Lambda - \frac{1}{\tau}\int_{L_c}^{\zeta} n(\Lambda)d\Lambda \qquad (3\text{-}7)$$

$$b(\zeta) = \alpha_1 e^{-\alpha_2(\zeta - L_c)} \qquad (3\text{-}8)$$

$$n(\zeta) = C_1\exp(-\gamma_1\zeta) + C_2\exp(-\gamma_2\zeta) \qquad (3\text{-}9)$$

Let $B(\zeta)$ be defined as follows,

$$B(\zeta) = \int_{L_c}^{\zeta} \alpha_1 e^{-\alpha_2(\Lambda - L_c)}\, d\Lambda = \int_{L_c}^{\zeta} b(\Lambda)d\Lambda \ . \qquad (B\text{-}1)$$

Let α denote the fractional error in the measurement of $n(\zeta)$ and let the corresponding birth and growth functions due

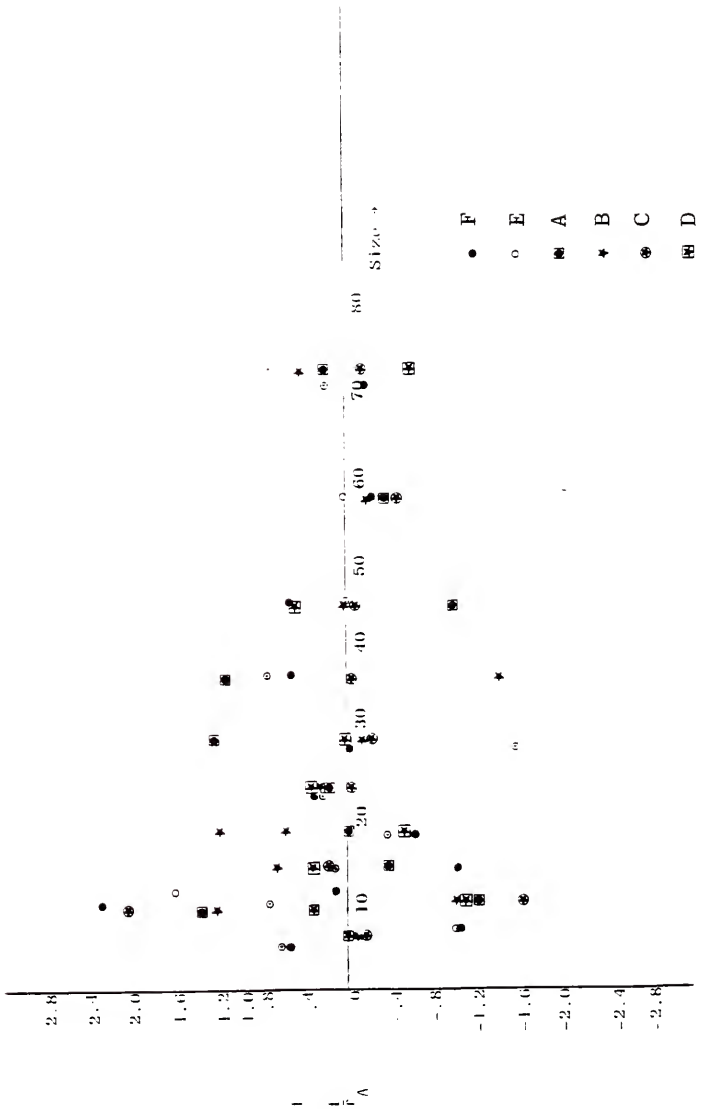

Figure 45. Plot of Standard Error Versus Size for Unsteady State Data. A, B, C, D in figure 11; E, F in figure 10.

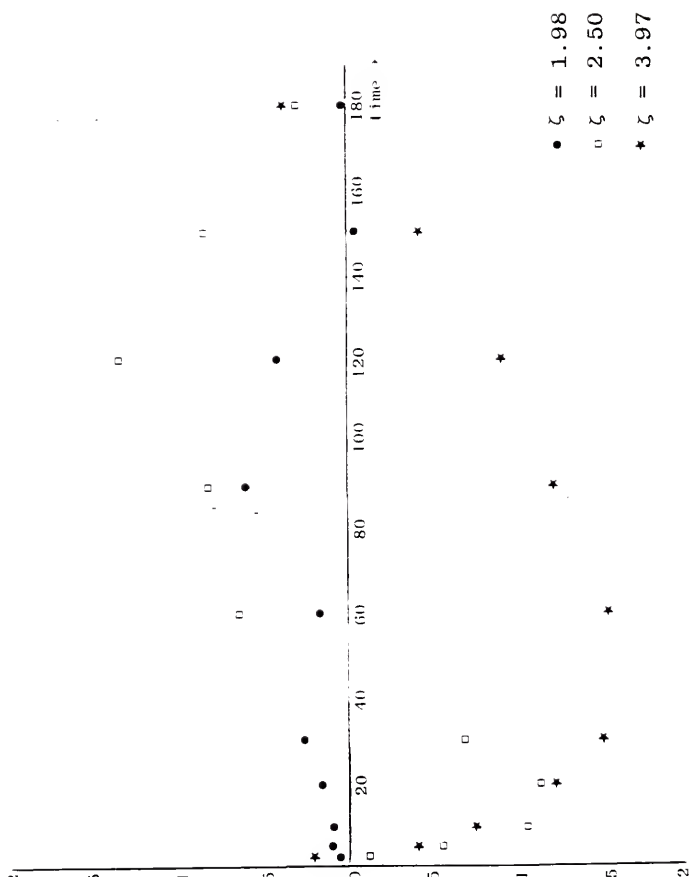

Figure 46. Plot of Standard Error Versus Time for Transient Data.

to this error be represented by B_1 and G_1 respectively. Thus we define B_1 in equation (B-2)

$$B_1(\zeta) = B(\zeta) + \varepsilon B(\zeta) \tag{B-2}$$

where ε represents the fractional error in $B(\zeta)$. Since equation (3-8) represents a model for $b(\zeta)$ the error in $B(\zeta)$, ε, is strictly the error arising from minimizing over α_1, α_2 and L_c. Combining equations (3-8), (B-1) and (B-2) we obtain

$$G_1 = \frac{B(\zeta) + \varepsilon B(\zeta) - \frac{1}{\tau}\int_{L_c}^{\zeta} (1+\alpha)n(\Lambda)d\Lambda}{(1+\alpha)n(\zeta)} \tag{B-3}$$

$$G_1(\zeta) < \frac{B(\zeta) - \frac{1}{\tau}\int_{L_c}^{\zeta} n(\Lambda)d\Lambda}{n(\zeta)} + \frac{\varepsilon B(\zeta) + \frac{1}{\tau}\alpha\int_{L_c}^{L_c} n(\Lambda)d\Lambda}{n}$$

$$G_1(\zeta) < G(\zeta) + \max(\varepsilon,\alpha)\left[B(\zeta) + \frac{1}{\tau}\int_{L_c}^{\zeta} n(\Lambda)d\Lambda\right] \tag{B-4}$$

Because the error, ε, arising from minimizing over α_1, α_2 and L_c was much less than α, we obtain

$$G_1(\zeta) << G(\zeta) + \alpha G(\zeta)$$

$$\frac{G_1(\zeta) - G(\zeta)}{G(\zeta)} = \frac{\Delta G}{G(\zeta)} < \alpha \tag{B-5}$$

Since $\varepsilon < \alpha/5$, the fraction error in $B(\zeta)$, is given by

$$\frac{\Delta B}{B} < \alpha/5 \ . \qquad \text{(B-6)}$$

The value of α for each of the plots is shown in table B-1

Table B-1
Values of α

Figure	Plot	α-values in percent
9	F	.064x100%
9	E	.086x100%
10	A	.066x100%
10	B	.098x100%
10	C	.060x100%
10	D	.064x100%

We present below a method for calculating α values. Define chi-square, χ^2, as follows

$$\chi^2 = \sum_{i=1}^{N} \left[(f_i - f_{Ai})/\alpha f_i\right]^2 \qquad \text{(B-7)}$$

where f_i and f_{Ai} are respectively the original data and the fitted value. Solving for α we obtain

$$\alpha = \left\{\frac{1}{df} \sum_{i=1}^{N} \left[(f_i - f_{Ai})/f_i\right]^2\right\}^{1/2} \qquad \text{(B-8)}$$

where df is the degrees of freedom, and plot $\Delta f_i/(\alpha f_{Ai})$ versus size as shown in figure 45 . The quantities,

$\Delta f_i/(\alpha f_{Ai})$, i=1,2,...,N are in units of standard deviation. It can be seen from figure 45 that the errors are randomly distributed for each i, and that the errors represent percent errors. In order to show what confidence level we place on the calculated values of $G(\zeta)$ and $B(\zeta)$ we use the student t distribution since N<30. Then $G(\zeta)$ and $B(\zeta)$ are represented respectively as $G(\zeta) \pm \alpha G(\zeta)$ and $B(\zeta) \pm \alpha B(\zeta)$ with a confidence level λ given by the t distribution $t_{df,\lambda}$. In other words, we are 100λ percent confident that the errors should lie within $t_{df,\lambda}$ times the standard deviation. We are, therefore, implying that $10(1-\lambda)$ out of every 10 data should lie outside the above limits, $t_{df,\lambda}$. The fact that all the data lie within these limits as shown in figure 45 is another indication that the fractional errors, α, determined above have been grossly overestimated. Given λ=.90 the student t values for the cases with eleven data points and twelve data points are given below,

$$N = 12 , \quad d_f = 8 , \quad t_{8,0.9} = 1.86$$
$$N = 11 , \quad d_f = 7 , \quad t_{8,0.9} = 1.90 .$$

Unsteady state (batch crystallizer) case. Consider the following equations,

$$\bar{N}(L_k,t_m) = -G(L_k)\bar{X}(L_k,t_m) + \bar{B}(L_k) \qquad (3\text{-}17)$$

$$\bar{B} = \int_{L_1}^{L_k} b(\zeta)d\zeta \qquad (3\text{-}17a)$$

$$\bar{X} = \frac{1}{t_m - t_1} \int_{t_1}^{t_m} n(L_k, \tau) d\tau \qquad (3\text{-}17b)$$

$$\bar{N} = \frac{\int_{L_1}^{L_k} n(\zeta, t_m) d\zeta}{t_m - t_1} - \frac{\int_{L_1}^{L_k} n(\zeta, t_1) d\zeta}{t_m - t_1} - \frac{G(L_1) \int_{t_1}^{t_m} n(L_1, \tau) d\tau}{t_m - t_1} \qquad (3\text{-}17c)$$

The error in the fit for $n(\zeta,t)$ which is shown in figure is a mixture of absolute, c_1, and percent error, c_1 . Let us denote this error by $c_1(1+\alpha)$. Let the fractional error in $G(L_1)$ and in the fit of equation (3-17) be denoted by λ and ε respectively. The error in $G(L_1)$ is very small compared to the error in the fit for $n(\zeta,t)$, that is, $\varepsilon << c_1(1+\alpha)$. The error in equation (3-17) is strictly due to the error in $\bar{N}$ and $\bar{X}$, which also have errors that arise from the error in $n(\zeta,t)$. The fact that the plot for $\bar{N}$ versus $\bar{X}$ is almost perfect (coefficient of determination, CD>0.98) suggests that $\lambda << c_1(1+\alpha)$.

For various values of α one can calculate the corresponding values of c_1 from equation (B-9),

$$c_1 = \left[\frac{1}{df} \sum_{i=1}^{N} \left((f_i - f_{Ai}) / (1+\alpha f_i) \right)^2 \right]^{1/2} . \qquad (B\text{-}9)$$

One then chooses the pair, (α, c_1) that best describes the data. This choice might be based on the randomness of the error. A pair, (α, c_1) that gives certain pattern of errors that is very unlikely to occur. The values of α examined

are .02, .05, .09, .11, .13, .15, .20, .25, .30. For the data under consideration the pair, (.30, .18) was chosen. The following equation taken from Chapter III is pertinent to this error analysis,

$$\int_{L_1}^{L_k} n(\zeta,t_m)d\zeta - \int_{L_1}^{L_k} n(\zeta,t_1)d\zeta + G(L_k)\int_{t_1}^{t_m} n(L_k,\tau)d\tau - G(L_1)\int_{t_1}^{t_m} n(L_1,\tau)d\tau = (t_m-t_1)\int_{L_1}^{L_k} b(\zeta)d\zeta \quad . \tag{B-10}$$

The error in n is $c_1\alpha+c_1$. The equation corresponding to equation (B-10) as a result of these errors would be

$$\int_{L_1}^{L_k} [(1+\alpha_2)n(\zeta,t_m) + c_1]d\zeta - \int_{L_1}^{L_k} [(1+\alpha_2)\, n(\zeta,t_1) + c_1]d\zeta + G(L_k)\int_{t_1}^{t_m} [(1+\alpha_2)n(L_k,\tau) + c_1]d\tau - G(L_1)\int_{t_1}^{t_m} [(1+\alpha_2)n(L_1,\tau) + c_1]d\tau = (t_m-t_1)\int_{L_1}^{L_k} b(\zeta)d\zeta$$

where $c_1\alpha = \alpha_2$.

Using the definitions of equations (3-17) through (3-17c) the above equation becomes

$$(1+\alpha_2)\bar{N} = -(1+\alpha_2)G(L_k)\bar{X} + \bar{B} + C_1[G(L_k - G(L_1)] \tag{B-11}$$

The worst that can happen is for the errors in $\overline{N}$ and $\overline{X}$ to be different in which case the following equation is obtained,

$$(1+\alpha_2)\overline{N} = -(1+\hat{\alpha}_2)G(L_k)\overline{X} + \overline{B} + C_1[G(L_k)-G(L_1)] \qquad \text{(B-12)}$$

where α_2 is different from $\hat{\alpha}_2$.

$$\left.\frac{\partial \overline{N}}{\partial \overline{X}}\right|_{L_k} = \frac{(1\pm\alpha_2)}{(1\pm\alpha_2)} G(L_k)$$

or

$$G(L_k) = \frac{(1\pm\alpha_2)}{(1\pm\hat{\alpha}_2)} \frac{\partial \overline{N}}{\partial \overline{X}} .$$

A one-term Taylor series expansion of $\frac{1}{1\pm\hat{\alpha}_2}$ is $1\mp\hat{\alpha}_2$ + higher order terms. Thus

$$G(L_k) = (1\pm\alpha_2)(1\mp\hat{\alpha}_2) \frac{\partial \overline{N}}{\partial \overline{X}} = [1\pm\alpha_2\mp\hat{\alpha}_2+\text{H.O.}] \frac{\partial \overline{N}}{\partial \overline{X}} . \qquad \text{(B-13)}$$

The error in $G(L_k)$ is approximately $\pm\alpha_2\mp\hat{\alpha}_2$. If the errors are totally uncorrelated, then the error, $\tilde{\alpha}$ in $G(L_k)$ is given by

$$\tilde{\alpha} \leq \left\{[\max(\alpha_2,\hat{\alpha}_2)]^2 + [\max(\alpha_2,\hat{\alpha}_2)]^2\right\}^{1/2} . \qquad \text{(B-14)}$$

Suppose $\max(\alpha_2,\hat{\alpha}_2) = \alpha_2$, then $\tilde{\alpha} \leq \sqrt{2}\alpha_2$. If the errors are correlated and equal, we obtain,

$$\tilde{\alpha} = \sqrt{2}\alpha_2 . \qquad \text{(B-15)}$$

The error in $\overline{B}$ is given by

$$C_1(G(L_k) - G(L_1)] \tag{B-16}$$

Hence we can write $G(L_k)$ and $\bar{B}(L_k)$ as shown below

$$G(L_k) \sim G(L_k) \pm \sqrt{2}\ \alpha_2 G(L_k) \tag{B-17}$$

$$\bar{B}(L_k) \sim \bar{B}(L_k) \pm C_1(G(L_k)-G(L_1)) \tag{B-18}$$

For the data under examination, equations (B-17) and (B-18) result in the expressions below

$$G(L_k) \sim G(L_k) \pm .08G(L_k) \tag{B-17a}$$

$$\bar{B}(L_k) \sim \bar{B}(L_k) \pm .18G(L_k) \tag{B-18a}$$

where $G(L_1) = 10^{-7}$ has been dropped.

The values of $G(L_k)$ and $\bar{B}(L_k)$ are tabulated below

Table B-2
Cummulative Birth and Growth Rates

L_k	$\bar{B}x10^{-6}$	G
2.25	.050303	.0073832
2.50	.085839	.014658
3.00	.14068	.032494
3.50	.18102	.056929
3.97	.20976	.088393

The values in equations (B-17a) and (B-18a) are valid to within a confidence level of 0.90. The confidence level of 0.9 is found in a way similar to the steady state case. The t-statistic for this case is $t_{18,0.9} = 1.73$. This concludes our discussion on error analysis.

APPENDIX C
THE DETERMINATION OF SEPARABLE GROWTH AND BIRTH FUNCTIONS

We take transient data for different concentrations $\sigma_1, \sigma_2, \ldots, \sigma_n$ as depicted in figures 47 and 48. We assume without loss of generality, and for the purpose of this illustration that the data represented in figures 47 and 48 are taken from a batch crystallizer. The batch crystallizer is chosen mainly because the data used for illustration in Chapter IV is taken from a batch crystallizer. We could have used a continuous unsteady state crystallizer.

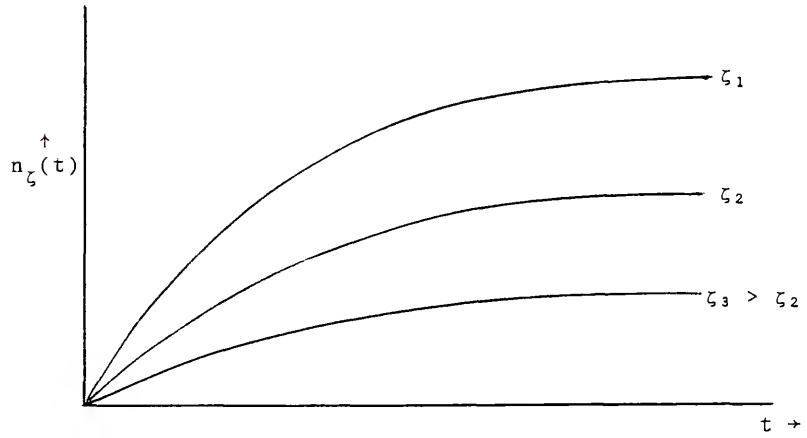

Figure 47. Time Dependent Number Size Distribution for a Fixed Concentration, σ_1.

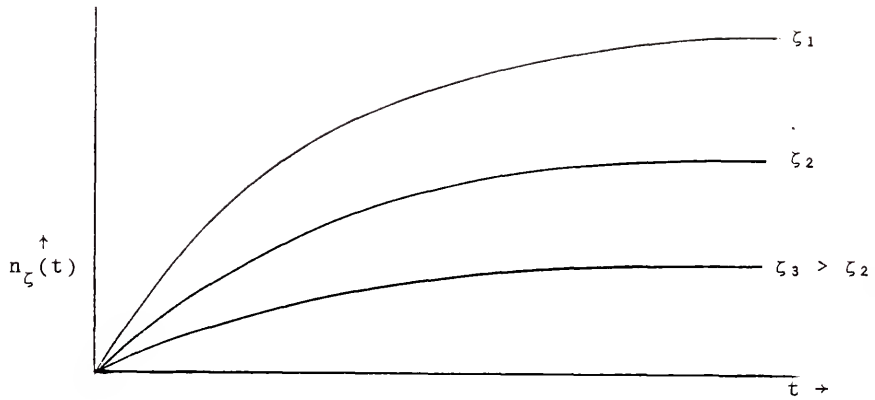

Figure 48. Time Dependent Number Size Distribution for a Fixed Concentration, C_2.

Here we adopt the notations $n(x,t) = n_x(t)$, which denotes $n(x,t)$ as a function of time for fixed x values. Similarly $G(c,\zeta)$ is represented as $G_c(\zeta)$ or $G_\zeta(c)$. The method for determining separable growth and birth functions represented by equations (3-44) and (3-45) is easily followed by the procedure outlined below,

$$G(c,\zeta) = g(c)\phi(\zeta) \qquad (3\text{-}44)$$

$$B(c,\zeta) = \sigma(c)b(\zeta) \ . \qquad (3\text{-}45)$$

Step 1. First obtain data as in figures and .

Step 2. For each fixed concentration use the already deviced method outlined in Chapter III to obtain size dependent growth and birth functions. For examle, the growth rate, G, obtained might look like the data shown in figure for different fixed concentrations.

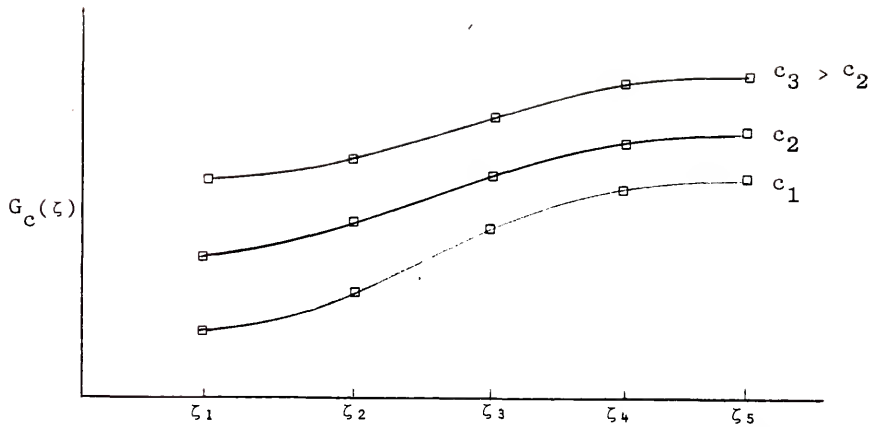

Figure 49. Growth Rate, $G(c,\zeta)$ as a Function of Size and Concentration.

Step 3. The separable form chosen for $G(c,\zeta)$ demands that the following be true if we let $\phi(x_1) = k$, where k is an arbitrary constant,

$$\frac{k\, G_{c_1}(\zeta_2)}{G_{c_1}(\zeta_1)} = \phi(\zeta_2)\,, \qquad \frac{k\, G_{c_2}(\zeta_2)}{G_{c_2}(\zeta_1)} = \phi(\zeta_2)$$

$$\frac{k\, G_{c_1}(\zeta_3)}{G_{c_1}(\zeta_1)} = \phi(\zeta_3)\,, \qquad \frac{k\, G_{c_2}(\zeta_3)}{G_{c_2}(\zeta_1)} = \phi(\zeta_3) \qquad \text{(C-1)}$$

$$\vdots \qquad\qquad \vdots$$

$$\frac{k\, G_{c_1}(\zeta_n)}{G_{c_1}(\zeta_1)} = \phi(\zeta_n)\,, \qquad \frac{k\, G_{c_2}(\zeta_n)}{G_{c_2}(\zeta_1)} = \phi(\zeta_n)\,.$$

Equating the ϕ's yield the following necessary conditions for separability,

$$\begin{aligned} G_{c_1}(\zeta_2)G_{c_2}(\zeta_1) &= G_{c_1}(\zeta_2)G_{c_1}(\zeta_1) \\ G_{c_1}(\zeta_3)G_{c_2}(\zeta_1) &= G_{c_2}(\zeta_3)G_{c_1}\zeta_1 \\ &\vdots \qquad\qquad \vdots \\ G_{c_1}(\zeta_n)G_{c_2}(\zeta_1) &= G_{c_2}(\zeta_n)G_{c_1}\zeta_1 \ . \end{aligned} \tag{C-2}$$

One can similarly obtain the functions, $g(c_i)$, i=1,2,...n as shown below

$$\begin{aligned} \frac{1}{k}\, G_{\zeta_1}(c_1) &= g(c_1) \\ \frac{1}{k}\, G_{\zeta_1}(c_2) &= g(c_2) \\ \vdots \qquad &= \vdots \\ \frac{1}{k}\, G_{\zeta_1}(c_n) &= g(c_n) \ . \end{aligned} \tag{C-3}$$

Also the functions, $g(c_i)$, i=1,2,...n, can be expressed as shown below,

$$\begin{aligned} \frac{1}{k}\, G_{\zeta_2}(c_1) \quad \left[\frac{G_{c_1}(\zeta_2)}{G_{c_1}(\zeta_1)}\right] &= g(c_1) \\ \frac{1}{k}\, G_{\zeta_2}(c_2) \quad \left[\frac{G_{c_1}(\zeta_2)}{G_{c_1}(\zeta_1)}\right] &= g(c_2) \ . \\ \vdots \qquad\qquad\qquad\quad \vdots \\ \frac{1}{k}\, G_{\zeta_2}(c_n) \quad \left[\frac{G_{c_1}(\zeta_2)}{G_{c_1}(\zeta_1)}\right] &= g(c_n) \end{aligned} \tag{C-4}$$

By factoring our "k" or "1/k" in equations (C-1), (C-3), and (C-4) one can obtain functional forms for $g(c)$ and $\phi(\zeta)$, each of which is determined up to a multiplicative constant. It is obvious that each form could be gotten from more than one set of equations. We note that all we are interested in are the functional forms of $g(c)$ and $\phi(\zeta)$ which would then suggest the form of $G(c,\zeta)$. We also note that if $g(c)$ and $\phi(\zeta)$ are combined to form $G(c,\zeta)$ the constant k cancels out. With the knowledge of the forms of the separate functions, $g(c)$ and $\phi(\zeta)$ a two-dimensional fit of the whole data in figure 49 could be obtained. This concludes the determination of the growth function, $G(c,\zeta)$, in separable form. The birth function, $B(c,\zeta)$, can be similarly obtained. Once these functions have been obtained they can be converted to the dimensionless versions as outlined in Chapter III.

APPENDIX D

COMPUTER PROGRAMS FOR THE ILLUSTRATION OF THE SUBROUTINE (SIMPLE) AND FOR THE MONITORING OF THE STABILITY OF THE COMPLEX CRYSTALLIZER

```
C THIS PROGRAM IS PROGRAM '' SIMPLE'' USED FOR MOST OF THE
C MINIMIZATION PROCEDURE OF THIS DISSERTATION.
      DIMENSION D1(3,4),F1(4),D0(3),D2(3)
      COMMON /FT/NW
      COMMON/CHAR/C1,C2,Q1,Q2
      COMMON/YU/U(140)
      NW=0
      TOL=.00000001
      NS=0
       N3=3
      ND=0
      N4=4
      NI=12000
C NI IS THE NUMBER OF ITERATIONS TO BE PERFORMED DURING
C THE MINIMIZATION.
      CALL SIMPLE(TOL,ND,NI,NS,N3,N4,D2,D1,F1,D0)
      NW=1
      FE=FTBM(D2)
       WRITE(6,*)D2
       WRITE(6,137)FE
C THE CHISQUARE IS SIMPLY THE THE SUM OF THE FRACTIONAL ERRORS
C DEFINED IN FUCTION SUBPROGAM FTBM.
137    FORMAT(' THE FINAL CHISQUARE IS',E20.6)
      T=9.
      N=9
      DO 3 I=1,N
      W1=(D2(1)/D2(2))*(1.-EMXP(-D2(2)*(U(I)-D2(3))))
      W2=(1./T)*(C1/Q1)*(EMXP(-Q1*D2(3))-EMXP(-Q1*U(I)))
      W3=(1./T)*(C2/Q2)*(EMXP(-Q2*D2(3))-EMXP(-Q2*U(I)))
      GR=(W1-W2-W3)/SS(U(I))
      BR=D2(1)*EMXP(-D2(2)*(U(I)-D2(3)))
      WRITE(6,2) I,U(I),W1,W2,W3,SS(U(I)),GR,BR
    2 FORMAT(1X,I4,7F10.4)
    3 CONTINUE
      X=D2(3)
```

```
      X1=D2(3)+0.5
      DO 4 I=1,140
      W1=(D2(1)/D2(2))*(1.-EMXP(-D2(2)*(X-D2(3))))
      W2=(1./T)*(C1/Q1)*(EMXP(-Q1*D2(3))-EMXP(-Q1*X))
      W3=(1./T)*(C2/Q2)*(EMXP(-Q2*D2(3))-EMXP(-Q2*X))
      GR=(W1-W2-W3)/SS(X)
      BR=D2(1)*EMXP(-D2(2)*(X-D2(3)))
      WRITE(6,5) I,X,W1,W2,W3,SS(X),GR,BR
    5 FORMAT(1X,I4,7F10.4)
      X=X+0.5
      IF(X.EQ.X1) X=FLOAT(IFIX(D2(3)))
    4 CONTINUE
      STOP
      END
C THE FUNCTION SUBPROGRAM FTBM IS WHERE THE FUNCTION TO BE
C MINIMIZED IS DEFINED. HERE FTBM IS EQUAL TO THE PERCENT
C ERROR SQUARE AND COULD BE DEFINED AS WISHED.THE ERROR IN THIS
C CASE IS THE DIFFENCE BETWEEN ORIGINAL DATA AND FIT.
      FUNCTION FTBM(D)
      EXTERNAL SS
      COMMON/FT/NW
      COMMON/CHAR/C1,C2,Q1,Q2
      DIMENSION D(1),E(140),F(140)
      COMMON/YU/U(140)
      DATA NFIRST,NP/0,1/
      IF(NFIRST .NE. 0) GO TO 40
      NFIRST=1
   40 CONTINUE
      FTBM =0.
      C1=26044.52
      C2=34.03978
      Q1=.87313032
      Q2=.03112719
      T=9.
      GLF=3.57
      WL=7.2
```

```
      WF=14.2
      XLM=71.7
      N=110
      U(1)=WF
      DO 6 I=2,N
      U(I)=U(I-1)+0.5
    6 CONTINUE
      DO 200 J=1,N
       F(J)= -GLF*SS(U(J))
      A=(D(1)/D(2))*(EMXP(-D(2)*(U(J)-D(3)))-1.)
      B=(1./T)*(C1/Q1)*(EMXP(-Q1*D(3))-EMXP(-Q1*U(J)))
      C=(1./T)*(C2/Q2)*(EMXP(-Q2*D(3))-EMXP(-Q2*U(J)))
      FA=A+B+C
      E(J)=F(J)
      IF(NW.EQ.0)GOTO 200
      ER=100.*(F(J)-FA)/F(J)
      WRITE(6,107) U(J),F(J),FA,ER
  107 FORMAT(4X,4E15.6)
  200 FTBM=FTBM+((F(J)-FA)/E(J))**2
      RETURN
      END
      SUBROUTINE SIMPLE(TOL,ND,NI,NS,N3,N4,D2,D1,F1,D0)
C   N3 IS THE NUMBER OF PARAMETERS BEING MINIMIZED, N4 IN GENERAL
C   IS N3+1,BUT THERE MAY BE CONDITIONS IN WHICH OTHER VALUS AREE
C   DESIRED. TOL IS THE LARGEST OF THE N4 LATEST VALUES OF THE
C   MINUS THE SMALLEST
C   MINUS THE SMALLEST
C   MINUS THE SMALLEST,THIS DIFFERENCE DIVIDED BY THE SMALLEST
C   IN GENERAL A VALUE OF ABOUT .0001 IS SUFFICIENT TO FIND
C   THE MINIMUM TO SINGLE PRECISION ACCURACY.
C   NOTICE THAT THE ROUTINE READS (4E20.6) THE N3 VALUES OF THE
C FIRST GUESS,AND THAT WITH VARIOUS SPECIFICATION FOR ND MAY READ
C EVEN MORE.
      DIMENSION D1(N3,N4),F1(N4),D0(N3),D2(N3)
C ND=0 READ FIRST GUESS  VALUES AND CALCULATE ALL FUNCTION
C VALUES.  WHEN ND=1 OR 2 PUT IN  4*N INITIAL GUESSES FOR AN
```

```
C N-PARAMETER OPTIMIZATION PROBLEM AND CALCULATE ALL 4*N
C CORRESPONDING 4*N FUNCTION VALUES FOR THE CASE ND=1. HOWEVER
C FOR THE CASE ND=2 DO NOT CALCULATE ANY FUNCTION VALUES.
C THE FIRST NS CONSTANTS ARE NOT VARIED.
C THE MINIMUM COEFFICIENTS ARE RETURNED AS D2
      NW=0
      NREFL=0
      WRITE(7,122)
122   FORMAT(' BEGIN OF SIMPLEX SUB')
101   FORMAT('  INIT',E20.7)
103   FORMAT(4E20.7)
104   FORMAT('  REFL',E20.7)
105   FORMAT('  CONT',F7.3,E20.7)
107   FORMAT('  EXPAND',E20.7)
108   FORMAT('  SHRINK',E20.7)
C     INITIAL LOOP
      SF=1.*N4
      NM=(N4-1)**2
      NC=0
      NIR=5
      DO20J=1,N4
      IF(J.GT.1.AND.ND.EQ.0)GOTO8
      READ(NIR,103)(D2(I),I=1,N3),F1(J)
      IF(NW.EQ.1)WRITE(6,103)(D2(I),I=1,N3)
8     CONTINUE
      DO10I=1,N3
10    D1(I,J)=D2(I)
      IF(ND.NE.2)F1(J)=FTBM(D2)
      IF(NW.EQ.2)WRITE(6,101)F1(J)
      IF(NW.EQ.1)WRITE(6,103)D2
      IF(ND.NE.0.OR.J.EQ.N4)GOTO20
      DO 15 I=1,N3
   15 D2(I)=D1(I,1)
      D2(J+NS)=1.001*D1(J+NS,1)
       IF(D2(J+NS).EQ.0.)D2(J+NS)=.1
20    CONTINUE
```

```
   40 CONTINUE
C  SORT LOOP
       I9=1
       I1=I9
       I2=2
       S=F1(1)
       B1=S
       B2=F1(2)
       NC=NC+1
       DO70 I=2,N4
       IF(S.LT.F1(I))GOTO50
       S=F1(I)
       I9=I
50     IF(B1.GT.F1(I))GOTO60
       B2=B1
       I2=I1
       B1=F1(I)
       I1=I
       GO TO 70
60     IF(B2.GT.F1(I))GOTO70
       B2=F1(I)
       I2=I
70     CONTINUE
       IF(S.EQ.0.)S=1.E-37
       IF(((B1-S)/S).LT.TOL  )GOTO800
       IF(NC.EQ.NI)GOTO800
       IF((B1-S)/S.LT.10.*TOL.AND.NREFL.GT.5*N4)GOTO300
C      FORMING DO
       DO100J=1,N3
       DO(J)=0.
       DO90I=1,N4
       IF(I.EQ.I1)GOTO90
       DO(J)=DO(J)+D1(J,I)
90     CONTINUE
       DO(J)=DO(J)/(N4-1)
100    CONTINUE
```

```
C       REFLECTION
        NREFL=NREFL+1
        DO110I=1,N3
110     D2(I)=2.*D0(I)-D1(I,I1)
        FT=FTBM(D2)
        IF(NW.EQ.2)WRITE(6,104)FT
        IF(FT.GE.B2)GOTO150
120     F1(I1)=FT
        DO130I=1,N3
130     D1(I,I1)=D2(I)
        IF(FT.LT.F1(I9).AND.NW.EQ.2)WRITE(6,109)FT
109     FORMAT(' NEW MIN',E15.6)
        IF(FT.LT.F1(I9).AND.NW.EQ.1)WRITE(6,119)(D2(I),I=1,N3)
119     FORMAT(' CONS FOR NEW MIN'/(4E20.6))
        IF(FT.LT.S)GOTO200
        GOTO40
C       CONTRACTION
150     CONTINUE
        IF(FT.GT.B1)GOTO165
        B1=FT
        DO160 I=1,N3
160     D1(I,I1)=D2(I)
165     CONTINUE
        AM=.75
168     CONTINUE
        DO170I=1,N3
170     D2(I)=AM*D1(I,I1)+(1.-AM)*D0(I)
        FT=FTBM(D2)
        IF(FT.GT.B1)GOTO 173
        B1=FT
        DO 172 I=1,N3
172     D1(I,I1)=D2(I)
173     CONTINUE
        IF(NW.EQ.2)WRITE(6,105)AM,FT
        S=-1.E64
        IF(FT.LT.B2)GOTO120
```

```
      IF(AM.LT..3)GOTO300
      AM=AM-.25
      GOTO168
C     EXPANSION
  200 S=FT
      DO210 I=1,N3
210   D2(I)=2*D2(I)-D0(I)
      FT=FTBM(D2)
      IF(NW.EQ.2)WRITE(6,107)FT
      IF(FT.GT.S)GOTO40
      S=-1.E64
      GOTO120
C     SHRINKAGE
300   CONTINUE
      NREFL=0
C FORMING THE AVERAGE OF THE SQUARES OF THE DISTANCES FROM THE MIN POINT
      NB=NS+1
      DO 280 J=NB,N3
      D0(J)=0.
      DO 270 I=1,N4
      IF(I.EQ.I9)GO TO 270
      D0(J)=D0(J)+(D1(J,I)-D1(J,I9))**2
270   CONTINUE
280   D0(J)=SQRT(D0(J)/(N4-1))
      SF=-.75*SF
      IF(NW.EQ.2)WRITE(6,103)SF
      MM=NS
      J=0
310   J=J+1
      IF(J.EQ.I9)GOTO310
      IF(J.GT.N4)GOTO 40
       MM=MM+1
      IF(MM.GT.N3)GOTO40
      DO340I=1,N3
340   D2(I)=D1(I,I9)
      D2(MM)=SF*(D0(MM))+D1(MM,I9)
```

```
      F1(J)=FTBM(D2)
      IF(NW.EQ.2)WRITE(6,108)F1(J)
      IF(NW.EQ.1)WRITE(6,103)D2
      DO 345 I=1,N3
345   D1(I,J)=D2(I)
      I1=J
      FT=F1(J)
      GOTO310
800   CONTINUE
      DO810J=1,N4
      IF(NW.EQ.1)WRITE(6,103)(D1(I,J),I=1,N3),F1(J)
      IF(NW.EQ.1)WRITE(7,103)(D1(I,J),I=1,N3),F1(J)
  810 CONTINUE
      WRITE(7,121)
121   FORMAT(' END OF SIMPLEX SUB')
      DO 820 J=1,N3
820   D2(J)=D1(J,I9)
      DO 3 J=1,N3
      WRITE(6,4) D2(J)
    4 FORMAT(4X,E15.6)
    3 CONTINUE
      RETURN
      END
      FUNCTION SS(XL)
      COMMON/CHAR/C1,C2,Q1,Q2
      SS =C1*EXP(-Q1*XL) + C2*EXP(-Q2*XL)
      RETURN
      END
      FUNCTION EMXP(X)
      IF(X .LT. 100.)GO TO 20
      EMXP=1.E64
      RETURN
   20 IF(X .GT. -100.)GO TO 30
      EMXP=0.E0
      RETURN
   30 EMXP=EXP(X)
```

```
      RETURN
      END
/DATA
438.8252              1.241923              2.994288
```

```
C STABILITY PROGRAM FOR THE COMPLEX CRYSTALLIZER
C    ****************************************************************
C
C        THE FOLLOWING PROGRAM IS IN CONJUNCTION WITH THE
C        DOCTORAL DISSERTATION SUBMITTED BY CHARLES OKONKWO
C        ON JUNE 9, 1982.
C
C    ****************************************************************
C
C     LIST OF VARIABLES (ALL QUANTITIES ARE DIMENSIONLESS
C          QUANTITIES):
C                        AL(I): RELATED TO RESIDENCE TIME, NU5
C                        B(I): (TAU)I = AL(I) * NU5
C                        EC: VOID FRACTION OF CRYSTALLIZER
C                        LF: LARGEST FINES SIZES
C                        LP: SMALLEST PRODUCT SIZE OR THE LARGEST
C                              INTERMEDIATE SIZE CRYSTALS
C                        A & ZS: REMOVAL RATES OF INTERMEDIATE
C                              AND PRODUCT SIZE CRYSTALS
C                        R: RECYCLE RATE OF DISSOLVED FINES
C                        THETA: RECYCLE RATE OF UNDISSOLVED FINES
C                        QSTAR: SAME AS Q* IN THE TEXT
C                        GAM2: SAME AS GAMMA2 IN THE TEXT
C                        YO: STEADY STATE CONCENTRATION
C                        VO: STEADY STATE CONCENTRATION DEPENDENT
C                              PART OF THE GROWTH FUNCTION
C                        VOP: CORRESPONDING DERIVATIVE OF VO
C                        UO: STEADY STATE CONCENTRATION DEPENDENT
C                              PART OF BIRTH FUNCTION
C                        UOP: CORRESPONDING DERIVATIVE OF UO
C                        B: RELATED TO PRODUCT WITHDRAWAL RATE,
C                              ZS, BY ZS(1-B)
C                        BIRTH FUNCTION, R(Z) = (EM2) EXP(-A3(Z-2))
C                        GROWTH FUNCTION, W(Z) = EM/(1+A1*EXP(-B1*Z))
C
```

```
C     ***********************************************************
C
C             DIMENSION STATEMENTS
C
      DIMENSION Z6(6),Z10(10)
      DIMENSION TLEG6(6),TLEG10(10),WLEG6(6),WLEG10(10)
      DIMENSION TLAG6(6),TLAG10(10),WLAG6(6),WLAG10(10)
      DIMENSION ALPHA(3,3),BETA(3,3),GAMMA(3),CHI(3)
      REAL LM1,LM2,LAM(3,3),MU5
      DIMENSION DELM(3),PSIM(3,3),P(3),COEF1(3),COEF2(5)
      REAL LP,LF
C     ***********************************************************
C
C             FORMAT STATEMENTS
C
11          FORMAT(1X,'I 0 =',E13.7,'   (FOR N=6)    ',E13.7,
     1              '    (FOR N=10)')
12          FORMAT(1X,'L 0 =',E13.7,'    (FOR N=6)    ',E13.7,
     1              '    (FOR N=10)')
13          FORMAT(2X,'DELM(2)=',E13.7)
21          FORMAT(1X,'I 1 =',E13.7,'    (FOR N=6)    ',E13.7,
     1              '    (FOR N=10)')
22          FORMAT(1X,'L 1 =',E13.7,'    (FOR N=6)   ',E13.7,
     1              '    (FOR N=10)')
25          FORMAT(1X,'DELTA 0',10X,E13.7,10X,E13.7///)
31          FORMAT(1X,'I 2 =',E13.7,'    (FOR N=6)    ',E13.7,
     1              '    (FOR N=10)')
32          FORMAT(1X,'L 2 =',E13.7,'    (FOR N=6)    ',E13.7,
     1              '    (FOR N=10)')
35          FORMAT(1X,'DELTA 1',10X,E13.7,10X,E13.7///)
45          FORMAT(1X,'DELTA 2',10X,E13.7,10X,E13.7///)
55          FORMAT(1X,'ALPHA 00',10X,E13.7,10X,E13.7///)
65          FORMAT(1X,'ALPHA 11',10X,E13.7,10X,E13.7///)
75          FORMAT(1X,'ALPHA 22',10X,E13.7,10X,E13.7///)
85          FORMAT(1X,'ALPHA 10 AND 01',10X,E13.7,10X,E13.7///)
95          FORMAT(1X,'ALPHA 12 AND 21',10X,E13.7,10X,E13.7///)
```

```
105         FORMAT(1X,'ALPHA 02 AND 20',10X,E13.7,10X,E13.7///)
115         FORMAT(1X,'BETA 00',10X,E13.7,10X,E13.7///)
125         FORMAT(1X,'BETA 11',10X,E13.7,10X,E13.7///)
135         FORMAT(1X,'BETA 22',10X,E13.7,10X,E13.7///)
145         FORMAT(1X,'BETA 12',10X,E13.7,10X,E13.7///)
155         FORMAT(1X,'BETA 21',10X,E13.7,10X,E13.7///)
165         FORMAT(1X,'BETA 10',10X,E13.7,10X,E13.7///)
175         FORMAT(1X,'BETA 01',10X,E13.7,10X,E13.7///)
185         FORMAT(1X,'BETA 02',10X,E13.7,10X,E13.7///)
195         FORMAT(1X,'BETA 20',10X,E13.7,10X,E13.7///)
205         FORMAT(1X,'GAMMA 0',10X,E13.7,10X,E13.7///)
215         FORMAT(1X,'GAMMA 1',10X,E13.7,10X,E13.7///)
225         FORMAT(1X,'GAMMA 2',10X,E13.7,10X,E13.7///)
235         FORMAT(1X,'CHI 0',10X,E13.7,10X,E13.7///)
245         FORMAT(1X,'CHI 1',10X,E13.7,10X,E13.7///)
255         FORMAT(1X,'CHI 2',10X,E13.7,10X,E13.7///)
265         FORMAT(1X,'A',10X,E13.7,10X,E13.7///)
321         FORMAT(1X,'QSTAR= ',E13.7)
323         FORMAT(3(2X,E13.7)/)
324         FORMAT((4X,E13.7)/)
325         FORMAT(1X,'4-TH ORDER STABILITY CRITERIA=',E13.7)
330         FORMAT(1X,'THE FOLLOWING COEFFICIENTS ',
     1              'WERE CALCULATED WITH THE INTEGRALS ',
     2              'EVALUATED FOR THE HIGHEST VALUE OF N')
335         FORMAT(1X,'COEF',I1,' FOR CASE 1 IS  ',E13.7)
355         FORMAT(1X,'COEF',I1,' FOR CASE 2 IS  ',E13.7)
C     ************************************************************
C
C
C             INPUT VALUES OF TLAG6, WLAG6, TLAG10,
C             WLAG10, TLEG6, WLEG6, TLEG10, & WLEG10
C
      DATA TLAG6/.2228466,1.1889321,2.99273633,5.77514357,
     1           9.83746742,15.98287398/
      DATA WLAG6/.45896467,.41700083,.11337338,.01039920,
     1           .00026102,.00000090/
      DATA TLAG10/.13779347,.72945455,1.80834290,3.40143370,
```

```
     1            5.55249614,8.33015275,11.84378584,16.27925783,
     2            21.99658581,29.92069701/
      DATA WLAG10/.30844112,.40111993,.21806829,.06208746,
     1            .00950152,.00075301,.00002826,.00000042,
     2            0.0,0.0/
      DATA TLEG6/0.0,0.0,0.0,.23861919,.66120939,.93246951/
      DATA WLEG6/0.0,0.0,0.0,.46791393,.36076157,.1732449/
      DATA TLEG10/0.,0.,0.,0.,0.,.14887434,.43339539,
     1            .67940957,.86506337,.97390653/
      DATA WLEG10/0.,0.,0.,0.,0.,.29552422,.26926672,.21908636,
     1            .14945135,.06667134/
         DO 10 I=1,3
            TLEG6(I)=(-TLEG6(7-I))
            WLEG6(I)=WLEG6(7-I)
10       CONTINUE
         DO 20 I=1,5
            TLEG10(I)=(-TLEG10(11-I))
            WLEG10(I)=WLEG10(11-I)
20       CONTINUE
C     ****************************************************************
C
C              DEFINE CERTAIN CONSTANTS WHICH APPEAR DUE
C              TO THE TRANSFORMATIONS OF THESE PARTICULAR
C              FUNCTIONS.  DIFFERENT FUNCTIONS WOULD
C              REQUIRE THIS SECTION OF THE PROGRAM TO
C              BE CHANGED.
C
         H=SQRT(2./(24.**3))
         H1=SQRT(2.)
         H2=2./SQRT(216.)
         H3= 1./SQRT(216.)
         H4=SQRT(2.*216.)
         H5=SQRT(2./(216.*(24.**3)))
C     ****************************************************************
C
C              INPUT VALUES OF THE PARAMETERS TO DEFINE
```

```
C              A PARTICULAR SYSTEM.
C
        THETA=0.0
        R=18.
        ZS=5.
        AL0=1./4.
        AL1=1./9.
        AL2=1./6.
        AL3=1./3.
        AL4=1./3.
        AL5=1.
        AL6=1./2.
        EC=.9
        LP=4.
        LP=30.
        UOP=.1
        VOP=4.67
        EMH=1000.
        B1=0.3
        A1=1000.
        A2=.21
        A3=.5
        EM=1.
        EM2=1000000.
        A=4.
        B=.6
        ENINT=8.
        NU5=1.
        VO=4.5
        UO=0.01
        YO=1.01
        R2=0.005
C     ****************************************************************
C
       C1=1./AL4-(1.-THETA)-(R-1.)/AL1
       C2=1./AL4-A
```

```
      C3=1./AL4-ZS*(1.-B)
      CS1=(1.-B)/AL1-1./AL4+THETA/AL6
      CS2=(-A/AL4)
      CS3=(-ZS/AL4)+ZS*B/AL6
C     ***************************************************************
C
C           DEFINE SOME CONSTANTS WHICH APPEAR IN
C           SEVERAL CALCULATIONS.  THESE ARE DUE TO
C           TRANSFORMATIONS OF THESE PARTICULAR
C           FUNCTIONS AND WOULD CHANGE WHEN USING
C           ANY OTHER FUNCTIONS.
C
        AK1=EC*EM2*EXP(-1.)/(A3+.5)
        AK2=EM*EMH*EXP(-1.)/(A2+0.5)
C     ***************************************************************
C
C           BEGIN INTEGRATING THE FUNCTIONS.  M IS
C           THE NUMBER OF THE PARTICULAR FUNCTION
C           BEING INTEGRATED AS THEY ARE NUMBERED
C           IN THE FUNCTION F.
C
C           U AND C ARE CONSTANTS WHICH APPEAR DUE
C           TO THE TRANSFORMATION OF THE FUNCTION.
C           THEY ARE USED IN THE GAUSS-LAGUERRE
C           INTEGRATION TO DETERMINE THE VALUE OF
C           A(I) BY THE EQUATION:
C                     A(I) = U * T(I) + C
C
C        FUNCTION 1
C     ***************
      U=1.
      C=2.*A3+1.
      M=1
        CALL GLAG(6,TLAG6,Z6,WLAG6,U,C,M,A1,B1,A2,A3)
        CALL GLAG(10,TLAG10,Z10,WLAG10,U,C,M,A1,B1,A2,A3)
C
```

```
C               S1 & S2 ARE THE VALUES OF THE INTEGRATION
C               AFTER EACH INTERVAL.  S1 IS THE VALUE
C               WHICH USES 6 INTERVALS AND S2 IS THE
C               VALUE WHICH USES 10 INTERVALS.
          S1=Z6(6)*AK1/(SQRT(2.)*(A3+0.5))
          S2=Z10(10)*AK1/(SQRT(2.)*(A3+0.5))
           WRITE(6,11)S1,S2
C
C
C          FUNCTION 2
C       ****************
       U =1./(A2+.5)
       C=2.
       M=2
         CALL GLAG(6,TLAG6,Z6,WLAG6,U,C,M,A1,B1,A2,A3)
         CALL GLAG(10,TLAG10,Z10,WLAG10,U,C,M,A1,B1,A2,A3)
           LM1=Z6(6)*AK2/SQRT(2.)
           LM2=Z10(10)*AK2/SQRT(2.)
       WRITE(6,12)LM1,LM2
          S1=S1*UOP-LM1*VOP
          S2=S2*UOP-LM2*VOP
           DELM(1)=S2
       WRITE(6,13) DELM(1)
       WRITE(6,25)S1,S2
C
C          FUNCTION 3
C       ****************
       U= 1./(A3+.5)
       C= 2.
       M=3
         CALL GLAG(6,TLAG6,Z6,WLAG6,U,C,M,A1,B1,A2,A3)
         CALL GLAG(10,TLAG10,Z10,WLAG10,U,C,M,A1,B1,A2,A3)
           S1=Z6(6)*AK1/SQRT(216.)
           S2=Z10(10)*AK1/SQRT(216.)
            WRITE(6,21)S1,S2
C
```

```
C          FUNCTION 4
C       ****************
        U= 1./(A2+.5)
        C= 2.
        M=4
          CALL GLAG(6,TLAG6,Z6,WLAG6,U,C,M,A1,B1,A2,A3)
          CALL GLAG(10,TLAG10,Z10,WLAG10,U,C,M,A1,B1,A2,A3)
            LM1=Z6(6)*AK2/SQRT(216.)
            LM2=Z10(10)*AK2/SQRT(216.)
             WRITE(6,22)LM1,LM2
            S1=S1*UOP-LM1*VOP
            S2=S2*UOP-LM2*VOP
        DELM(2)=S2
        WRITE(6,13) DELM(2)
        WRITE(6,35)S1,S2
C
C          FUNCTION 5
C       ****************
        U= 1./(A3+.5)
        C= 2.
        M=5
          CALL GLAG(6,TLAG6,Z6,WLAG6,U,C,M,A1,B1,A2,A3)
          CALL GLAG(10,TLAG10,Z10,WLAG10,U,C,M,A1,B1,A2,A3)
            S1=Z6(6)*AK1*H
            S2=Z10(10)*AK1*H
             WRITE(6,31)S1,S2
C
C          FUNCTION 6
C       ****************
        U=1./(A2+.5)
        C= 2.
        M=6
          CALL GLAG(6,TLAG6,Z6,WLAG6,U,C,M,A1,B1,A2,A3)
          CALL GLAG(10,TLAG10,Z10,WLAG10,U,C,M,A1,B1,A2,A3)
            LM1=Z6(6)*AK2*H
            LM2=Z10(10)*AK2*H
```

```
      WRITE(6,32) LM1,LM2
      S1=S1*UOP-LM1*VOP
      S2=S2*UOP-LM2*VOP
    DELM(3)=S2
    WRITE(6,13) DELM(3)
    WRITE(6,45) S1,S2
C
C       FUNCTION 7
C   ****************
    M=7
      CALL GLEG(2.,LP,6,TLEG6,Z6,WLEG6,M,A1,B1,A2,A3)
      CALL GLEG(2.,LP,10,TLEG10,Z10,WLEG10,M,A1,B1,A2,A3)
        S1=Z6(6)*CS1/2.
        S2=Z10(10)*CS1/2.
      CALL GLEG(LP,LP,6,TLEG6,Z6,WLEG6,M,A1,B1,A2,A3)
      CALL GLEG(LP,LP,10,TLEG10,Z10,WLEG10,M,A1,B1,A2,A3)
        S1=S1+Z6(6)*CS2/2.
        S2=S2+Z10(10)*CS2/2.
C
C       FUNCTION 8
C   ****************
    U=1.
    C=LP
    M=8
      CALL GLAG(6,TLAG6,Z6,WLAG6,U,C,M,A1,B1,A2,A3)
      CALL GLAG(10,TLAG10,Z10,WLAG10,U,C,M,A1,B1,A2,A3)
        S1=S1+Z6(6)*EXP(-LP)*CS3/2.
        ALPHA(1,1)=S2+Z10(10)*EXP(-LP)*CS3/2.
    WRITE(6,55) S1,ALPHA(1,1)
C
C       FUNCTION 9
C   ****************
    M=9
      CALL GLEG(2.,LP,6,TLEG6,Z6,WLEG6,M,A1,B1,A2,A3)
      CALL GLEG(2.,LP,10,TLEG10,Z10,WLEG10,M,A1,B1,A2,A3)
        S1=Z6(6)*CS1/216.
```

```
          S2=Z10(10)*CS1/216.
        CALL GLEG(LP,LP,6,TLEG6,Z6,WLEG6,M,A1,B1,A2,A3)
        CALL GLEG(LP,LP,10,TLEG10,Z10,WLEG10,M,A1,B1,A2,A3)
          S1=Z6(6)*CS2/216.+S1
          S2=Z10(10)*CS2/216.+S2
C
C         FUNCTION 10
C       *****************
        U=1.
        C=LP
        M=10
          CALL GLAG(6,TLAG6,Z6,WLAG6,U,C,M,A1,B1,A2,A3)
          CALL GLAG(10,TLAG10,Z10,WLAG10,U,C,M,A1,B1,A2,A3)
            S1=S1+Z6(6)*CS3*EXP(-LP)/216.
            ALPHA(2,2)=S2+Z10(10)*CS3*EXP(-LP)/216.
        WRITE(6,65)S1,ALPHA(2,2)
C
C         FUNCTION 11
C       *****************
        M=11
          CALL GLEG(2.,LP,6,TLEG6,Z6,WLEG6,M,A1,B1,A2,A3)
          CALL GLEG(2.,LP,10,TLEG10,Z10,WLEG10,M,A1,B1,A2,A3)
            S1=Z6(6)*CS1*(2./(24**3))
            S2=Z10(10)*CS1*(2./(24**3))
          CALL GLEG(LP,LP,6,TLEG6,Z6,WLEG6,M,A1,B1,A2,A3)
          CALL GLEG(LP,LP,10,TLEG10,Z10,WLEG10,M,A1,B1,A2,A3)
            S1=S1+Z6(6)*CS2*(2./(24**3))
            S2=S2+Z10(10)*CS2*(2./(24**3))
C
C         FUNCTION 12
C       *****************
        U=1.
        C=LP
        M=12
          CALL GLAG(6,TLAG6,Z6,WLAG6,U,C,M,A1,B1,A2,A3)
          CALL GLAG(10,TLAG10,Z10,WLAG10,U,C,M,A1,B1,A2,A3)
```

```
          S1=S1+Z6(6)*CS3*EXP(-LP)*(2./(24**3))
          ALPHA(3,3)=S2+Z10(10)*CS3*EXP(-LP)*(2./(24**3))
        WRITE(6,75)S1,ALPHA(3,3)
C
C          FUNCTION 13
C       ****************
        M=13
          CALL GLEG(2.,LF,6,TLEG6,Z6,WLEG6,M,A1,B1,A2,A3)
          CALL GLEG(2.,LF,10,TLEG10,Z10,WLEG10,M,A1,B1,A2,A3)
            S1=Z6(6)*CS1/SQRT(2.*216.)
            S2=Z10(10)*CS1/SQRT(2.*216.)
          CALL GLEG(LF,LP,6,TLEG6,Z6,WLEG6,M,A1,B1,A2,A3)
          CALL GLEG(LF,LP,10,TLEG10,Z10,WLEG10,M,A1,B1,A2,A3)
            S1=S1+Z6(6)*CS2/SQRT(2.*216.)
            S2=S2+Z10(10)*CS2/SQRT(2.*216.)
C
C          FUNCTION 14
C       ****************
        U=1.
        C=LP
        M=14
          CALL GLAG(6,TLAG6,Z6,WLAG6,U,C,M,A1,B1,A2,A3)
          CALL GLAG(10,TLAG10,Z10,WLAG10,U,C,M,A1,B1,A2,A3)
            S1=S1+Z6(6)*CS3*EXP(-LP)/SQRT(2.*216.)
            ALPHA(2,1)=S2+Z10(10)*CS3*EXP(-LP)/SQRT(2.*216.)
        ALPHA(1,2)=ALPHA(2,1)
        WRITE(6,85)S1,ALPHA(2,1)
C
C          FUNCTION 15
C       ****************
        M=15
          CALL GLEG(2.,LF,6,TLEG6,Z6,WLEG6,M,A1,B1,A2,A3)
          CALL GLEG(2.,LF,10,TLEG10,Z10,WLEG10,M,A1,B1,A2,A3)
            S1=Z6(6)*CS1*H5
            S2=Z10(10)*CS1*H5
          CALL GLEG(LF,LP,6,TLEG6,Z6,WLEG6,M,A1,B1,A2,A3)
```

```
      CALL GLEG(LF,LP,10,TLEG10,Z10,WLEG10,M,A1,B1,A2,A3)
        S1=S1+Z6(6)*CS2*H5
        S2=S2+Z10(10)*CS2*H5
C
C        FUNCTION 16
C     ******************
      U=1.
      C=LP
      M=16
      CALL GLAG(6,TLAG6,Z6,WLAG6,U,C,M,A1,B1,A2,A3)
      CALL GLAG(10,TLAG10,Z10,WLAG10,U,C,M,A1,B1,A2,A3)
        S1=S1+Z6(6)*CS3*EXP(-LP)*H5
        ALPHA(2,3)=S2+Z10(10)*CS3*EXP(-LP)*H5
      ALPHA(3,2)=ALPHA(2,3)
      WRITE(6,95)S1,ALPHA(2,3)
C
C        FUNCTION 17
C     ******************
      M=17
      X= SQRT(1./(24**3))
      CALL GLEG(2.,LF,6,TLEG6,Z6,WLEG6,M,A1,B1,A2,A3)
      CALL GLEG(2.,LF,10,TLEG10,Z10,WLEG10,M,A1,B1,A2,A3)
        S1=Z6(6)*CS1*X
        S2=Z10(10)*CS1*X
      CALL GLEG(LF,LP,6,TLEG6,Z6,WLEG6,M,A1,B1,A2,A3)
      CALL GLEG(LF,LP,10,TLEG10,Z10,WLEG10,M,A1,B1,A2,A3)
        S1=S1+Z6(6)*CS2*X
        S2=S2+Z10(10)*CS2*X
C
C        FUNCTION 18
C     ******************
      U=1.
      C=LP
      M=18
      CALL GLAG(6,TLAG6,Z6,WLAG6,U,C,M,A1,B1,A2,A3)
      CALL GLAG(10,TLAG10,Z10,WLAG10,U,C,M,A1,B1,A2,A3)
```

```
          S1=S1+Z6(6)*CS3*EXP(-LP)*X
          ALPHA(1,3)=S2+Z10(10)*CS3*EXP(-LP)*X
        ALPHA(3,1)=ALPHA(1,3)
        WRITE(6,105) S1,ALPHA(1,3)
C
C          FUNCTION 19
C       ******************
        U=1.
        C=2.
        M=19
          CALL GLAG(6,TLAG6,Z6,WLAG6,U,C,M,A1,B1,A2,A3)
          CALL GLAG(10,TLAG10,Z10,WLAG10,U,C,M,A1,B1,A2,A3)
            S1=Z6(6)*EM*EXP(-2.)/H1
            BETA(1,1)=Z10(10)*EM*EXP(-2.)/H1
        WRITE(6,115) S1,BETA(1,1)
C
C          FUNCTION 20
C       ******************
        M=20
          CALL GLAG(6,TLAG6,Z6,WLAG6,U,C,M,A1,B1,A2,A3)
          CALL GLAG(10,TLAG10,Z10,WLAG10,U,C,M,A1,B1,A2,A3)
            S1=Z6(6)*EM*EXP(-2.)*H3
            BETA(2,2)=Z10(10)*EM*EXP(-2.)*H3
        WRITE(6,125) S1,BETA(2,2)
C
C          FUNCTION 21
C       ******************
        M=21
          CALL GLAG(6,TLAG6,Z6,WLAG6,U,C,M,A1,B1,A2,A3)
          CALL GLAG(10,TLAG10,Z10,WLAG10,U,C,M,A1,B1,A2,A3)
            S1=Z6(6)*EM*EXP(-2.)*H
            BETA(3,3)=Z10(10)*EM*EXP(-2.)*H
        WRITE(6,135) S1,BETA(3,3)
C
C          FUNCTION 22
C       ******************
```

```
      M=22
        CALL GLAG(6,TLAG6,Z6,WLAG6,U,C,M,A1,B1,A2,A3)
        CALL GLAG(10,TLAG10,Z10,WLAG10,U,C,M,A1,B1,A2,A3)
          S1=Z6(6)*EM*EXP(-2.)*H
          BETA(2,3)=Z10(10)*EM*EXP(-2.)*H
      WRITE(6,145)S1,BETA(2,3)
C
C        FUNCTION 23
C     *****************
      M=23
        CALL GLAG(6,TLAG6,Z6,WLAG6,U,C,M,A1,B1,A2,A3)
        CALL GLAG(10,TLAG10,Z10,WLAG10,U,C,M,A1,B1,A2,A3)
          S1=Z6(6)*EM*EXP(-2.)*H3
          BETA(3,2)=Z10(10)*EM*EXP(-2.)*H3
      WRITE(6,155)S1,BETA(3,2)
C
C        FUNCTION 24
C     *****************
      M=24
        CALL GLAG(6,TLAG6,Z6,WLAG6,U,C,M,A1,B1,A2,A3)
        CALL GLAG(10,TLAG10,Z10,WLAG10,U,C,M,A1,B1,A2,A3)
          S1=Z6(6)*EM*EXP(-2.)/H1
          BETA(2,1)=Z10(10)*EM*EXP(-2.)/H1
      WRITE(6,163)S1,BETA(2,1)
C
C        FUNCTION 37
C     *****************
      M=37
        CALL GLAG(6,TLAG6,Z6,WLAG6,U,C,M,A1,B1,A2,A3)
        CALL GLAG(10,TLAG10,Z10,WLAG10,U,C,M,A1,B1,A2,A3)
          S1=Z6(6)*EM*EXP(-2.)*H3
          BETA(1,2)=Z10(10)*EM*EXP(-2.)*H3
      WRITE(6,175)S1,BETA(1,2)
C
C        FUNCTION 25
C     *****************
```

```
      M=25
        CALL GLAG(6,TLAG6,Z6,WLAG6,U,C,M,A1,B1,A2,A3)
        CALL GLAG(10,TLAG10,Z10,WLAG10,U,C,M,A1,B1,A2,A3)
          S1=Z6(6)*EM*EXP(-2.)*H
          BETA(1,3)=Z10(10)*EM*EXP(-2.)*H
      WRITE(6,185)S1,BETA(1,3)
C
C         FUNCTION 26
C     *****************
      M=26
        CALL GLAG(6,TLAG6,Z6,WLAG6,U,C,M,A1,B1,A2,A3)
        CALL GLAG(10,TLAG10,Z10,WLAG10,U,C,M,A1,B1,A2,A3)
          S1=Z6(6)*EM*EXP(-2.)/H1
          BETA(3,1)=Z10(10)*EM*EXP(-2.)/H1
      WRITE(6,195)S1,BETA(3,1)
C
C         FUNCTION 27
C     *****************
      U =2.
      C=2.
      M=27
        CALL GLAG(6,TLAG6,Z6,WLAG6,U,C,M,A1,B1,A2,A3)
        CALL GLAG(10,TLAG10,Z10,WLAG10,U,C,M,A1,B1,A2,A3)
          S1=Z6(6)
          GAMMA(1)=Z10(10)
      WRITE(6,205)S1,GAMMA(1)
C
C         FUNCTION 28
C     *****************
      M=28
        CALL GLAG(6,TLAG6,Z6,WLAG6,U,C,M,A1,B1,A2,A3)
        CALL GLAG(10,TLAG10,Z10,WLAG10,U,C,M,A1,B1,A2,A3)
          S1=Z6(6)
          GAMMA(2)=Z10(10)
      WRITE(6,215)S1,GAMMA(2)
C
```

```
C          FUNCTION 29
C       ******************
        M=29
          CALL GLAG(6,TLAG6,Z6,WLAG6,U,C,M,A1,B1,A2,A3)
          CALL GLAG(10,TLAG10,Z10,WLAG10,U,C,M,A1,B1,A2,A3)
            S1=Z6(6)
            GAMMA(3)=Z10(10)
        WRITE(6,225)S1,GAMMA(3)
C
C          FUNCTION 30
C       ******************
        M=30
          CALL GLEG(2.,LP,6,TLEG6,Z6,WLEG6,M,A1,B1,A2,A3)
          CALL GLEG(2.,LP,10,TLEG10,Z10,WLEG10,M,A1,B1,A2,A3)
            S1=C1*Z6(6)
            S2=C1*Z10(10)
          CALL GLEG(LP,LP,6,TLEG6,Z6,WLEG6,M,A1,B1,A2,A3)
          CALL GLEG(LP,LP,10,TLEG10,Z10,WLEG10,M,A1,B1,A2,A3)
            S1=S1+C2*Z6(6)
            S2=S2+C2*Z10(10)
C
C          FUNCTION 31
C       ******************
        U=2.
        C=LP
        M=31
          CALL GLAG(6,TLAG6,Z6,WLAG6,U,C,M,A1,B1,A2,A3)
          CALL GLAG(10,TLAG10,Z10,WLAG10,U,C,M,A1,B1,A2,A3)
            S1=(S1+C3*EXP(-LP/2.)*Z6(6))
            CHI(1)=(S2+C3*EXP(-LP/2.)*Z10(10))
        WRITE(6,235)S1,CHI(1)
C
C          FUNCTION 32
C       ******************
        M=32
          CALL GLEG(2.,LP,6,TLEG6,Z6,WLEG6,M,A1,B1,A2,A3)
```

```
      CALL GLEG(2.,LP,10,TLEG10,Z10,WLEG10,M,A1,B1,A2,A3)
        S1=C1*Z6(6)
        S2=C1*Z10(10)
      CALL GLEG(LP,LP,6,TLEG6,Z6,WLEG6,M,A1,B1,A2,A3)
      CALL GLEG(LP,LP,10,TLEG10,Z10,WLEG10,M,A1,B1,A2,A3)
        S1=S1+C2*Z6(6)
        S2=S2+C2*Z10(10)
C
C        FUNCTION 33
C     ******************
      M=33
      CALL GLAG(6,TLAG6,Z6,WLAG6,U,C,M,A1,B1,A2,A3)
      CALL GLAG(10,TLAG10,Z10,WLAG10,U,C,M,A1,B1,A2,A3)
        S1=S1+C3*EXP(-LP/2.)*Z6(6)
        CHI(2)=S2+C3*EXP(-LP/2.)*Z10(10)
      WRITE(6,245)S1,CHI(2)
C
C        FUNCTION 34
C     ******************
      M=34
      CALL GLEG(2.,LP,6,TLEG6,Z6,WLEG6,M,A1,B1,A2,A3)
      CALL GLEG(2.,LP,10,TLEG10,Z10,WLEG10,M,A1,B1,A2,A3)
        S1=C1*Z6(6)
        S2=C1*Z10(10)
      CALL GLEG(LP,LP,6,TLEG6,Z6,WLEG6,M,A1,B1,A2,A3)
      CALL GLEG(LP,LP,10,TLEG10,Z10,WLEG10,M,A1,B1,A2,A3)
        S1=S1+C2*Z6(6)
        S2=S2+C2*Z10(10)
C
C        FUNCTION 35
C     ******************
      M=35
      CALL GLAG(6,TLAG6,Z6,WLAG6,U,C,M,A1,B1,A2,A3)
      CALL GLAG(10,TLAG10,Z10,WLAG10,U,C,M,A1,B1,A2,A3)
        S1=S1+C3*EXP(-LP/2.)*Z6(6)
        CHI(3)=S2+C3*EXP(-LP/2.)*Z10(10)
```

```
      WRITE(6,255) S1,CHI(3)
C
C        FUNCTION 36
C     *****************
      M=36
        CALL GLEG(2.,LP,6,TLEG6,Z6,WLEG6,M,A1,B1,A2,A3)
        CALL GLEG(2.,LP,10,TLEG10,Z10,WLEG10,M,A1,B1,A2,A3)
          S1=C1*Z6(6)*EMH
          S2=C1*Z10(10)*EMH
        CALL GLEG(LP,LP,6,TLEG6,Z6,WLEG6,M,A1,B1,A2,A3)
        CALL GLEG(LP,LP,10,TLEG10,Z10,WLEG10,M,A1,B1,A2,A3)
          S1=S1+C2*Z6(6)*EMH
          S2=S2+C2*Z10(10)*EMH
C
C        FUNCTION 38
C     *****************
      U=1./A2
      C=LP
      M=38
        CALL GLAG(6,TLAG6,Z6,WLAG6,U,C,M,A1,B1,A2,A3)
        CALL GLAG(10,TLAG10,Z10,WLAG10,U,C,M,A1,B1,A2,A3)
          S1=S1+Z6(6)*C3*EXP(-LP*A2)*EMH
          S2=S2+Z10(10)*C3*EXP(-LP*A2)*EMH
       QS=S2
      WRITE(6,265) S1,S2
          GAM2=(1.+R2)/AL2-1./AL1-1.
          QSTAR=(GAM2+QS+ENINI/AL0)/(EC*NU5)
          WRITE(6,321) QSTAR
           DO 301 L=1,3
301         P(L)=(GAMMA(L)-AL4*YO*CHI(L))/(EC*AL4*NU5)
              DO 300 J=1,3
              DO 300 K=1,3
               PSIM(J,K)=ALPHA(J,K)/NU5-VO*BETA(J,K)
               LAM(J,K)=DELM(J)*P(K)
300         CONTINUE
C     ************************************************************
```

```
C
C                CALCULATE THE COEFFICIENTS OF THE
C                QUADRATIC WITH THE FORM:
C          COEF1(1)  X**2  +  COEF1(2)  X  +  COEF1(3)  =  0
C
                  COEF1(1)=1.
                  COEF1(2)=QSTAR+PSIM(1,1)
C     ************************************************************
C
C                CALCULATE SOME CONSTANTS WHICH
                  COEF1(3)=QSTAR*PSIM(1,1)+DELM(1)*P(1)
C                APPEAR FREQUENTLY IN THE CALCULATION
C                OF THE COEFICIENTS OF THE QUARTIC.
C
C                THEN CALCULATE THE COEFICIENTS
C                FOR A QUARTIC EQUATION OF THE FORM:
C
C          COEF2(1)  X**4  +  COEF2(2)  X**3  +
C               COEF2(3)  X**2  +  COEF2(4)  X  +  COEF2(5)  = 0
C
C            CONSTANTS
C           *************
               X1=PSIM(1,1)+PSIM(2,2)
               X2=LAM(1,1)+LAM(2,2)
               X3=PSIM(1,1)*PSIM(2,2)-PSIM(1,2)*PSIM(2,1)
               X4=PSIM(2,2)*LAM(1,1)+PSIM(1,1)*LAM(2,2)
     1            -PSIM(1,2)*LAM(2,1)-PSIM(2,1)*LAM(1,2)
C
C            COEFICIENTS
C           ***************
               COEF2(1)=1.
               COEF2(2)=2.*QSTAR+X1
               COEF2(3)=QSTAR*(1.+2.*X1)+X2+X3
               COEF2(4)=QSTAR*(QSTAR*X1+X2+2.*X3)+X4
               COEF2(5)=(QSTAR**2)*X3+QSTAR*X4+LAM(1,1)*LAM(2,2)
     1                  -LAM(1,2)*LAM(2,1)
```

```
C     ************************************************************
C
C               OUTPUT ALL PSI'S, P'S, AND LAMBDA'S
C
      WRITE(6,322)
322   FORMAT(2X,'COMPUTATION OF PSIM,P,LAM IN THIS ORDER')
      WRITE(6,323)((PSIM(I,J),J=1,3),I=1,3)
      WRITE(6,324)(P(I),I=1,3)
      WRITE(6,323)  ((LAM(I,J),J=1,3),I=1,3)
C     ************************************************************
C
C               CALCULATE THE 4TH ORDER STABILITY CRITERION.
C               DIVIDE ALL OF THE NUMBERS BY 10 TO THE
C               POWER 30 IN ORDER TO AVOID AN ERROR FOR
C               TOO LARGE A NUMBER.
C
          TF2 = (1./1.E30) *
     1          (-COEF2(2) * COEF2(3) + COEF2(4)) * (-COEF2(4))
          TF1=(1./1.E30)*((COEF2(2))**2)*COEF2(5)
          TF =TF2-TF1
C
C           OUTPUT 4TH ORDER STABILITY CRITERION
C         ***************************************
            WRITE(6,325) TF
C
C     ************************************************************
C
C                 OUTPUT THE COEFICIENTS OF QUADRATIC AND
C                 THE QUARTIC, EXPLAINING THAT ONLY THE
C                 VALUES FOR THE GAUSS-LAGUERRE AND THE
C                 GAUSS-LEGENDRE INTEGRATIONS USING
C                 INTERVALS OF 10 WERE USED.
C
              WRITE(6,330)
            DO 340 I=1,3
               WRITE(6,335)I,COEF1(I)
```

```
340         CONTINUE
            DO 350 I=1,5
               WRITE(6,355)I,COEF2(I)
350         CONTINUE
          STOP
          END
        FUNCTION F(M,Z,A1,B1,A2,A3)
C     ***********************************************************
C
C            F IS FUNCTION SUBPROGRAM WHICH IS A
C            LISTING OF ALL THE FUNCTIONS TO BE
C            INTEGRATED IN THE MAIN PROGRAM THROUGH
C            THE SUBROUTINES GLEG AND GLAG.
C
C            THE NUMBER OF FUNCTION TO BE USED
C            AT ANY GIVEN TIME IS PASSED FROM
C            THE CALLING PROGRAM AS THE VARIABLE M.
C
C            ALSO PASSED TO THIS ROUTINE ARE ANY
C            PARAMETERS NEEDED TO EVALUATE ANY OF
C            THE FUNCTIONS.  IN ORDER TO EMPLOY
C            ONLY ONE SUBPROGRAM, THESE VALUES
C            ARE PASSED EACH TIME THE PROGRAM IS
C            CALLED REGARDLESS OF WHETHER THEY ARE
C            USED BY THEFUNCTION OF INTEREST.
C     ***********************************************************
C
C            DEFINE SOME COMMONLY USED QUANTITIES.
C
               W=1.+A1*EXP(-B1*Z)
               E1=W*W
               D=A1*(EXP(-B1*Z))*(B1-A2)-A2
               B2=Z*(-6.*Z+18.)
               G1=Z*(12.*Z*Z-96.*Z+144.)
               W1=1./W
               WD=(A1*B1*EXP(-B1*Z))/E1
```

```
                F0D=(1.-Z/2.)/SQRT(2.)
                F1D=(Z*Z-7.*Z+6.)/(2.*SQRT(6.))
                F2D=(-(Z**3)/2.+7.*Z*Z-22.*Z*12.)/(4.*SQRT(3.))
                H=SQRT(2./(24.**3))
                H1=SQRT(2.)
                H2=(2./SQRT(216.))
                H3=(1./SQRT(216.))
C     ************************************************************
C
C
C           RETRIEVE THE FUNCTION OF INTEREST
C
       GOTO (1,2,3,4,5,6,7,8,9,10,11,12,13,14,15,
      1       16,17,18,19,20,21,22,23,24,25,26,27,
      2       28,29,30,31,32,33,34,35,36,37,38)     M
C     ************************************************************
C
C           LIST OF FUNCTIONS
C      **************************
1      F=Z
         RETURN
2      F=Z*D/E1
         RETURN
3      F=E2
         RETURN
4      F=E2*(D/E1)
         RETURN
5      F=G1
         RETURN
6      F=G1*D/E1
         RETURN
7      F=Z*Z*EXP(-Z)
         RETURN
8      F=Z*Z
         RETURN
9      F=E2*F2*EXP(-Z)
         RETURN
```

```
10      F=E2*E2
          RETURN
11      F=G1*G1*EXP(-Z)
          RETURN
12      F=G1*G1
          RETURN
13      F=Z*E2*EXP(-Z)
          RETURN
14      F=Z*E2
          RETURN
15      F=E2*G1*EXP(-Z)
          RETURN
16      F=E2*G1
          RETURN
17      F=Z*G1*EXP(-Z)
          RETURN
18      F=Z*G1
          RETURN
19      F=(WD*Z/H1+F0D/W)*Z
          RETURN
20      F=(WD*E2*H3+F1D/W)*E2
          RETURN
21      F=(WD*H*G1+F2D/W)*G1
          RETURN
22      F=(WD*E2*H3+F1D/W)*G1
          RETURN
23      F=(WD*G1*H+F2D/W)*E2
          RETURN
24      F=(WD*E2*H3+F1D/W)*Z
          RETURN
25      F=(WD*Z/H1+F0D/W)*G1
          RETURN
26      F=(WD*G1*H+F2D/W)*Z
          RETURN
27      F=(EXP(-1.))*H1*Z**4
          RETURN
```

```
28      F=(EXP(-1.))*H2*E2*Z**3
          RETURN
29      F=(EXP(-1.))*H*G1*(Z**3)
          RETURN
30      F=(1./H1)*(EXP(-Z/2.))*(Z**4)
          RETURN
31      F=H1*(Z**4)
          RETURN
32      F=H3*(EXP(-Z/2.))*E2*(Z**3)
          RETURN
33      F=H2*E2*(Z**3)
          RETURN
34      F=H*(EXP(-Z/2.))*G1*(Z**3)
          RETURN
35      F=H*G1*(Z**3)
          RETURN
36      F=(EXP(2.*A2))*EXP(-A2*Z)*(Z**3)
          RETURN
37      F=(WD*Z/H1+FOD/W)*E2
          RETURN
38      F=((EXP(2.*A2))/A2)*(Z**3)
        RETURN
        END
        SUBROUTINE GLEG(LF,LP,N,T,Z,E,M,A1,B1,A2,A3)
C     ********************************************************
C
C            GLEG USES THE GAUSS-LEGENDRE METHOD OF
C            INTEGRATION TO INTEGRATE A FUNCTION
C            WITH FINITE LIMITS.
C
C     ********************************************************
C
C       DIMENSION STATEMENTS
C       ************************
        REAL S(11),A(10),T(N),Z(N),LP,LF,W(N)
C
```

```
C       FORMAT STATEMENTS
C      *********************
40     FORMAT(1X,'FOR F',I2,5X,'N=',I2)
60     FORMAT(5X,E13.7)
C
C         INITIALIZE THE SUM
       S(1)=0.
C
       B=(LP+LF)/2.
       C=(LP-LF)/2.
C
       DO 10 I=1,N
         A(I)=B+(C*T(I))
10     CONTINUE
C     ****************************************************************
C          PERFORM THE INTEGRATION--EVALUATE
C          THE SUM INTERVALS.
C     ****************************************************************
       DO 20 I=1,N
         MZ=I+1
         S(MZ)=S(I)+F(M,A(I),A1,B1,A2,A3)*W(I)
         Z(I)=C*S(MZ)
20     CONTINUE
C     ****************************************************************
C
C          OUTPUT THE NUMBER OF THE FUNCTION
C          AND THE NUMBER OF INTERVALS USED.
C
       WRITE(6,40)M,N
C     ****************************************************************
C          OUTPUT THE VALUE OF THE SUM AT THE
C          END OF EACH INTERVAL.
C
C
       DO 50 I=1,N
          WRITE(6,60)Z(I)
```

```
50    CONTINUE
C
      RETURN
      END
      SUBROUTINE GLAG(N,T,Z,E,U,C,M,A1,B1,A2,A3)
C     ************************************************************
C
C         GLAG CALCULATES THE VALUE OF AN INTEGRAL
C         FROM ZERO TO INFINITY FOR ANY FUNCTION
C         OF INTEREST.
C
C     ************************************************************
C
C         DIMENSION STATEMENTS
C      ****************************
      REAL A(10),T(N),S(11),W(N),Z(N)
C
C         FORMAT STATEMENTS
C      ************************
40    FORMAT(1X,'FOR F',I2,5X,'N=',I2)
60    FORMAT(5X,E13.7)
C
      DO 10 I=1,N
        A(I)=U*T(I)+C
10    CONTINUE
C
C         INITIALIZE THE SUM
C      ************************
      S(1)=0.
C     ************************************************************
C
C         PERFORM THE INTEGRATION--EVALUATE
C         THE SUM OF THE INTERVALS.
C
      DO 20 I=1,N
        MZ=I+1
```

```
          S(MZ)=S(I)+F(M,A(I),A1,B1,A2,A3)*W(I)
          Z(I)=S(MZ)
20      CONTINUE
C     ************************************************************
C
C
C           OUTPUT THE NUMBER OF FUNCTION BEING
C           INTEGRATED AND THE NUMBER OF INTERVALS
C           USED
C
        WRITE(6,40)M,N
C     ************************************************************
C
C           OUTPUT THE VALUE OF THE SUM AFTER
C           EACH INTERVAL
C
        DO 50 I=1,N
50      WRITE(6,60)Z(I)
C
        RETURN
        END
```

BIBLIOGRAPHY

Abegg, C.F., and N.S. Balakrishnan, A.I.Ch.E. Symp. Series 67, 88 (1971).

Bauer, L.G., M.A. Larson, and V.J. Dallons, Chem. Eng. Sci. 29, 1253 (1974).

Beckman, J.R., Ph.D. Dissertation, Dept. of Chemical Engineering, University of Arizona, Tucson (1976).

Bennema, P., in Industrial Crystallization, J.W. Mullin, ed. Plenum Press, New York (1976), p. 91.

Bennett, R.C., Chem. Eng. Progr. 9, 76 (1962).

Bennett, R.C., and M. Van Buren, A.I.Ch.E. Symp. Series 65, 44 (1969).

Bollinger, R.E., and D.E. Lamb, Ind. Eng. Chem. Fundamentals 1, 245 (1962).

Bujac, P.D.B., in Industrial Crystallization, J.W.Mullin, ed. Plenum Press, New York (1976), p. 23.

Burton, W.K., N. Cabrera, and F.C. Frank, Phil. Trans. Roy. Soc. A243, 299 (1951).

Canning, T.F., and A.D. Randolph, A.I.Ch.E. J. 13, 5 (1967).

Clontz, N.A., and W.L. McCabe, Chem. Eng. Progr. Symp. Series 67, 6 (1971).

Cohen, D.S., and J.P. Keener, SIAM J. Appl. Math. 28, 307 (1975).

Finn, R.K., and R.E. Wilson, Agr. Food Chem. 2, 66 (1954).

Garside, J., and R.J. Davey, Chem. Eng. Commun. 4, 393 (1980).

Garside, J., and S.J. Jancic, A.I.Ch.E. J. 22, 887 (1976).

Garside, J., and S.J. Jancic, A.I.Ch.E. J. 25, 948 (1979).

Garside, J., and M.A. Larson, J. Cryst. Growth 43, 694 (1978).

Garside, J., I.T. Rusli, and M.A. Larson, A.I.Ch.E. J. 25, 57 (1979).

Han, C.D., paper presented at the Symposium on Selected Papers. Part 1 61st Annual Meeting, A.I.Ch.E., Los Angeles (1967).

Helwig, J.T., and K.A. Council, eds., SAS User's Guide 1979 edition, SAS Institute Inc., Raleigh, North Carolina (1979).

Hulburt, H.M., and S. Katz, Chem. Eng. Sci. 19, 555 (1964).

Hulburt, M.A., and D.G. Stefango, C.E.P. Symp. Series 5, 50 (1969).

Janse, A.H., and E.J. de Jong, in Industrial Crystallization, J.W. Mullin, ed. Plenum Press, New York (1976), p. 145.

Khambaty, S., and M.A. Larson, Ind. Eng. Chem. Fundamentals 17, 160 (1978).

Larson, M.A., and A. D. Randolph, C.E.P. Symp. Series 65, 95 (1969).

Lee, H.H., A.I.Ch.E. J. 24, 535 (1978).

Lei, S.J., R. Shinnar, and S. Katz, A.I.Ch.E. J. 17, 1459 (1971a).

Lei, S.J., R. Shinnar, and S. Katz, C.E.P. Symp. Series, 67, 129 (1971b).

Luyben, W.L., and D.E. Lamb, C.E.P. Symp. Series 59, 165 (1963).

McCabe, W.L., and R.P. Stevens, Chem. Eng. Progr. 47, 168 (1951).

Miller, P., and W.C. Saeman, Chem. Eng. Progr. 43, 667 (1947).

Miller, P., and W.C. Saeman, Chem. Eng. Progr. 47, 168 (1951).

Murray, D.C., and M.A. Larson, A.I.Ch.E. J. 11, 728 (1951).

Ottens, E.P.K., and E.J. de Jong, Ind. Eng. Chem. Fundamentals 12, 179 (1973).

Nyvlt, J., and J.W. Mullin, Chem. Eng. Sci. 25, 131 (1970).

Randolph, A.D., Ph.D. Dissertation, Dept. of Chemical Engineering, Iowa State University of Science and Technology, Ames (1962).

Randolph, A.D., Can. J. Chem. Eng. 42, 280 (1964).

Randolph, A.D., G.L. Beer, and J.P. Keener, A.I.Ch.E. J. 19, 1140 (1973).

Randolph, A.D., and M.D. Cise, A.I.Ch.E. J. 18, 789 (1972).

Randolph, A.D., and M.A. Larson, A.I.Ch.E. J. 8, 639 (1962).

Randolph, A.D., and M.A. Larson, Chem. Eng. Progr. Symp. Series 61, 147 (1965).

Randolph, A.D., and M.A. Larson, C.E.P. Symp. Series 65, 95 (1969).

Randolph, A.D., and M.A. Larson, Theory of Particulate Processes, Academic Press, New York (1971).

Randolph, A.D., and A.D. Puri, A.I.Ch.E. J. 27, 92 (1981).

Robinson, J.N., and J.E. Roberts, Can. J. Chem. Eng. 35, 105 (1957).

Rousseau, R.W., Chemteck 10, 566 (1980).

Rousseau, R.W., and R.M. Parks, Ind. Eng. Chem. Fundamentals 20, 71 (1981).

Rumford, F., and J. Bain, Trans. Inst. Chem. Engrs. 38, 10 (1960).

Saeman, W.C., A.I.Ch.E. J. 2, 107 (1956).

Sherwin, M.B., S. Katz, and R. Shinnar, C.E.P. Symp. Series 65, 75 (1969).

Sherwin, M.B., R. Shinnar, and S. Katz, A.I.Ch.E. J. 13, 1141 (1967).

Shinnar, R., J. Fluid Mech. 10, 259 (1961).

Sidkar, S.K., and A.D. Randolph, A.I.Ch.E. J. 22, 110 (1976).

Song, Y.H., and J.M. Douglas, A.I.Ch.E. J. 21, 924 (1975).

Strickland-Constable, R.F., A.I.Ch.E. Symp. Series 68, 1 (1972).

Sung, C.Y., J. Estrin, and G.R. Youngquist, A.I.Ch.E. J. 19, 957 (1973).

Thomas, W.M., and W. C. Mallison, Petrol. Refiner. 5, 211 (1961).

Timm, D.C., and G. Gupta, paper presented at the 63rd Annual A.I.Ch.E. Meeting, Chicago (1970).

Timm, D.C., and M.A. Larson, A.I.Ch.E. J. 14, 452 (1968).

Van Hook, A., Crystallization: Theory and Practice, ACS Monograph 152, Reinhold, New York (1961), p. 94.

Youngquist, G.R., and A.D. Randolph, A.I.Ch.E. J. 18, 421 (1972).

Yu, K.M., and J.M. Douglas, A.I.Ch.E. J. 21, 917 (1975).

BIOGRAPHICAL SKETCH

Charles Umejei Onwuegbunem Okonkwo was born in Lagos, Nigeria, to Clara and Francis Onwochei Okonkwo. Upon graduating from high school, he worked as a quality controller for International Paints Company in Lagos for about two years and commenced undergraduate studies in 1971. He received a Bachelor of Science degree in December, 1974, from Iowa State University, in Ames, Iowa. He later graduated from the same school with a Master of Science degree in chemical engineering in August, 1977. He wrote a thesis for the Master of Science degree.

Charles began work for the doctoral degree in chemical engineering at the University of Florida under the guidance of H.H. Lee. He was accepted to candidacy for the Doctor of Philosophy degree in September, 1978, defended his dissertation in June, 1982, and expects to officially receive the doctoral degree in August, 1982.

Upon graduation Charles will assume a position with the Systems Engineering Division of Tennessee Eastman Kodak, Tennessee.

Charles has interests in boxing and was the captain of his high school boxing team. He has had the opportunity to train with very talented boxers. While an undergraduate, he was a member of the Iowa State University wrestling team. He is one of the top ranked power lifters in the world. In July, 1981, he attempted a world record in the bench press and was ranked number one in this event in the United States. His other hobbies include karate, table tennis, jogging, playing checkers and swimming.

I certify that I have read this study and that in my opinion it conforms to acceptable standards of scholarly presentation and is fully adequate, in scope and quality, as a dissertation for the degree of Doctor of Philosophy.

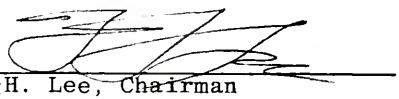

HongH. Lee, Chairman
Associate Professor of Chemical Engineering

I certify that I have read this study and that in my opinion it conforms to acceptable standards of scholarly presentation and is fully adequate, in scope and quality, as a dissertation for the degree of Doctor of Philosophy.

John P. O'Connell
Professor and Acting Chairman of Chemical Engineering

I certify that I have read this study and that in my opinion it conforms to acceptable standards of scholarly presentation and is fully adequate, in scope and quality, as a dissertation for the degree of Doctor of Philosophy.

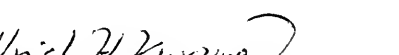

Ulrich H. Kurzweg
Professor of Engineering Sciences

I certify that I have read this study and that in my opinion it conforms to acceptable standards of scholarly presentation and is fully adequate, in scope and quality, as a dissertation for the degree of Doctor of Philosophy.

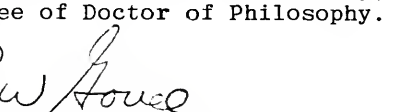

Robert W. Gould
Professor of Materials Science Engineering

I certify that I have read this study and that in my opinion it conforms to acceptable standards of scholarly presentation and is fully adequate, in scope and quality, as a dissertation for the degree of Doctor of Philosophy.

R. Narayanan

Ranganathan Narayanan
Visiting Assistant Professor of
Chemical Engineering

This dissertation was submitted to the Graduate Faculty of the College of Engineering and to the Graduate Council, and was accepted as partial fulfillment of the requirements for the degree of Doctor of Philosophy.

August 1982

Hubert A. Lewis

Dean, College of Engineering

Dean for Graduate Studies and
Research